

University  
of Ljubljana  
Faculty  
*for Civil and Geodetic  
Engineering*



**LIVIA BEATRIZ MACHADO DE ALMEIDA**

**FLOOD RISK AND DAMAGE INVESTIGATION IN  
AREAS OF HIGH CULTURAL HERITAGE VALUE**

MASTER'S THESIS

MASTER STUDY PROGRAMME FLOOD RISK MANAGEMENT



Univerza v Ljubljani



Ljubljana, 2023



University  
of Ljubljana  
Faculty  
for Civil and Geodetic  
Engineering



Candidate

**LIVIA BEATRIZ MACHADO DE ALMEIDA**

**FLOOD RISK AND DAMAGE INVESTIGATION IN  
AREAS OF HIGH CULTURAL HERITAGE VALUE**

Master's thesis no .:

**Mentor:**

Simon Rusjan

**Co-mentor:**

Andrej Kryžanowski

Andrej Vidmar

**Commission member:**

**Chairman of the Commission:**

izr. prof. dr. Nataša Atanasova, Ph.D.

Ljubljana, 28. August. 2023



UNIVERSITAT POLITÈCNICA  
DE CATALUNYA  
BARCELONATECH

Univerza v Ljubljani



*"This page is intentionally blank"*

## **ERRATA**

Error page	Error bar	Instead	Let it be
------------	-----------	---------	-----------

## ACKNOWLEDGEMENTS

It is an immense privilege and pleasure to convey my sincere gratitude and appreciation to the following people, whose advice, assistance, and guidance were extremely helpful in the completion of this master's thesis.

To my research mentors, Dr. Simon Rusjan and Dr. Andrej Kryžanowski, for their supervision, constant support, and continuous assistance throughout the whole thesis process. Thank you, Dr. Simon Rusjan, for always being available to answer my questions, inquiries, and doubts concerning which direction to take with this work with patience and openness. I deeply appreciate your disposition to teach and share part of your knowledge and experience with me. Your knowledgeable opinions, comments, and excellent guidance allowed me to successfully complete this study. I am also thankful for all the support provided by Dr. Andrej Kryžanowski especially regarding the comprehension of the hydrologic, social, and political aspects of the present case study, highlighting the obstacles and difficulties that the municipality face. Furthermore, I would like to thank Dr. Andrej Vidmar for taking the time to explain KR PAN's operation and limitations to me and presenting me with diverse platforms and documents that could help the development of my thesis. I am also grateful for the time and effort he invested in altering his model to accommodate the changes I suggested, which allowed me to obtain this thesis results.

To my friends from Batch 10, I honestly don't believe I had such intense experiences with no other group of people in my life. We were a part of each other's life in such a close manner for so long that it felt like family. We shared, laughed, and learned with each other every day. We even lived together! You gave me so much perspective about the world and realities that were so different that mine. You made me reflect on my own life and grow. I will always remember all the talks, dinners, parties, trips, and hikes we shared. You pushed me to do things I never thought I would be capable of doing. I would like to thank you for the endless times you made yourselves available to help me, either emotionally or academically. I don't think I could ever ask for a better Batch, you made these past two years incredible. I would like to especially thank Gina, Cristiane, Liza, Andres, Doreen, Paolo, Moe, Emiel, and Kristina, for hanging in there with me, I want to take you with me.

To my friends in Brazil, for all their love and support from far away in all the difficult moments. I thank you for your patience to listen to my complaints about the cold, the struggle with the subjects and the thesis, and especially for making me feel that independent of what happened they would always be there for me and make me feel like I am a part of something, that I always had something to get back to.

To Patrick, for being my partner along this whole way. The past two years have been hard for both of us, but you always found a way to support me despite your struggles. Thank you for stepping up whenever I needed you to and being understanding whenever I was drained and didn't have much of me to give you.

To my family and especially my mum. I will never be able to thank you enough for all the unconditional love in every single step of this process, from the period before the program with all the doubts about being able to attend the program to the times when I doubted myself and my capacity to keep moving forward and finally through the thesis journey, that ends up being a very lonely and introspective process. Thank you for all the visits, all the trips here we could enjoy together, and all the food from home you brought me and made me feel like there was a piece of home in Europe. You have supported me in every moment ever since I can remember.

Lívia Beatriz Machado de Almeida  
Ljubljana, Slovenia

**BIBLIOGRAPHIC-DOCUMENTALISTIC INFORMATION AND ABSTRACT**

<b>UDC:</b>	<b>556.166:725(043.3)</b>
<b>Author:</b>	<b>Livia Beatriz Machado de Almeida</b>
<b>Supervisor:</b>	<b>Assist. Prof. Simon Rusjan, Ph.D.</b>
<b>Co-supervisor:</b>	<b>Assoc. Prof. Andrej Kryžanowski, Ph.D.</b>
<b>Title:</b>	<b>Flood Risk and Damage Investigation in Areas of High Cultural Heritage Value</b>
<b>Document type:</b>	<b>Master thesis</b>
<b>Notes:</b>	<b>121 p., 19 tab., 67 fig., 5 eq., 117 ref.</b>
<b>Keywords:</b>	<b>coastal floods, cultural heritage, climate change, sea level rise, depth-damage function, KRPAN model, the city of Piran</b>

**Abstract**

Floods affect more than a billion people every year, bringing direct damage through the destruction of buildings, infrastructure, and loss of life. On the other hand, it results in indirect social and economic damage through well-being and revenue reduction. Floods also impact irreplaceable cultural heritage, especially in coastal areas such as Piran, in Slovenia. Piran is known for its rich cultural heritage, having been occupied by several relevant civilizations, such as the Romans and the Byzantines. This municipality is constantly affected by floods and the tendency, according to climate change and sea level rise predictions, is for those floods to become more frequent and more destructive in the following years. The loss of cultural heritage is disastrous not only for tangible reasons, associated with the destruction of buildings or historical areas, their use, and the tourism it promotes but also because it erases part of the cultural identity and history of a community.

To assess the financial impact of floods in Slovenia, Vidmar et al. 2019 created the KRPAN model, which uses depth-damage curves of residential buildings, businesses, and infrastructure to calculate annual damage. KRPAN provides the possibility to consider the damage on cultural heritage, however without accounting for its specific characteristics. The depth-damage curve used in the model is derived from FEMA (2014) and is not well-adapted to historical buildings. This work aims to improve the original KRPAN depth-damage curves for cultural heritage by making them more accurate with the aid of field data collected in Piran and a literature review of damage on cultural heritage and specific building materials found in the area. The literature research also comprises the impact of saltwater on cultural heritage buildings. Nevertheless, this impact was not considered directly in the damage calculation due to a lack of available data and resources to perform an in-depth chemical analysis of saltwater impacts on construction materials.

A qualitative risk assessment was also performed in the area, according to the estimated vulnerability of the buildings, represented by a flood vulnerability index. Most of the assets are found to have a moderate or high flood vulnerability index (FVI). Besides that, intersecting FVIs values with flood hazard, the 51 buildings analyzed are classified in flood risk classes. Interpreting the results, it can be concluded that the influence of the sea level rise variation on the determination of flood risk classes (highest shift of 35% between classes) is bigger than the impact of the change of flood return periods (highest shift of 25% between classes). This means that cultural heritage in Piran is significantly vulnerable to floods, and, with the increasing sea level rise and the consequent deterioration of the buildings, the tendency is for these assets to become even more vulnerable. A superficial qualitative analysis of the long-term evolution of salt deterioration with the effect of climate change was also performed. This analysis led to the conclusion that the combination of the predicted increase in the

number of cycles and increased flood event frequency would undoubtedly result in the augmentation of cultural heritage losses.

In order to evaluate the calculated flood damage, the costs computed in the present work are compared with cultural heritage renovation data estimated and provided by the Ministry of Culture of the Republic of Slovenia and the results presented by Alivio (2020). The damage values increase as the sea level rise scenarios get more extreme. For a 10-year return period, values for a 1.46m sea level rise reach up to 529% of the costs for a 0.3m scenario and 25 times the costs for a no sea level rise scenario. Additionally, the impact of the sea level rise on the damage cost for cultural heritage buildings gets smaller as the return period gets longer. It should be noted that, in every scenario, the building located in Tartini Square 2 is the one that contributed the most to total damage, with damage costs up to 530 thousand euros for a 1000-year return period and a 1.46m sea level rise. The improvement of these curves would allow the designated authorities to better reduce and mitigate flood risk and the impact of climate change on cultural heritage, through the prioritization of sites to protect and a better understanding of the severity and financial consequences of these processes.

**BIBLIOGRAFSKO – DOKUMENTACIJSKA STRAN IN IZVLEČEK**

<b>UDK:</b>	<b>556.166:725(043.3)</b>
<b>Avtor:</b>	<b>Livia Beatriz Machado de Almeida</b>
<b>Mentor:</b>	<b>doc. dr. Simon Rusjan</b>
<b>Somentor:</b>	<b>izr. prof. dr. Andrej Kryžanowski</b>
<b>Naslov:</b>	<b>Analiza poplavne ogroženosti in škode za objekte kulturne dediščine na območju mesta Piran</b>
<b>Tip dokumenta:</b>	<b>magistrsko delo</b>
<b>Obseg in oprema:</b>	<b>121 str., 19 pregl., 67 sl., 5 en., 117 ref.</b>
<b>Ključne besede:</b>	<b>poplave morja, kulturna dediščina, podnebne spremembe, dvig gladine morja, škodne krivulje, model KRPAN, mesto Piran</b>

**Izveček:**

Poplave vsako leto prizadenejo več kot milijardo ljudi in povzročijo neposredno škodo z uničenjem stavb, infrastrukture in izgubo življenj. Po drugi strani se posledice poplav odražajo v socialnih stiskah in posredni gospodarski škodi zaradi zmanjšanja blaginje ter prihodkov. Poplave prizadenejo tudi nenadomestljivo kulturno dediščino, za tovrstno škodo so dovzetna zlasti obalna območja, kot je npr. območje starega mesta Piran na slovenki obali. Piran je znan po svoji bogati kulturni dediščini, ki je posledica prisotnosti številnih starih civilizacij, med drugimi Rimljani in Bizantinci. Območje mesta Piran pogosto prizadene poplavljanje morja, glede na podnebne spremembe in napovedi dviga morske gladine bodo zelo verjetno poplave v naslednjih letih vse pogostejše in bolj uničujoče. Izguba kulturne dediščine je problematična ne samo zaradi neposredne škode, povezanih z neposrednim uničenjem stavb ali zgodovinskih območij, njihovo uporabo in turističnimi dejavnostmi, ki jih spodbuja, temveč tudi zato, ker se s poplavno škodo pogosto izbriše del kulturne identitete in zgodovine skupnosti.

Za oceno ekonomskih posledic poplav v Sloveniji so Vidmar in sod. (2019) ustvarili model KRPAN, ki vključuje škodne krivulje stanovanjskih zgradb, raznih gospodarskih dejavnosti in infrastrukture za izračun škode zaradi poplav. KRPAN omogoča tudi upoštevanje škode na kulturni dediščini, vendar brez upoštevanja njenih posebnosti. Škodne krivulje, uporabljene v modelu, izhajajo iz FEMA (2014) in niso prilagojene specifičnim lastnostim objektov kulturne dediščine. Namen naše naloge je bil opraviti analizo poplavne škode na kulturni dediščini v modelu KRPAN z vključitvijo specifičnih škodnih krivulj z upoštevanjem natančnejših terenskih podatkov o lastnostih raznih elementov kulturne dediščine, zbranih v mestu Piran ter pregledom svetovne literature o poškodbah kulturne dediščine in dovzetnosti specifičnih gradbenih materialov na poškodbe zaradi poplavljanja. Pregled literature je zajemal tudi vpliv slane vode na objekte kulturne dediščine, vendar vpliv slane vode ni bil neposredno upoštevan pri izračunu poplavne škode zaradi pomanjkanja razpoložljivih podatkov in virov za izvedbo poglobljene kemijske analize vplivov slane vode na različne gradbene materiale.

Na območju mesta Piran je bila izvedena tudi kvalitativna ocena ogroženosti glede na ocenjeno ranljivost objektov, ki jo predstavlja indeks poplavne ogroženosti. Za večino objektov s statusom kulturne dediščine je bilo ugotovljeno, da imajo zmeren do visok indeks poplavne ranljivosti (FVI). Poleg tega smo s kombiniranjem vrednosti FVI z ugotovljenim obsegom poplavne nevarnosti za različne scenarije dvigov morja analizirali 51 stavb in jih razvrstili v razrede poplavne ogroženosti. Na podlagi rezultatov lahko sklepamo, da je vpliv spremenljivosti dviga morske gladine na določitev razredov poplavne ogroženosti (največje razlike med razredi 35%) večji od vpliva spremembe povratnih dob poplav (največje razlike med razredi 25%). To pomeni, da je kulturna dediščina v Piranu močno poplavno ranljiva, z naraščajočim dvigom morske gladine in posledičnim večanjem poškodb pa bo dovzetnost za poškodbe še bistveno večja. Izvedena je bila tudi ocena dolgoročnega vpliva soli na gradbene materiale v povezavi s pričakovanimi podnebnimi spremembami. Ta analiza je vodila do zaključka, da bo kombinacija vplivov soli na gradbene materiale in povečane pogostosti poplav nedvomno povzročila povečanje poškodb na elementih kulturne dediščine.

Za ovrednotenje izračunane škode zaradi poplav so stroški, izračunani v pričujočem delu, primerjani s podatki o ocenjenih sredstvih potrebnih za prenavo nekaterih objektov kulturne dediščine, ki jih je ocenilo in posredovalo Ministrstvo za kulturo Republike Slovenije, ter rezultati, ki jih je predstavil Alivio (2020). Vrednosti škode se pričakovano povečujejo, ko upoštevamo bolj ekstremne

scenarije dviga morske gladine. V primeru dogodka z 10-letno povratno dobo ob upoštevanem ekstremnem scenariju dviga srednje gladine morja za 1,46 m je povečanje škode za 529% v primerjavi scenarija dviga morske gladine za 0,3 m (najverjetnejši scenarij dviga srednje gladine morja do leta 2100) in kar 25-kratno povečanje škode v primerjavi s sedanjim srednjim nivojem morske gladine. Poleg tega se vpliv dviga morske gladine na škodo na objektih kulturne dediščine manjša z daljšanjem povratnem dobe poplavnega dogodka. Opozoriti je treba, da je v vsakem upoštevanem scenariju stavba na Tartinijevem trgu 2 tista, ki največ prispeva k skupni škodi, ocenjena škoda znaša do 530 tisoč evrov v primeru ekstremnega dogodka s 1000-letno povratno dobo in upoštevanjem dviga morske gladine za 1,46 m. Naše izboljšave ocene škode na elementih kulturne dediščine lahko pristojnim inštitucijam omogočijo boljši vpogled v posledice prisotnosti poplavne ogroženosti in vpliva podnebnih sprememb na različne elemente kulturne dediščine ter identifikacijo prednostnih območij, ki jih bo treba obvarovati. Rezultati analiz bodo prispevali k boljšemu razumevanju problematike izpostavljenosti kulturne dediščine poplavam in finančnih posledic povečane pojavnosti poplavnih dogodkov.

**TABLE OF CONTENTS**

<b>ERRATA</b> .....	<b>I</b>
<b>ACKNOWLEDGEMENTS</b> .....	<b>II</b>
<b>BIBLIOGRAPHIC-DOCUMENTALISTIC INFORMATION AND ABSTRACT</b> .....	<b>III</b>
<b>TABLE OF CONTENTS</b> .....	<b>VII</b>
<b>LIST OF FIGURES</b> .....	<b>IX</b>
<b>LIST OF TABLES</b> .....	<b>XII</b>
<b>ABBREVIATIONS AND SYMBOLS</b> .....	<b>XIII</b>
<b>1 INTRODUCTION</b> .....	<b>1</b>
<b>1.1 Context</b> .....	<b>1</b>
<b>1.2 Motivation</b> .....	<b>3</b>
<b>1.3 Objectives</b> .....	<b>4</b>
<b>1.4 Research questions</b> .....	<b>4</b>
<b>1.5 Innovation and Practical Value</b> .....	<b>5</b>
<b>2 LITERATURE REVIEW</b> .....	<b>6</b>
<b>2.1 Impact of Climate Change on Cultural Heritage</b> .....	<b>7</b>
<b>2.2 Impact of Climate Change on Coastal Cities</b> .....	<b>13</b>
<b>2.3 Flood Risk Assessment of Cultural Heritage Sites</b> .....	<b>14</b>
<b>2.4 Impact of Salt on Cultural Heritage</b> .....	<b>18</b>
<b>2.5 Depth-damage curves</b> .....	<b>22</b>
<b>2.6 Slovenian and European Policies, Guidelines, and Projects for The Protection and Conservation of Cultural Heritage</b> .....	<b>27</b>
<b>3 CASE STUDY – PIRAN</b> .....	<b>32</b>
<b>3.1 Geographical Location</b> .....	<b>32</b>
<b>3.2 Climate and Hydrological Context</b> .....	<b>33</b>
<b>3.3 Socio-Economic Context</b> .....	<b>34</b>
<b>3.4 Cultural Heritage in Piran</b> .....	<b>35</b>
<b>4 RESEARCH METHODOLOGY</b> .....	<b>37</b>
<b>4.1 Methodological Framework</b> .....	<b>37</b>
<b>4.2 Data sources</b> .....	<b>37</b>
<b>4.3 GIS Analysis</b> .....	<b>38</b>
<b>4.4 Flood Vulnerability Index (FVI)</b> .....	<b>39</b>
4.4.1 Coastal City Flood Vulnerability Index (CCFVI).....	<b>50</b>
<b>4.5 Depth-Damage Curves</b> .....	<b>52</b>
<b>4.6 Evolution of the number of salt transition cycles</b> .....	<b>54</b>
<b>5 RESULTS</b> .....	<b>55</b>
<b>5.1 Qualitative Flood Risk</b> .....	<b>55</b>
<b>5.2 Quantitative Flood Risk</b> .....	<b>61</b>
5.2.1 Comparison with Previous Studies in Piran.....	<b>73</b>
5.2.2 Comparison with Renovation Costs.....	<b>77</b>

---

<b>5.3</b>	<b>Evolution of the number of salt transition cycles .....</b>	<b>80</b>
<b>6</b>	<b>DISCUSSION.....</b>	<b>81</b>
<b>6.1</b>	<b>Second-Tier Flood Vulnerability and Risk Assessment.....</b>	<b>81</b>
<b>6.2</b>	<b>Evaluation of Flood Adaptation Strategies .....</b>	<b>84</b>
<b>6.3</b>	<b>Flood Risk Reduction Measures Proposed for Piran .....</b>	<b>85</b>
<b>6.4</b>	<b>Damage Assessment of Saltwater Floods.....</b>	<b>89</b>
<b>7</b>	<b>CONCLUSION .....</b>	<b>91</b>
<b>7.1</b>	<b>Summary .....</b>	<b>91</b>
<b>7.2</b>	<b>Conclusions .....</b>	<b>92</b>
<b>7.3</b>	<b>Recommendations.....</b>	<b>95</b>
<b>8</b>	<b>REFERENCES .....</b>	<b>96</b>

**LIST OF FIGURES**

Figure 1: Total Expected Annual Flood Damage in Piran for different SLR scenarios (Alivio, 2020)..	6
Figure 2: Potential adaptation tipping points for the flood risk index and the erosion risk index (Reimann et al, 2018).....	7
Figure 3: Conversion functions for specific materials or object type (upper part) and the weight attributed to a key risk indicator (KRI) (lower part.).....	9
Figure 4: Incorporation of a long-term monitoring program in a Cultural Heritage Integrated.....	11
Figure 5: Qualitative matrix of the urgency of the intervention (Loli and Bertolin, 2018).....	12
Figure 6: Interaction between coastal vulnerability subsystems (Balica et al., 2012).....	14
Figure 7: Level of physical damage in cultural assets related to flood depth and velocity (Dassanayake et al., 2012).....	15
Figure 8: Proposed risk analysis methodology: assessment of the level of risk of the cultural heritage (CH) unit. (Romão et al., 2016) .....	17
Figure 9: Pictures representing several deterioration processes observed at the sites. (a,b) at Panamá	19
Figure 10: Depth-damage curves for cultural heritage in Piran .....	22
Figure 11: Flowchart of the development of depth-damage curves for Spanish municipalities (Martínez-Gomariz et al., 2020).....	23
Figure 12: Relative depth-damage curves for buildings in Spanish cities (Martínez-Gomariz et al., 2020) .....	24
Figure 13: Temporal adjustment indices until the year 2060. (Martínez-Gomariz et al., 2020).....	24
Figure 14: Flowchart for flood risk assessment with a building-material-based vulnerability approach (Englhard et al., 2019).....	25
Figure 15: Stage-damage curves for four building-material-based vulnerability classes. For classes III and IV the one- and two-floor curves are denoted by (a) and (b).....	26
Figure 16: Geographic location of Piran, Slovenia (Alivio, 2020) .....	32
Figure 17: Elevations of Piran, Slovenia (Alivio, 2020).....	33
Figure 18: Temperature in Piran over the year (Weatherspark.com, 2023).....	33
Figure 19: Precipitation in Piran over the year (World Weather & Climate Information, 2023).....	34
Figure 20: Population distribution in Piran (Alivio, 2020) .....	35
Figure 21: Culture heritage locations and heritage status in Piran.....	36
Figure 22: Methodology Flowchart.....	37
Figure 23: Framework for simplified flood vulnerability assessment (Miranda and Ferreira, 2019) ...	40
Figure 24: Frequency of Flood Vulnerability Indexes .....	42
Figure 25: Cumulative distribution of Flood Vulnerability Indexes .....	42
Figure 26: Mary of Health's Church/ Cerkev Marije Zdravja – One of the four buildings with the highest FVI.....	43

Figure 27: 10 most vulnerable buildings in Piran according to FVI .....	43
Figure 28: Flood Vulnerability Index classes in Piran .....	44
Figure 29: Age of cultural heritage buildings in Piran .....	45
Figure 30: Condition of cultural heritage buildings in Piran .....	46
Figure 31: Exposure of cultural heritage buildings in Piran .....	47
Figure 32: Heritage Status of cultural heritage buildings in Piran .....	48
Figure 33: Presence of limestone base on cultural heritage buildings in Piran .....	48
Figure 34: Numbers of stories of cultural heritage buildings in Piran.....	49
Figure 35: Presence of ornaments on cultural heritage buildings in Piran .....	49
Figure 36: Occurrence of recent renovation on cultural heritage buildings in Piran.....	50
Figure 37: Depth-damage curves selected for the present work. General (blue), raw sandstone, more fragile materials (green), and sandstone masonry (red).....	54
Figure 38: Flood Risk Distribution for the cultural heritage buildings in Piran.....	56
Figure 39: Risk Classes for the 10-year return period and no sea level rise (S0).....	56
Figure 40: Risk Classes for the 10-year return period for a 0.3m mean sea level rise (S3). .....	57
Figure 41: Risk Classes for the 10-year return period for a 1.46m mean sea level rise (S7). .....	58
Figure 42: Risk Classes for the 100-year return period and no sea level rise (S0).....	59
Figure 43: Risk Classes for the 100-year return period for a 0.3m mean sea level rise. ....	60
Figure 44: Risk Classes for the 100-year return period for a 1.46m mean sea level rise. ....	61
Figure 45: Damage per flood scenario and depth-damage curve .....	62
Figure 46: Damage per flood scenario and depth-damage curve with uncertainty bands (purple stripes) .....	63
Figure 47: Comparison between damage estimates: Damage per flood scenario (in millions of euros) and depth-damage curve with uncertainty bands (purple stripes) .....	64
Figure 48: Damage per (a) building and (b) curve for a 10-year period and no sea level rise .....	65
Figure 49: Damage per (a) building and (b) curve for a 100-year period and no sea level rise .....	66
Figure 50: Damage per (a) building and (b) curve for a 1000-year period and no sea level rise .....	67
Figure 51: Damage per (a) building and (b) curve for a 10-year period and 0.3m mean sea level rise	68
Figure 52: Damage per (a) building and (b) curve for a 100-year period and 0.3m mean sea level rise .....	69
Figure 53: Damage per (a) building and (b) curve for a 1000-year return period and 0.3m mean sea level rise.....	70
Figure 54: Damage per (a) building and (b) curve for a 10-year return period and 1.46m sea level rise .....	71
Figure 55: Damage per (a) building and (b) curve for a 100-year return period and 1.46m mean sea level rise.....	72

Ljubljana, UL FGG, Masters of Science Thesis in Flood Risk Management.

Figure 56: Damage per (a) building and (b) curve for a 1000-year return period and 1.46m mean sea level rise .....	73
Figure 57: Shares of flood damages by sectors (cultural heritage sector in blue) for façade 10-year; (d) 100-year; and (f) 1000-year recurrence intervals at varying SLR scenarios (Alivio, 2020) .....	74
Figure 58: Damage-probability curves for Piran according to different SLR scenarios (Alivio, 2020)	74
Figure 59: Comparison between depth-damage curves for cultural heritage: Alivio (2020) – blue, FD12 – red, and FD13+FD14 – green.....	75
Figure 60: Expected Annual Damage (General and Cultural Heritage) in Piran according to different mean SLR scenarios (Alivio, 2020) .....	77
Figure 61: Condition of buildings after the impact caused by the sea flood in November 2019 (0.4m flood depth): (a) Obzidina ulica 2; (b) Tartini Square 2; .....	78
Figure 62: Yearly evolution of the number of salt crystallization cycles.....	80
Figure 63: Workflow of the proposed flood vulnerability modeling approach for .....	81
Figure 64: Susceptibility index per building type (Figueiredo R. et al., 2021).....	82
Figure 65: Structural measures proposed to Piran – (1) Gate: (a) section view, (b) top view .....	86
Figure 66: Structural measures proposed to Piran – (2a) Park – top-side view .....	87
Figure 67: Structural measures proposed to Piran – (2b) Park–section C-C.....	87
Figure 68: Structural measures proposed to Piran – (3a) Promenade – top view .....	88
Figure 69: Structural measures proposed to Piran – (3b) Promenade – section A.....	88
Figure 70: Structural measures proposed to Piran – (4a) Wall–top view.....	89
Figure 71: Structural measures proposed to Piran – (4b) Wall–section B-B .....	89

**LIST OF TABLES**

Table 1: Causes of climate change effects, results, materials affected, and proposed level of urgency for acting, with comments on relevance to the case study (Carroll and Aarrevaara, 2018). .....	9
Table 2: The table of risk assessment for the main deterioration variables (Loli and Bertolin, 2018)..	12
Table 3: Flood risk matrix (Davis et al., 2023). .....	18
Table 4: Datasets used in the study .....	38
Table 5: Extreme sea level elevations for various return periods using GEV and Gumbel distribution models (Alivio, 2020).....	39
Table 6: Sea level rise scenarios (Alivio, 2020).....	39
Table 7: Sensitivity and Exposure parameters with their class and rating .....	41
Table 8: Ranking of the most vulnerable buildings.....	42
Table 9: CCVI indicators for the city of Piran .....	50
Table 10: Explanation of the 2 simulations executed in KR PAN .....	53
Table 11: Flood risk matrix – present work. H is water height in m. ....	55
Table 12: Cost of damage to cultural heritage (Alivio, 2020).....	74
Table 13: Comparison between costs of damage to cultural heritage in Alivio (2020) and the present work.....	75
Table 14: Comparison between EAD to cultural heritage in Alivio (2020) and the present work.....	76
Table 15: Comparison between renovation interventions costs for exceptional and ordinary buildings (Institute for the Protection of the Cultural Heritage of Slovenia, 2020). .....	78
Table 16: Comparison between damage and renovation costs for the buildings analyzed in the Ministry of Culture report (Institute for the Protection of the Cultural Heritage of Slovenia, 2020). .....	79
Table 17: Scale of susceptibility indices (Figueiredo R. et al., 2021). ....	82
Table 18: Three-level scale to score the value of each component (Figueiredo R. et al., 2021). ....	83
Table 19: Average level of flood risk for depth damage curve and adjustment factors (Davis et al., 2023).....	84

## **ABBREVIATIONS AND SYMBOLS**

ARSO	Agencija Republike Slovenije za Okolje
CCI	Cultural and Creative Industries
DEM	Digital Elevation Model
EAD	Expected Annual Damage
FVI	Flood Vulnerability Index
GIS	Geographic Information System
GDP	Gross Domestic Product
IPCC	Intergovernmental Panel on Climate Change
KRPAN	Kumulativni Računi Poplavnih škod in Analize
LiDAR	Light Detection and Ranging
OECD	Organisation for Economic Co-operation and Development
RCP	Representative Concentration Pathway
RMSE	Root Mean Square Error
SLR	Sea Level Rise
UL	University of Ljubljana
WHS	World Heritage Site



# 1 INTRODUCTION

## 1.1 Context

Historically, the first settlements were established by the water, either a river or the sea. This location choice is associated with the several benefits derived from water availability such as drinking water, transportation, irrigation, fisheries, etc. The importance of those areas increased their value and encouraged migration to those areas, which became gradually more subjected to human impact.

The human impact was translated in many ways and one of them was the construction of buildings, squares, and monuments that were testimony to unique and exceptional cultural traditions or human interactions between civilizations (UNESCO, 2018). These constructions are now considered cultural heritage sites, and not only do they have economic value, associated with their construction material and tourist attractiveness, but also an intangible one, related to the identification of the population to those specific sites and how they reflect a society's way of living and evolving. Nevertheless, the anthropogenic effect is harmful in many aspects, such as wildlife survival and air quality. This effect is particularly detrimental to flood risk, as it translates into soil impermeabilization and construction in naturally flooded areas, increasing the risk of inundation in densely populated regions.

The high exposure of coastal areas also amplifies their flood risk, especially in low-lying regions. Their sensitive condition is expected to become even more critical as climate change and its consequent global warming increase the sea level, raising the risk to the population, the infrastructure and services they depend on, the environment, and commercial activities.

According to Oppenheimer et al. (2019), the increase in sea level rise incurs the exponential augmentation of flood risk. Even the most optimistic scenarios of sea level rise, as RCP 2.6 (associated with an increase in water depth from 30 to 80 cm), are expected to cause the amplification of the severity and frequency of floods from 100 years return period to yearly in coastal areas until the middle of the 21st century (Nicholls et al., 2008; Nicholls and Cazenave, 2010; Oppenheimer et al., 2019; Alivio, 2020). This higher frequency of floods can magnify the exfoliation, powdering, detachment, worsening of crack formation, and deformation of cultural heritage sites in coastal cities (Sesana et al., 2019).

The augmentation of the risk of floods in coastal areas reaffirms the necessity of formulating comprehensive flood risk management plans that include hazard, exposure, and vulnerability analysis for those areas. Hazard assessments aim to predict the probability of extreme events in the future and reduce their impact through the probabilistic and statistical analysis of past data and studies. Flood hazard is expressed by the number of years within which a flood with a certain intensity (e.g. depth or velocity) is expected to reoccur (also known as the return period) (Wang, 2015; Foudi et al., 2015; Foudi & Osés-Eraso, 2014).

Regarding exposure, its assessment is based on the spatial distribution of flood prone-areas and the presence of threatened assets in the area. In addition, vulnerability is associated with the inherent characteristics of an element and how it affects its susceptibility to forces and impacts and its value when affected by extreme events (Wang, 2015; Foudi et al., 2015; Foudi & Osés-Eraso, 2014).

To obtain reliable flood hazard estimates, it is important to have access to detailed and accurate topographic data. Digital Elevation Models or DEMs are the main source of topographic data, and, for that reason, their spatial resolution must be as high as possible (Casas et al., 2010). One method that allows the acquisition of accurate DEMs is Light Detection and Ranging (LiDAR), which generates 3D

data of Earth's surface characteristics and shape elevation through airborne laser scanning technology (NOAA Coastal Services Center, 2018; Alivio, 2020; Webster et al., 2006). The data obtained with LiDAR could be further used in 1D-2D hydrological models and flood prediction models (Ernst, 2010; Erpicum et al., 2010).

In the interest of assessing exposure, it is fundamental to properly delimitate the flood-prone area. This area is determined by the flood characteristics (water level, volume of water, depth of water, flow velocity, etc.), the topography of the area, and hydrologic connectivity. Hydrologic connectivity is defined as the condition by which different regions on the hillslope are connected via water flow. In this way, the consideration of this condition in flood assessments is crucial to guarantee that flooded areas are directly linked to the source of flooding (Stieglitz et al., 2003; Gesch, 2018; Alivio, 2020).

Poulter and Halpin (2008) present two options of rules that can be implemented in hydrologic connectivity models: four-side and eight-side connectivity. In case the four-side connectivity rule is applied, a cell is inundated if one to four cells in the cardinal directions are flooded or directly connected to water bodies. On the other hand, the eight-side connectivity rule considers the cells evaluated by the four-side and, additionally, whether the diagonal neighborhoods are flooded or directly connected to the source of flooding. Generally, the four-side rule underestimates flood impacts while the eight-side one overestimates them. However, as the eight-side rule is the more conservative one, it is usually the one employed for elevation-based sea level rise damage assessments (Breilh et al., 2013; Fereshtehpour and Karamouz, 2018; Li et al., 2009; Poulter and Halpin, 2008; Yunus et al., 2016; Alivio, 2020).

Vulnerability assessments are closely related to the estimation of flood damage since the damage is a consequence of the impact of a certain hazard in an element according to its characteristics. Damage can be categorized according to whether it is a result of direct contact with water (direct or indirect) and the possibility of estimating it in financial terms (tangible or intangible) (Messner et al., 2007).

The loss due to floods can be assessed qualitatively or quantitatively, depending on data availability and the nature of the loss. Quantitative loss models are especially useful, as they can enable improved decision-making through cost-benefit analysis, which can further guide flood mitigation, relief, and recovery plans, and help establish priority areas of action (Kang et al., 2005; Middelman-Fernandes, 2010; Alivio, 2020).

Flood damage assessments are mainly executed with the aid of post-flood surveys or loss functions. Loss functions tend to be the chosen method by the scientific community due to the difficulties associated with the conduction of a comprehensive post-flood survey, as the collected information varies according to the perception of the interviewers and interviewees and its elevated cost (Herath, 2003; Smith, 1994; Alivio, 2020).

Flood damage functions describe the extent of damage in a particular element depending on flood parameters such as depth, velocity, duration, sediment concentration, and level of water contamination (Merz et al., 2010). Among these parameters, depth is considered to be the most relevant for quantitative assessments based on monetary terms. Consequently, depth-damage curves are the most frequently applied flood damage function. This is chiefly due to the large availability of depth data when compared to the other parameters and the lack of understanding of the coupling between the other factors (Burnham and Davis, 1997; Dutta et al., 2003; Merz et al., 2007; Smith, 1994; Schröter et al., 2014; Alivio, 2020).

To create damage functions, two methods can be selected, empirical and synthetic, according to the availability of data. The empirical approach is based on historical flood data, namely the real losses from a flood event. Conversely, the synthetic approach is hypothetical. It estimates flood damage

according to expert knowledge, land use/cover information, and the composition of the elements for which damage must be calculated. The bias embedded in the empirical approach combined with its lack of adaptability and large data requirement results in a larger use of the synthetic method. Nevertheless, ideally, the two methods would be coupled, through the adjustment of the synthetic approach with historical data (Merz et al., 2010; Gerl et al., 2016; Dutta et al., 2003; Pistrika et al., 2014; Middelmann-Fernades, 2010; Merz et al., 2004; Smith, 1994; Alivio, 2020).

In addition, damage functions can further be classified as absolute or relative. Absolute functions assess damage according to the value of the unit area of a given built asset, that can be adequate for commercial and industrial properties. Consequently, as this value changes, the functions must be adapted. On the other hand, relative functions calculate damage proportionally to the affected percentage of the element, only requiring the total value of the item (Messner et al., 2007; Gerl et al., 2016; Pistrika et al., 2014; Olesen et al., 2017; Alivio, 2020).

In the present work, the expected damage will be calculated with the use of synthetic depth-damage curves and empirical data included in the KR PAN methodology. KR PAN is the Cumulative Calculation of Flood Damage and Analyses model created by Vidmar et al. (2019) for the Slovenia territory that is used to estimate the tangible monetary consequences of floods on buildings, businesses, building contents, infrastructure, cultural heritage, and watercourses, also considering vehicles and cleaning costs. To develop this model, depth-damage curves adapted from FEMA (2014) and historical data from flood events archived in AJDA (the Slovenian web application for damage assessment on agricultural products and property) were combined. KR PAN's goal is to assist decision-making related to flood mitigation measures, as it calculates the economic benefits of possible interventions.

## 1.2 Motivation

Floods pose significant risks to individuals, residential buildings, socio-economic activities, infrastructure, cultural heritage, and the environment, having directly affected approximately 1.81 billion people, or 23% of the world population in 2022. This risk is substantially higher in low- and middle-income countries (where 89% of the affected individuals were located) and in coastal areas (World Bank Blogs, 2022).

In the selected area for this study, the coastal city of Piran, Slovenia, flood is a major concern due to its geographical location and the combined influence of winds, astronomical tides, and heavy rain, characteristic of the Adriatic Sea. A recent devastating event occurred in the area was the flood of November 2019, when the low-lying parts of cities along the Slovenian coast (Piran, Izola, and Koper) were inundated overnight due to the coupling of intense rainfall, a cyclone, southerly wind, and a full moon which resulted in an abnormally high tide (STA, 2019). According to unofficial information, the sea level reached the second-highest point in the last 50 years.

Flood risk is expected to become even higher due to climate change and its consequent sea level rise. The predicted sea level rise in the area would not only heighten flood depth but also increase the frequency of high return periods floods. Floods with a 100-year return period are predicted to occur yearly, for example (Nicholls et al., 2008; Nicholls and Cazenave, 2010; Oppenheimer et al., 2019; Alivio, 2020). Piran has no structural measures in place to help protect it from the impact of storm surges with such small intervals between one another.

Cultural heritage sites are among the most vulnerable assets in Piran due to the city's ancient history. Piran was incorporated into the Roman Empire in 178 and 177 BC and after that was ruled by

the Byzantines, Frankish and Istria, German Empire, and Venetians, among others (Archive.org, 2019; Expoaus.org, 2015). These rulers left marks of their culture and traditions in the city of Piran in the form of fortresses, churches, statues, and imposing buildings. As flood risk increases and these elements get older and under a higher stage of deterioration, the need to create specific strategies to protect them becomes more pressing.

To support decision-making associated with flood management in Slovenia, the KR PAN methodology was developed by Vidmar et al. (2019). The methodology enables the calculation of the monetary consequences of floods in many sectors, including cultural heritage. Nevertheless, the depth-damage curves included in this model are very general and do not contemplate the particularities of cultural heritage elements.

The motivation of the present work is to create a more reliable quantitative method for assessing flood damage in cultural heritage sites that could be subsequently used to assist decision-making regarding the protection and preservation of these sites. The increase in reliability of flood damage assessments to cultural heritage sites will be a result of research on the deterioration of cultural heritage sites when submitted to floods and climate change, according to the material they are composed of and their building techniques. In this way, decision-making will also be assisted with the comparison of restoration costs with the improved estimates of damage costs by considering specific depth-damage curves for cultural heritage sites.

### 1.3 Objectives

The main objective of this work is to assess the impact of coastal flooding and its future damage caused by sea level rise on cultural heritage sites located in the coastal city of Piran, Slovenia. This objective can be broken down into the following goals:

- a) Evaluate the exposure and vulnerability of cultural heritage sites at flood risk, under different sea level rise scenarios;
- b) Qualitatively assess flood risk to cultural heritage;
- c) Apply specific depth-damage curves adapted to cultural heritage sites (considering building characteristics);
- d) Calculate the direct flood damage cost brought upon cultural heritage sites for different return period events and foreseen sea level rise scenarios.

### 1.4 Research questions

This work aims to answer the following research questions:

- a) How do floods affect the deterioration of cultural heritage depending on their material and building typology?
- b) Which cultural heritage sites would be most affected by sea floods in case of extreme sea level rise scenarios?
- c) What are the direct costs caused by the damage to cultural heritage sites and how will the cost change in view of the future SLR?

## **1.5 Innovation and Practical Value**

The novelty of this study lies in the specific attention given to the quantitative damage in cultural sites. The fact that Slovenia has a quantitative flood damage assessment method that includes cultural heritage is, by itself, an exception, since the evaluation of the impact in this type of site tends to be an afterthought when flood risk is assessed. The exclusion of cultural heritage from flood risk assessments is usually associated with the intangible and highly qualitative nature of its value, associated with community identity, culture, and traditions. Nevertheless, it is possible and extremely relevant to consider at least the tangible damage to cultural heritage in monetary terms also for planning the flood risk reduction measures for such sites.

Even though KR PAN, a Cumulative Calculation of Flood Damage and Analyses model, created to assess the benefits of structural and non-structural flood reduction measures in Slovenia, considers cultural heritage as part of the direct damage assessment, it must be highlighted that the damage to these sites is calculated according to general depth-damage curves adapted from FEMA (2014). This document only presents depth-damage curves for 5 categories: buildings, transportation, utility facilities, agriculture products, and vehicles. This way, the depth-damage curve used to calculate the loss of cultural heritage is rough, not being able to properly portray the damage for different types of structures.

In this context, this study will deliver particular depth-damage curves adapted for different groups of buildings and sites (depending on their typology and the material they are made of) in the city of Piran, Slovenia. The discretization of depth-damage curves will allow the obtention of more precise economic loss results that can better direct government interventions to protect cultural heritage (through the prioritization of the buildings with higher damage potential). These alterations can also assist the damage assessment of cultural heritage sites in other coastal areas, especially in the Adriatic Sea and the Mediterranean area.

## 2 LITERATURE REVIEW

Flood risk assessment of cultural heritage sites is a recurrent theme in recent studies due to the recognition of the historical and societal (among others social, aesthetic, spiritual, recreational, and educational) significance of these assets and the understanding of the tendency of flood risk to considerably increase due to climate change. These studies follow different approaches and some of the examples are: the focus on the prediction of damage under extreme conditions, the assessment of the number of cultural heritage sites at risk under different flood scenarios, the implementation of an integrated vulnerability assessment (a mix of top-bottom and bottom-up approaches) of the consequences of climate change, the assessment of qualitative vulnerability and exposure according to UNESCO criteria, the incorporation of flood vulnerability indexes in the flood risk assessment, among others. Some of these studies will be further described in the following sections.

Alivio (2020) has developed a general flood risk assessment in Piran, Slovenia which will help orientate the current study. Alivio's (2020) work aimed to evaluate the potential flood damage to the population, built-up structures, public infrastructures, and cultural heritage under different sea level rise scenarios and estimate the future return periods of these extreme events in view of climate change. To predict the influence of sea level rise on the frequency of severe flood events, a statistical analysis was conducted, and sea level rise scenarios were established. Regarding damage assessment, first, a bathtub model was created to determine the flood extent and depth and then, this information was used as inputs to the depth-damage curves predetermined by the KR PAN model. In this way, the cost of flood loss for the chosen flood scenarios, and the total expected annual flood damage (EAD) in the area was computed (Figure 1) (Alivio, 2020).

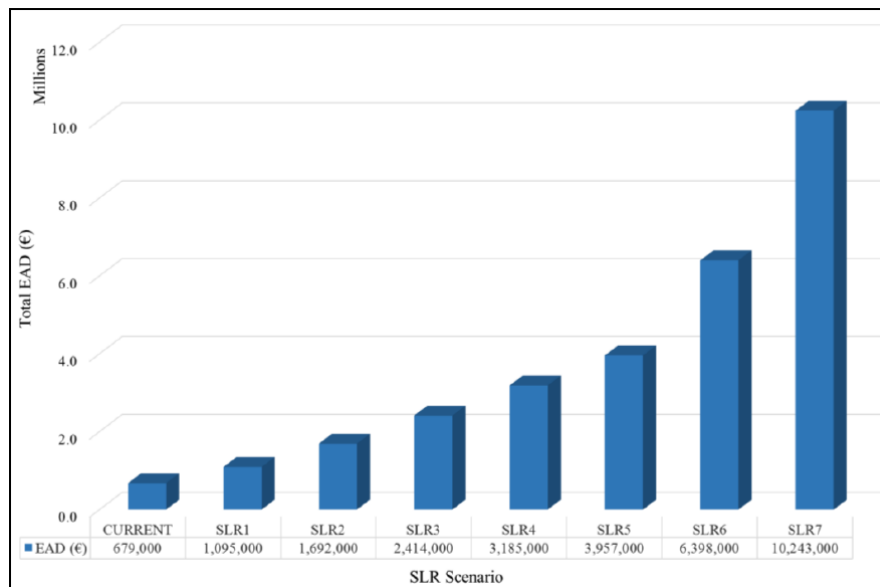


Figure 1: Total Expected Annual Flood Damage in Piran for different SLR scenarios (Alivio, 2020)

The importance of salt presence in sea floods that frequently affect the cultural heritage in Piran is clear. In this way, even though the impact of salt weathering due to sea floods on cultural heritage was not assessed in detail in the present work, a literature review was conducted on the topic. The most relevant parameters to be analyzed, the impact of climate change, and the most common consequences of salt deterioration were presented.

## 2.1 Impact of Climate Change on Cultural Heritage

Sesana et al (2019) presented an integrated approach (a mix of a top-bottom approach, a framework in which the government makes a decision and the population is informed about it, and a bottom-up one, which includes public participation) for the vulnerability assessment of World Heritage Sites (WHS) under the impact of climate change. This approach consists, initially, of the attribution of values to cultural heritage sites, according to the quantity of UNESCO WHS criteria it fulfills. Subsequently, an assessment of the impact of climate change on cultural heritage is executed. This impact is evaluated according to the exposure (climate conditions that can bring adverse consequences), sensitivity (level of susceptibility to the exposure), and adaptability capacity of the site (ability of the site to cope with the sensitivities related to climate change) (Sesana et al, 2019).

This research defined the main conditions that impact adaptability capacity: technical resources, information and awareness, leadership, economic resources, management capacities, communication and collaboration, human resources, learning capacity, and governance. The bottom-up character of the study lies in the inclusion of semi-structured interviews with academics and experts in the management and conservation of cultural heritage, managers, and coordinators of WHS through which they could share their expertise concerning the sensitivity and adaptation capacity of the sites (Sesana et al, 2019).

Concerning the impacts of sea level rise on coastal flood risk and erosion, Reimann et al (2018) worked on the determination of tipping points at which cultural heritage sites would be exposed to non-acceptable risks (Figure 2). To help determine those tipping points, flood risk, and erosion indexes were created. The flood risk index was a function of the flooded area and flood depth while the erosion index depended on the distance from the shore to the site, the granulometry of the coastal material, the wave height, and the rate of sediment supply brought by the waves. Figure 2 represents with red points and labels with the cultural heritage ID the point at which the asset is considered to be under a flood risk or erosion risk higher than acceptable (that would be a flood risk index of more than 6.5 or an erosion risk index of more than 7.5) (Reimann et al, 2018).

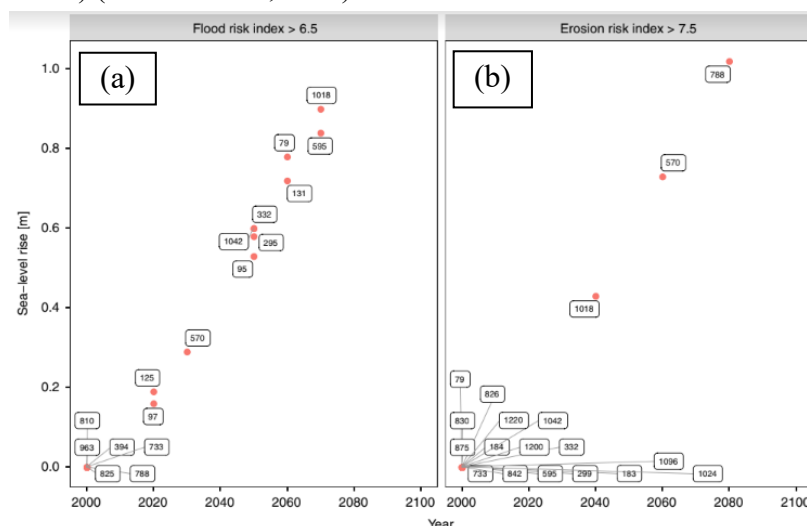


Figure 2: Potential adaptation tipping points for the flood risk index and the erosion risk index (Reimann et al, 2018)

Bertolin (2019) was responsible for the special issue “Preservation of Cultural Heritage and Resources Threatened by Climate Change” of the *Geosciences Journal*. This document aimed to unify knowledge on the conservation of cultural heritage to better predict the behavior of the materials that



Figure 3: Conversion functions for specific materials or object type (upper part) and the weight attributed to a key risk indicator (KRI) (lower part)

Further on, KRIs would be weighted, taking into account the importance of the KRI per material and the sensitivity of the material. The IAQ index would be the result of  $1 - R_{max}$ , being  $R_{max}$  the maximum result of the multiplication of  $R_i$  (risk) by  $W_i$  (weight) for each one of the markers. Finally, the obtained indexes were later used to support the development of mitigation actions in a church located in Belgium (Anaf et al, 2018).

Carroll and Aarrevaara’s (2018) paper aimed to review the potential future risk factors to cultural heritage, especially in Nordic countries, to better direct efforts to adapt and/or mitigate the impacts of climate change (helping define which buildings to prioritize). To attain that, they classified the materials and structures that are expected to be the most affected by climate change according to a numeric scale ranging from 1 to 10, with being 1 the class in which a mild or minor impact would be observed in the long-term and 10 the class where a major short- to mid-term effect would be perceived.

According to the literature review performed by Carroll and Aarrevaara’s (2018), there are 9 categories of impacts on cultural heritage resultant of climate change: physical damage; soil instability; likelihood of soil moisture changes; changes in hydrology; alteration in humidity cycles; modification in vegetation; migration of damaging pests; climatic zone movements impacting cultural landscapes; and changing economic and social patterns of settlements. For Carroll and Aarrevaara’s (2018) work, these categories were summarized in Table 1, where only 5 categories of climate change impacts are presented, along with their units, result or effect, materials or structures affected, their rating, and an example of its occurrence in the case study presented in the paper (a Finnish farmhouse complex consisting of several buildings).

Table 1: Causes of climate change effects, results, materials affected, and proposed level of urgency for acting, with comments on relevance to the case study (Carroll and Aarrevaara, 2018)

Climate Change Category	Measure or scale	Result/Effect	Materials/ Structures Affected	Proposed Urgency rating	Case Study: Application of the Criteria
Warmer Climate	Rise in °C/year	Freeze-thaw damage	Stone Brick	3	Partly visible in stone constructions (cow house), although the structure is also affected by the current use and site conditions
		Rust	Metal	5	Limited use in case study buildings. Non-painted roofs are suffering from rust
		New fauna–pests	Wood Brick	5	Clearly visible increased effect, especially in wooden facades, but also brick facades.
Longer Growing Season	Days/year	New/increased flora, algae, moss, root damage	Wood Brick Stone	5	Clearly visible increased effect, especially in wooden facades, but also, cement surfaces like staircases and foundations (moss).
Increased Precipitation: rain or snow	mm/year	Humidity	Wood Brick Structures	10	Clearly visible effect in all facades, especially in northern and shaded facades and wooden building parts.
		Increased loads (snow)	Wood Brick Roof/Roof Structures (Typically Wood)	5 - 10	Depending on the roof material and declination; the lower the declination, the higher the risk of damage due to the increased load.

		Soil and material degradation	Foundations Base Floor	5	Depending on the roof material and declination; the lower the declination, the higher the risk of damage due to the increased load.
		Flooding (from any increased precipitation effect)	Wood Brick Structures	10	The highest risk with the buildings situated on the slopes of the site (surface runoff gathering).
Severe rain incidents	mm/hour	Erosion	Wood Brick Stone	5	The highest risk is with the buildings situated on slopes of the site (possible soil erosion).
Extreme Winds	m/s	Damage to structures through falling trees or wind causing damage to the roof	Metal Roofs Wood & Brick Structures	5-10	High steel roofs facing the dominating wind direction are subject to the largest threat of damage from extreme winds (residential buildings, cow houses high roof).

Regarding climate change impact assessments, Haugen et al. (2018) proposed a methodology for long-term monitoring of climate change's effects on cultural heritage. The framework would assist the planning and organization of a monitoring program in order to support decision-making taking climate change into account. The estimated duration of the monitoring campaign is from 30 to 50 years, comprising a zero-level registration and an interval-based registration system in order to catch climate change effects as soon as possible.

According to Haugen et al. (2018), when designing monitoring programs, it is crucial to have a monitoring context based on a solid overview of current and future climate; and on social, economic, and environmental exposure, sensitivity, and vulnerability to climate change. As expected, the indicators required and organizations responsible for the monitoring must be defined. Additionally, financial and legal support must be guaranteed (Haugen et al., 2018).

Concerning the procedures, it is essential to ensure clarity and structure in the description of information requirements, the monitoring objectives and procedures (such as data collection and reporting), and stakeholder participation. In addition, the concept of adaptive monitoring should be integrated into the campaign (Haugen et al., 2018).

Besides assisting in the creation of a monitoring program, the research points out some of the general challenges this type of initiative could face and possible solutions. The challenges comprise the collection of useful information; the assurance of the quality, communicative value, and efficiency of the indicators; the credibility of the information; and the feasibility of the monitoring program (Haugen et al., 2018).

The work presents a step-to-step manual of how to develop the monitoring campaign and, additionally, introduces the possibility of incorporating the long-term monitoring campaign in a Cultural Heritage Integrated Management Plan (CHIMP) through monitoring reports, as described in Figure 4 below (Haugen et al., 2018).

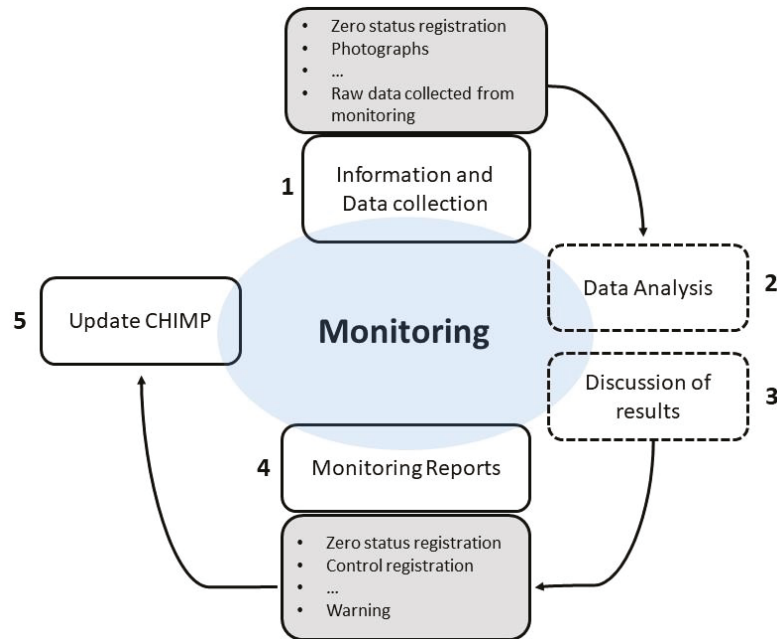


Figure 4: Incorporation of a long-term monitoring program in a Cultural Heritage Integrated Management Plan (CHIMP) (Haugen et al., 2018)

Concerning cultural heritage intervention restrictions and climate change risks, Loli and Bertolin (2018)'s article associates climate-induced decay variables (relative humidity and temperature) for various construction materials located inside cultural heritage buildings with the historic assets' adaptation capacity related to their protection status. The general method developed in this research determines the deterioration degree for varied building materials, sizes, and locations.

The previously mentioned decay-linked variables were simulated in the Climate for Culture (CfC) project, which assessed the possible climate change effects on indoor and outdoor European cultural heritage and presented that information in high-resolution risk maps. The CfC project identified mechanical, chemical, and biological deterioration mechanisms for wood, masonry, and concrete buildings. The main variables selected to estimate the indoor deterioration in wooden buildings were the moisture content of the panel, the joined and the cylindrical element (mechanical), the lifetime multiplier (chemical), and the presence of mold and insects (biological). In the case of masonry and concrete buildings, the mechanical variables are salt crystallization cycles, thenardite-mirabite cycles, freeze-thaw cycles, and frosting time. The chemical and biological mechanisms are the same as in wooden buildings, excluding the presence of insects (Loli and Bertolin, 2018).

To assess risk, initially, weights are assigned to all decay variables according to the threshold presented in Table 2. Subsequently, the risk is assessed for each deterioration mechanism (in case various decay variables are relevant for a mechanism, the one that presents the highest weight or risk level is chosen). Finally, to obtain the total degree of deterioration of the construction, the highest level of risk between the 3 mechanisms is chosen (Loli and Bertolin, 2018).

Table 2: The table of risk assessment for the main deterioration variables (Loli and Bertolin, 2018)

Variable Name	Unit	Very Low	Low	Medium	Medium-High	High	Very High
Panel—base material	[-]	0.333	0.667	1	1.333	1.667	2
Panel—pictorial layer	[-]	0.333	0.667	1	1.333	1.667	2
Jointed element	[-]	0.333	0.667	1	1.333	1.667	2
Cylindrical element	[-]	0.333	0.667	1	1.333	1.667	2
Salt crystallisation cycles	[no/year]	30	60	90	120	150	180
Thenardite-Mirabilite cycles	[no/year]	30	60	90	120	150	180
Freeze-thaw cycles	[no/year]	15	30	45	60	75	90
Frosting time	[h/year]	1200	2400	3600	4800	6000	7200
Lifetime multiplier—Wood	[-]	1.5	1.25	1	0.75	0.5	0.25
Lifetime multiplier—Masonry	[-]	1.5	1.25	1	0.75	0.5	0.25
Lifetime multiplier—Concrete	[-]	1.5	1.25	1	0.75	0.5	0.25
Mould growth	[mm/year]	25	50	125	200	400	600
Insects—humidity dependent	[DD/year]	500	1000	1500	2000	2500	3000
Insects—temp. dependent	[DD/year]	500	1000	1500	2000	2500	3000

To better plan the degree and urgency of interventions that would reduce or mitigate climate change effects, the obtained level of risk was intersected with the level of adaptation allowed in the building. The visual aspect of that intersection is a qualitative matrix (Figure 5) in which 3 different color codes define the emergency of the intervention (Loli and Bertolin, 2018).

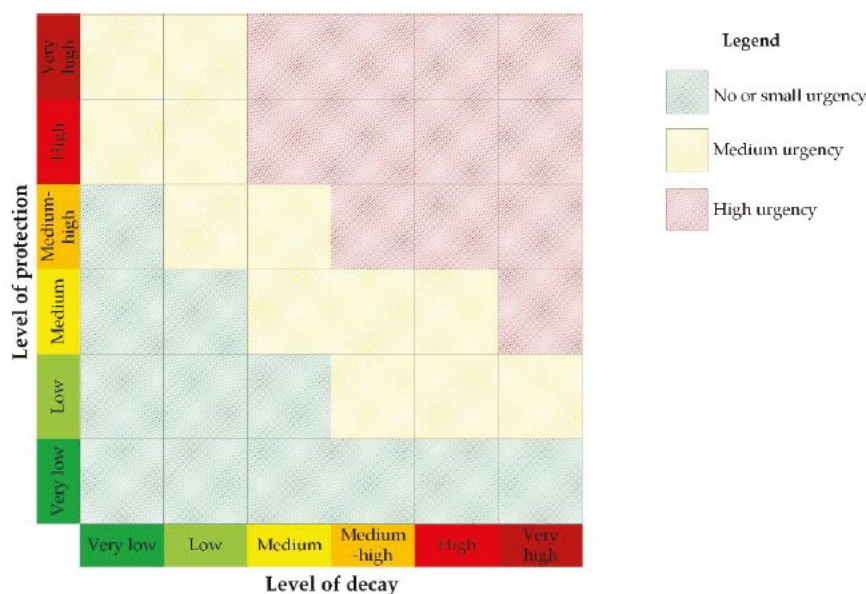


Figure 5: Qualitative matrix of the urgency of the intervention (Loli and Bertolin, 2018)

Focusing on climate change impact in indoor environments, Melin et al. (2018) conducted simulations of moisture gradients in wood elements present in historic buildings that are subjected to climate-induced damage, caused by changes in temperature and relative humidity. This paper compared data on relative humidity and temperature collected in a previous work, where these two parameters were monitored at different depths of wooden samples, with results from two methods that predict the influence of climate change. The two models chosen were the simplified model and the hygrothermal building simulation software WUFI. The research concluded that the two simulation methods display excellent compliance with the monitored data and that the maximum and minimum values of relative humidity would change according to the scenario and building chosen for the simulation (Melin et al., 2018).

Supporting a participatory approach, Sesana et al.'s (2018) paper aimed to understand climate change adaptation perspectives from cultural heritage experts. With that goal, the study included the

identification of obstacles to and prerequisites, opportunities, and determinant factors for the climate adaptation of immovable and tangible cultural heritage. An additional objective of the research was to find examples of best practice strategies and methodologies to prepare heritage sites for climate change.

In order to obtain the previously mentioned information, 45 semi-structured interviews were conducted with experts (academics and researchers, governmental institutions, and cultural heritage professionals) from countries in Europe and the UK and workshops were organized with different stakeholders. The main topics the interviewees were questioned about were their belief in the possibility of adaptation of cultural heritage to climate change; their knowledge of examples of management methodologies that could prevent or mitigate the damage caused by climate change; their awareness of best practice examples of climate adaptation of heritage assets; and their vision on which considerations should be made when adapting cultural heritage to climate change (Sesana et al., 2018).

Regarding the study results, most participants showed confidence in the possibility of adapting cultural heritage to future impacts of climate change and were unaware of climate adaptation strategies for cultural heritage. Some of the managerial and decisional best practices identified in the research were the enhancement of monitoring and maintenance; the promotion of participatory planning and engagement with stakeholders such as owners, citizens, and tourists; the reinforcement of regulations and guidelines; the encouragement of a research boost; the spread of knowledge; and the increase in funding for climate adaptation of cultural heritage. Additionally, between the practical actions proposed were the construction of coastal defense structures, the amelioration of drainage systems, the implementation of interventions compatible with heritage sites, the intensification and digitalization of data collection on heritage sites, and the relocation of the sites when possible (Sesana et al., 2018).

## **2.2 Impact of Climate Change on Coastal Cities**

Focusing on the threat of climate change in coastal cities, Balica et al. (2012) created a Coastal City Flood Vulnerability Index (CCFVI) to identify the most vulnerable cities to coastal flooding now and in the future. This index was developed considering the exposure, susceptibility, and resilience of nine large urban cities in different regions of the globe to coastal flooding.

For Balica et al.'s (2012) study, the coastal vulnerability system was subdivided into three subsystems: natural (associated with a hydro-geological component), socio-economic (related to a socio-economic component), and institutional (linked to a politico-administrative component). Additionally, each subsystem is vulnerable to floods due to one or more of the 3 following factors: exposure, susceptibility, and resilience (Balica et al., 2012).

Those 3 subsystems interact with one another in a way that the natural subsystem is expected to cause and suffer impacts from the socio-economic one and the institutional component provides the infrastructure to support the natural one and creates mechanisms to enhance services and benefits to the socio-economic component (Figure 6) (Balica et al., 2012).

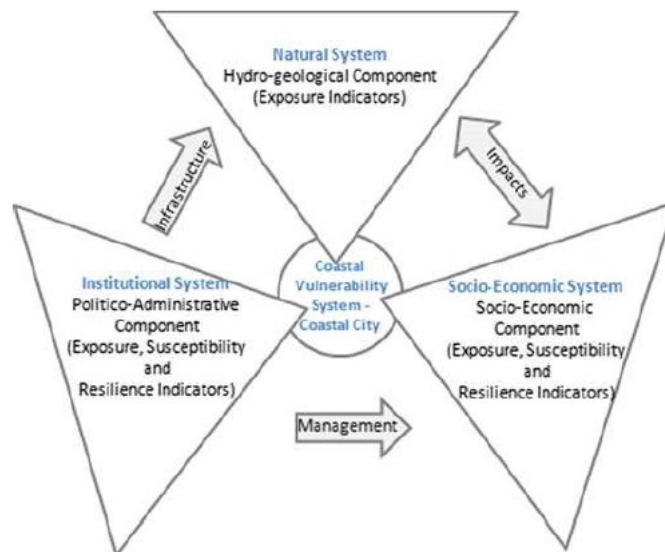


Figure 6: Interaction between coastal vulnerability subsystems (Balica et al., 2012)

The calculation of the vulnerability index was based on the use of indicators. Indicators would be characteristics that qualitatively describe the conditions of a system. For each one of the components, indicators with units and associated with the 3 vulnerability factors were defined. Some of the determined indicators were sea level rise, storm surge, and number of cyclones for the hydrological component; number of cultural heritage assets affected, number of people exposed, and growth population factor in the last 10 years for the socio-economic component; and the existence of flood hazard maps, the number of institutional organizations and the existence of flood protection measures for the politico-administrative component. To obtain Coastal City Flood Vulnerability Indexes (CCFVI) for each one of the components, equations were defined based on the contribution of each one of the chosen indicators. The total FVI (Balica et al., 2012) was calculated as follows:

$$\begin{aligned}
 & \text{Total FVI} = \text{Hydro - Geological} + \text{Social} + \text{Economic} + \text{Politico - administrative} \\
 \text{Total FVI: } & \left\{ (SLR, SS, \#Cyc, FS, RD, Soil, CL) + \left( \frac{CH, PCL, \%Disable}{S, \frac{A}{P}} \right) + \left( \frac{GCP}{RT, Drainage} \right) \right. \\
 & \left. + \left( \frac{FHM, UP}{IO, FP} \right) \right\}
 \end{aligned}$$

The research compared the CCFVI (normalized to values from 0 to 1) of 9 cities for each of the hydro-geological, social, economic, and political-administrative components and the overall index (sum of the individual components). The work allowed a general understanding of flood vulnerability in multiple cities and a way of analyzing measures that could reduce the impact of climate change (the one that affects the index as positively as possible) (Balica et al., 2012).

### 2.3 Flood Risk Assessment of Cultural Heritage Sites

Holický and Sýkora (2009) developed a work focused on the 2002 flood that severely affected the historic center of Prague, which incurred high levels of damage due to, according to the results of investigations, geotechnical aspects, inadequate structural properties, and insufficient communication. Their work proposed a framework of risk assessment that accounts for the specificities of cultural

heritage sites with the aid of Bayesian networks associated with statistical models which predict the extent and discharge of future floods. The Bayesian or casual network assists the risk analysis of exposed technical systems through the determination of chance, decision, utility nodes, and directional arrows, representing the causal links between the nodes. The statistical methods considered adequate to predict future floods in the area were Pearson III and lognormal distribution (Holický and Sýkora, 2009).

To execute a flood risk assessment in Taiwan, Wang (2015) created risk maps that portrayed the number of affected cultural heritage sites according to different rainfall intensity scenarios (200, 350, 450, and 600 mm). Once having assessed cultural heritage vulnerability, the study analyzed solutions for heritage preservation that considered sustainable management, climate change, and adaptation, as, for example, the possibility of artificially inundating areas near the cultural heritage sites to lower their damage (Wang, 2015).

To perform a qualitative flood risk assessment of cultural heritage, in-depth research was carried out by Dassanayake et al (2012). Extensive data on depth-damage and depth-velocity curves and damage matrices that differentiated buildings components (reinforced-concrete frames, structural steel columns, concrete-block walls, masonry bearing walls doors, windows, utilities, and finishes, etc.) and flood types (river floods, storm surges, and tsunamis) were collected. These data were combined to generate depth-velocity curves according to depth-velocity product thresholds. These curves allowed the attribution of levels of physical damage to cultural assets from very low to very high (Figure 7) (Dassanayake et al., 2012).

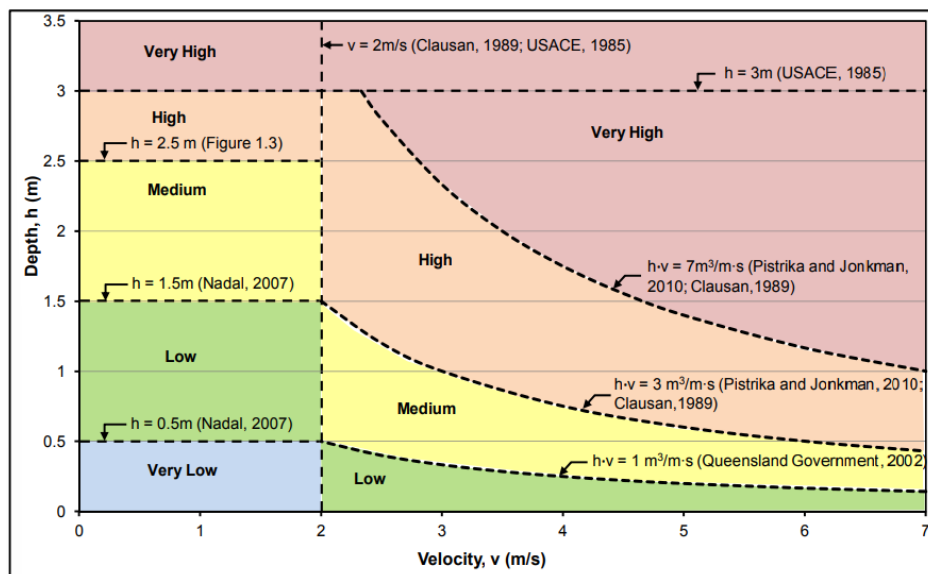


Figure 7: Level of physical damage in cultural assets related to flood depth and velocity (Dassanayake et al., 2012)

Another possibility of flood risk analysis, based on the qualitative assessment of potential damage of tangible UNESCO World Heritage (UNWH), was exposed by Arrighi (2021). Arrighi's (2021) work presented a risk matrix including hazard, exposure, and vulnerability. The vulnerability was determined according to the typology of the built asset, with hydraulic structures having the smallest value of vulnerability ( $V=1$ ) and cities having the highest ( $V=7$ ). Concerning exposure, cultural heritage sites were ranked on a scale from 1 to 6 according to the number of UNESCO selection criteria assigned by the committee (e.g. "an important interchange of human values on developments in architecture or technology, monumental arts, town-planning or landscape design" (UNESCO, 2018); "a unique or at

least exceptional testimony to a cultural tradition or to a civilization which is living, or which has disappeared”(UNESCO, 2018)) (UNESCO, 2018). In addition, hazard was divided into 5 classes associated to return periods from 10 to 500 years (Arrighi, 2021).

Concerning flood risk assessments in historical cities, Arrighi (2015) conducted research that considered the losses associated with structures, building contents, economic activities, and cultural heritage in Florence. The work gathered data from hydraulic simulations, historical reports of destructive floods, and cultural heritage recognition sheets to determine the spatial distribution of the cultural sites that would be lost in case risk mitigation measures were not implemented. The study presented which cultural works would be exposed to different flood return periods and the resultant level of risk they would be subjected to (from low to high) (Arrighi, 2015).

In order to further structure flood risk assessments in historic cities, Garrote et al. (2020) created a framework for analyzing flood risk in cultural heritage sites and elements in the Castile and León Region. The work comprised the analysis of 2155 cultural heritage assets scattered across an area of 94,226 km<sup>2</sup>. The research created a GIS database in which the flood extent for different return periods is superposed with the location of the heritage elements and a risk matrix that would allow the determination of flood risk levels according to the assets’ vulnerability and the hazard they are exposed to (Garrote et al., 2020).

For the determination of hazard, a flood hazard matrix was developed. The flood hazard level obtained in the matrix is a result of the intersection of flood frequencies of 10, 100, and 500-year return periods and severities that depend on whether the flood is considered normal or flash, on the time lag for precipitation to become runoff, and the area of the basin. The levels go from 1, corresponding to a low hazard level, to 6, linked to an extreme hazard level (Garrote et al., 2020).

Regarding flood vulnerability, flood vulnerability levels from 1 to 5, with being 5 the highest flood vulnerability level, were assigned to the assets’ building material, structure characteristics, and content. The vulnerability level also accounted for the building typology, such as civil, industrial, religious, or archeological. For each one of the elements (material, structure, and content), vulnerability values were assigned according to the susceptibility of the component to floods. For example, buildings made of earth with crypts and documents were the ones subjected to the highest vulnerability (Garrote et al., 2020). The total vulnerability level was a result of the following equation:

$$Total_{vulnerability} = 0.1 \times V_{material} + 0.2 \times V_{structure} + 0.7 \times V_{content}$$

A more general framework of flood risk assessment of cultural heritage that could be applied to different types of disasters, such as fires and earthquakes was developed by Romão et al. (2016). The framework consisted in a set of flowcharts that would help estimate flood risk according to the probability of the hazard, the vulnerability of the assets, the consequences of the hazard, the assets’ depreciation, and the recovery capacity of the element (Romão et al., 2016).

The study identified the following main challenges to executing comprehensive risk assessments of cultural heritage: the availability of trustworthy data to apply hazard models adequately and assess the current state of the threatened elements, the implementation of suitable vulnerability models, and of access to necessary human, time, and economic resources. Faced with these challenges, a general qualitative risk assessment shows itself as suitable for cases in which resources are limited and many assets must be analyzed (Romão et al., 2016).

The framework is composed of two flowcharts, one linked to cultural heritage vulnerability and the second one associated with disaster risk it is under. The vulnerability flowchart (Figure 8) took into

consideration the exposure of the asset, its level of damage, whether its damages are expected to be repairable, whether the function of the heritage can be easily restored, and whether its loss in value is relevant. The output of the first flow chart is a level of vulnerability from I to V, with V being the highest level of vulnerability. On the other hand, the disaster risk flowchart accounted for the likelihood of the hazard affecting cultural heritage elements to determine risk levels from I to V being the highest disaster risk. Disasters with a higher likelihood are expected to result in a smaller risk because it is assumed that their impact would be smaller than the one of events with a small frequency (Romão et al., 2016).

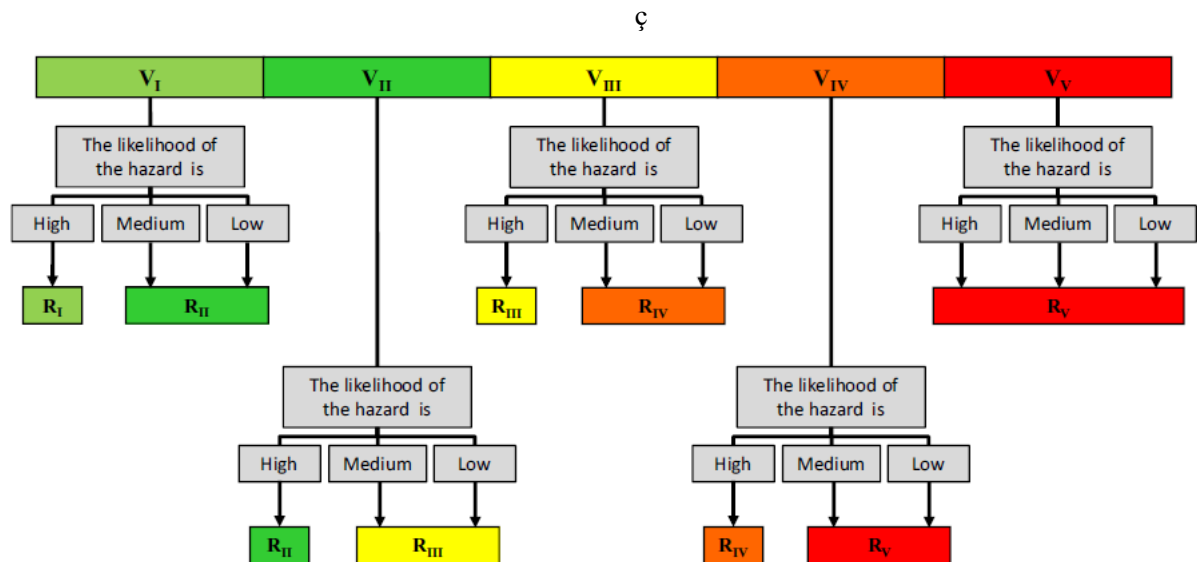


Figure 8: Proposed risk analysis methodology: assessment of the level of risk of the cultural heritage (CH) unit. (Romão et al., 2016)

A flood risk assessment was performed in the historic center of Tomar, Portugal by Davis et al. (2023) including vulnerability quantification, creation of depth-damage curves, and analysis of flood reduction actions. The work's objective was to disseminate knowledge regarding the creation of matrices that describe the physical vulnerability of buildings, the development of damage curves for specific hazard scenarios, and the evaluation of retrofitting interventions as flood adaptation measures (Davis et al., 2023).

To assess flood risk on the building scale, the research initially evaluated the buildings' vulnerability and then combined that information with hazard scenarios for 20 and 100-year return periods. Further, this paper evaluated flood reduction interventions with the aid of a cost-benefit analysis and adapted depth-damage curves (Davis et al., 2023).

To determine flood vulnerability, Davis et al. (2023) followed the index-based methodology presented by other studies, such as Miranda and Ferreira (2019) and Stephenson and D'Ayala (2014), both previously mentioned in this work in section 4.4 and used as a basis of the FVI calculated for Piran. Nevertheless, in the article, the FVI was calculated according to different parameters. Seven sensitivity components were selected: state of conservation, structural material, finishing material of the façade, type, and condition of window/door frames, opening at ground floor (presence of windows and large openings), existence of basements, and height of the door threshold. In addition, the 3 exposure components chosen were the type of use or activity (commercial, religious, etc.), surface condition (characteristic of the inclination of the ground), and heritage value. The classes and ranking chosen by

Davis et al. (2023) were similar to Stephenson and D'Ayala (2014), with 4 classes associated with values from 10 to 100.

Regarding hazard assessment, both flood depth and velocity were taken into consideration. Their values were acquired, evaluated, and processed with the aid of hydrologic and hydraulic models from the Portuguese Environmental Agency and the contribution of the Institute of Geography and Spatial Planning at the University of Lisbon (Brandao et al., 2014). The hydrologic assessment comprised a probabilistic and statistical approach and a physically-based model that described the rainfall-runoff relationship. Whereas, for the hydraulic component, 2D hydraulic MOHID land and water models were utilized (Davis et al., 2023).

After obtaining flood vulnerability and hazard values, Davis et al. (2023) determined flood risk according to the flood risk matrix below (Table 3: Flood risk matrix (Davis et al., 2023)Table 3):

Table 3: Flood risk matrix (Davis et al., 2023)

		Hazard level [FHI= Depth (velocity+ 0.5)]				
		Negligible	Low	Moderate	High	Extreme
Flood risk		[H ≤ 0.5]	[0.75 < H ≤ 1.25]	[1.25 < H ≤ 2.5]	[2.5 < H ≤ 7.0]	[H > 7.0]
Vulnerability level	Extreme [ > Mean + SD]	Moderate	High	Extreme	Extreme	Extreme
	High [Mean to (Mean+SD)]	Low	Moderate	High	Extreme	Extreme
	Moderate [(Mean- SD) to Mean]	Low	Low	Moderate	High	Extreme
	Low [ < Mean - SD]	Negligible	Low	Low	Moderate	High

Note: The greens, yellow and reds are used to illustrate the different risk levels.

## 2.4 Impact of Salt on Cultural Heritage

Ciantelli et al.'s (2018) work aims to assess the impact of climate change on UNESCO cultural heritage sites in coastal areas in Panama. Initially, the buildings' main construction materials were identified and the meteorological conditions in the region surrounding the sites were analyzed (such as near-surface air temperature, relative humidity, and precipitation). Subsequently, historical and future simulations were executed in EC-Earth and the obtained results were analyzed, run, and utilized with damage functions to project the future deterioration (surface recession, biomass accumulation, and results of salt crystallization cycles) of the cultural heritage sites in question.

To characterize the construction materials, the following mineralogical-petrographic, physical, and chemical analyses were conducted: stereomicroscope observations, polarized light microscopy observations, X-ray powder diffraction analysis, environmental scanning electron microscopy, and microchemical investigations, X-ray fluorescence, mercury intrusion porosimetry, and ion chromatography. After executing those tests, the most common deterioration phenomena identified were biological growth, material loss, disintegration, salt encrustations, the existence of soluble salts, and chromatic alteration (Figure 9) (Ciantelli et al., 2018).



Figure 9: Pictures representing several deterioration processes observed at the sites. (a,b) at Panamá Viejo, (a) biological growth; (b) surface recession/material loss; (c) encrustation at Fort San Fernando (Portobelo); (d) biological growth at Fort San Lorenzo (Ciantelli et al., 2018)

Concerning porosity, very high inter and intragranular porosity was identified in coral boundstones and packstones whereas sandstones and tuffites were found to have higher compacity and be prone to cracks. In addition, it was observed that the presence of salt water can result in the formation of sulphuric and nitric acids that would cause the dissolution of carbonates. These carbonates might recrystallize inside the stones and originate internal tensions or superficial incrustations (Ciantelli et al., 2018).

Regarding the selection of damage functions, three phenomena were further analyzed: surface recession due to rain washout, described by an equation that accounted for the solubility of the most relevant building material and precipitation; salt transition cycles, which were considered by counting the number of times the average daily relative humidity crossed the equilibrium of NaCl (75.3% relative humidity at 25°C) when decreasing; and biomass accumulation, based on the Gomez-Bolea et al. function, considering annual precipitation and annual mean temperature. The damage functions combined with the response from future climate projections would allow the effective implementation of predictive maintenance in cultural heritage sites (Ciantelli et al., 2018).

Fermo et al. (2018) conducted a study whose objective was the chemical characterization of environmental deposition in real exposure conditions of marble and surrogate substrates of the main façade of the Milano cathedral. The field exposure at two different heights in the façade started being conducted in 2014 and lasted 3 years. The research results show the significant deterioration potential of the deposits, especially sulfates, soluble salts, and silicatic compounds. Some of these compounds, such as sulfates, may have an anthropogenic or marine origin and their source has to be identified to better plan interventions. The article highlights the fact that the deposition volume and composition on cultural heritage depend on the subject height, the particular geometry of the façade's components, and the presence of urban canyons' effects (Fermo et al., 2018).

Concerning salt weathering, Menéndez (2018) performed estimations of the impact of several salts, such as sulfates, mixtures of chlorides, and nitrates, or the combination of them on cultural heritage

deterioration. The methodology involved the estimation of present and future phase changes of the selected salts in 41 French locations. The study points out that, generally, salts are omnipresent in cultural heritage buildings and most of them are originated from the interaction among building materials (stones, mortars, plasters) or with external agents such as sea salt, pollution, and underground water (Menéndez, 2018).

Salt weathering mechanisms can generate different decay forms and development degrees depending on material characteristics, its pore system, the source of the salt, and the position of the material in the construction. Despite this issue's complexity, temperature and relative humidity are considered to be its most relevant environmental parameters. For that research, only the geographical location of the salts was taken into consideration to differentiate climate conditions (Menéndez, 2018).

After applying different salt weathering estimation methods, the results were compared and together indicated more severe impacts when considering the combination of salts instead of single ones. The information obtained can better direct cultural heritage managers when selecting the best restoration treatments (Menéndez, 2018).

A large literature review was performed by Charola (2000), concentrating on the most important subjects regarding the salt-induced deterioration of inorganic porous materials. These topics include the transport of water, moisture, and salts in the pore network; impact of salt on moisture absorption; consequences of the presence of multiple salts; salt distribution in masonry; weathering mechanisms; and deterioration patterns. The goal of this research was to provide a comprehensive understanding of the various processes comprised in salt weathering of porous materials (Charola, 2000).

The research presents the origins of the salts that cause stone weathering: "air pollution, deicing salts, soil, sea spray, inappropriate treatments, or interaction between building materials" (Charola, 2000). It also mentions the primary mechanisms by which salt penetrates porous materials in buildings: "capillary rise of groundwater and infiltration by rainwater" (Charola, 2000). An accessory mechanism would be surface condensation. After entering a porous material, salt will move according to the environment it is exposed to (characterized by its temperature, relative humidity, and the presence of other salts) (Massari and Massari, 1993). The most usual weathering patterns formed after the salts crystallize in porous materials are flaking (or contour scaling) and powdering (or sanding). The accumulation of salts occurs in the zone of maximum moisture content, usually located 1 to 5cm away from the material's surface. (Snethlage and Wendler, 1997; Weber, 1984; Charola, 2000).

The study also gathers information on the influence of the size of pores and the presence of a second salt. According to field measurements executed by Zehnder and Arnold (1989), salt crystals primarily develop in pores with 1-10 $\mu$ m of diameter, and the relative humidity necessary for salt precipitation is reduced when a second salt is present (Price and Brimblecombe, 1994; Steiger and Dannecker 1995), which increases the frequency of the crystallization-dissolution cycles (Charola, 2000).

Regarding stone conservation measures, consolidation, and hydrophobization treatments are examples of interventions that could be implemented. However, it must be highlighted that the implementation of such treatments in salt-containing masonry could lead to the alteration of the distribution of salts in the material. In case the hydrophobization is not performed adequately or unhydrophobized joints are present, the salts concentrate in nonhydrophobized areas and behind the hydrophobized front (Franke and Pinsler, 1998; Charola, 2000).

The weathering mechanisms and weathering forms of stones utilized in cultural heritage on the SW coast of France are the subject of Cardell (2003)'s paper. The study identified mineralogical,

chemical, textural, and pore-system characteristics of recently quarried and decayed stones from quarries, exceptional and ordinary constructions. Cardell (2003) compared crystallization pressures, which are dependent on the pore size distribution, with the tensile strengths determined by Auger (1987) to assess the stones' resistance to salt deterioration. As a result, different deterioration effects resulting from salt crystallization stresses were observed in the stones. The patterns, such as alveolar weathering, granular disintegration, flaking, and micro-fissuring were greatly impacted by the distribution of the stone pores. The salt-induced decay is primarily caused by marine aerosols and atmospheric pollution. In this way, it is a major issue in coastal cities and one of the main contributors to the deterioration of stonework and masonry used in architectural heritage in these areas.

Regarding stone resistance, salt crystallization processes are capable of damaging even the strongest stones. Nevertheless, the deterioration rate and lifespan of a building stone vary according to its characteristics (mineralogy, texture, and structure) and surrounding conditions (Cardell, 2003).

Stone samples were obtained from structures, monuments, and quarries to compare the composition and texture of fresh and decaying elements. When performing the sampling, the following factors were considered: distance from the coast; kind of calcareous stone; weathering pattern; and orientation and elevation of samples in buildings and monuments. The samples were used to assess seawater's contribution to their total salt content and potential susceptibility to salt decay (Cardell, 2003).

The vulnerability to salt weathering was estimated by computing NaCl crystallization pressures (considering that NaCl is the most common salt in the analyzed stones). Fractures are expected to occur in case the crystallization pressure against pore walls, caused by salt nucleation and growth, is greater than the tensile strength of the stone. In this way, it would be assumed that stones with smaller pores are more prone to salt crystallization fractures (Cardell, 2003).

In order to protect the analyzed buildings exposed to the marine environment, broader chemical, physical and mechanical studies of building stones were encouraged, and the enhancement of frequent and continuous maintenance was suggested. To perform such maintenance, adequate salt extraction techniques must be developed, accompanied by the execution of appropriate consolidation and protection treatments based on the stone's characteristics (Cardell, 2003).

Grossi et al., (2011) present in their paper the concept of salt climatology while analyzing meteorological observation data from Western Europe and outputs from climate change models. The study demonstrates how climate impacts salt thermodynamics and how long-term salt damage can be linked to climate types. The number of dissolution-crystallization cycles for unhydrated (sodium chloride) and hydrated (sodium sulphate) systems were used as parameters for salt weathering. The findings indicate that the Köppen-Geiger climatic types can be related to potential salt damage. The temperate humid climate appears to be the most prone to salt weathering. Temperature, precipitation, and relative humidity data obtained from Climate Models indicate a future change in the Köppen-Geiger climate types and patterns of salt damage (Grossi et al., 2011).

The article discusses how stone decay is influenced by stone microstructure and the environment to which it is exposed. The main identified causes of building stone degradation are atmospheric pollution, frost, and salt weathering (Honeycombe, 1990). Even subtle climatic alterations may result in phase transitions, as in salt and frost weathering, and induce degradation within porous materials (Brimblecombe and Grossi, 2007). Phase transitions in salt that lead to damage, also known as crystallization-dissolution cycles, take place under specific thermo-hygrometric conditions (Grossi et al., 2011).

Grossi et al. (2011) included salt climatology in the scope of heritage climatology. Heritage climatology can be defined as “the study of the climate parameters that affect monuments, materials, and sites” (Grossi et al., 2011). It should be highlighted that heritage climatology is associated with variables that are distinct from the standard meteorological ones (such as temperature or relative humidity). This type of climatology concentrates on cycles and combinations of meteorological variables that can be linked to material degradation (Grossi et al., 2011).

## 2.5 Depth-damage curves

Based on the past few flood events, analyzed damage and the reconstruction costs of some selected buildings and the cultural heritage building characteristics, the Ministry of Culture in collaboration with the Faculty of Civil and Geodetic Engineering of the University of Ljubljana suggested three depth-damage curves that are used to conduct flood assessments, associated with different numbers of stories (1, 2 and 3 stories). The reason why the one-story curve diverges so much from the others is related to the fact that, according to the resolutions of disaster renovation, many times, it is only required to renovate the first story, which is usually the most affected story in the building (Ministry of Culture of Slovenia, 2023).

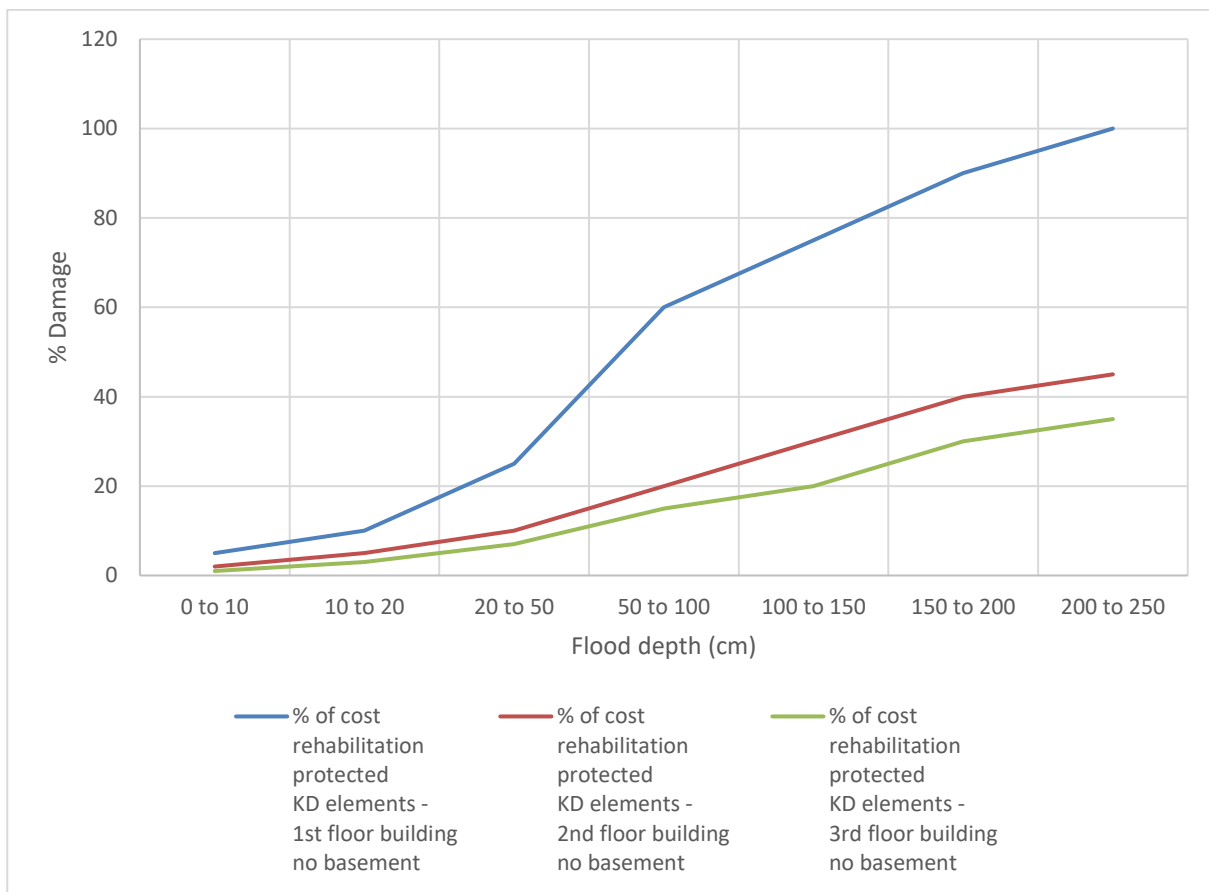


Figure 10: Depth-damage curves for cultural heritage in Piran

Aiming to contribute with depth-damage curves suitable to flood damage assessments throughout the entire country of Spain, Martínez-Gomariz et al. (2020) performed a literature review of depth-damage curves in Spain and all over the world. Additionally, they created spatial and temporal

adjustment indexes to transfer depth-damage curves to specific Spanish municipalities and different time horizons (to estimate future flood damage). The semi-empirical depth-damage curves used as a basis for Martínez-Gomariz et al.'s (2020) work were created in the framework of the RESCCUE project for the city of Barcelona. This project developed 14 curves, one for each of the most usual types of properties present in urban areas (restaurant, sport, education, etc.).

To develop such site-specific curves, the methodology present in Figure 11 was followed. Initially, relative depth-damage curves were derived from the ratio between economic damage and total property value for each of the building typologies. For that, the object value was determined according to either insured data or assessment of the flood surveyor, in case the property was not previously evaluated. Then, monetized depth-damage curves were obtained dividing the damage values by the asset area. As, in Martínez-Gomariz et al.'s (2020) work, differently from the present study, content damage is considered, the next step was to aggregate the three monetized curves (building, furniture, and inventory). Furthermore, to transfer the curves regionally and temporally, indexes based on Barcelona and 2020 damage values were created. These indexes would be used to evaluate loss in different cities in Spain and in the future (Martínez-Gomariz et al., 2020).

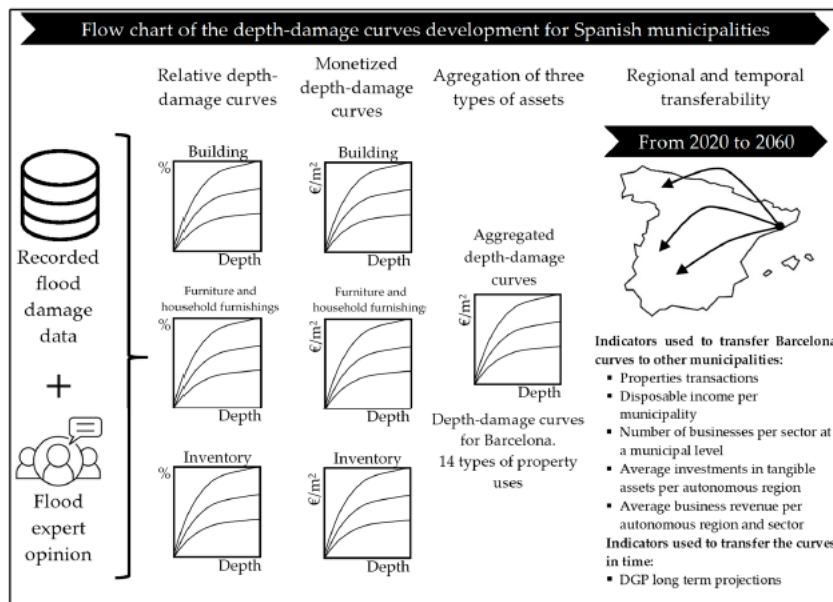
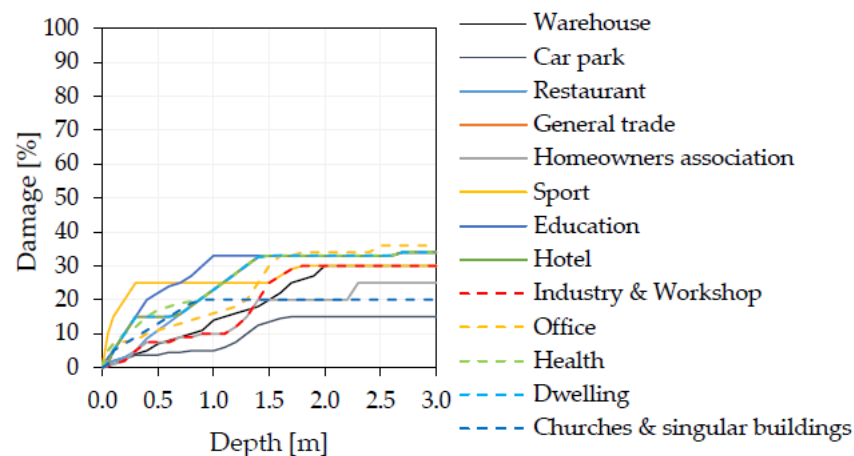


Figure 11: Flowchart of the development of depth-damage curves for Spanish municipalities (Martínez-Gomariz et al., 2020)



\* The depth-damage curve related to churches and singular buildings was created based on a single record available for their typology and flood expert knowledge.

Figure 12: Relative depth-damage curves for buildings in Spanish cities (Martínez-Gomariz et al., 2020).

In order to obtain spatial indexes for buildings, the economic level of the cities was considered. More specifically, a regional adjustment index for construction assets was estimated as the mean of the tax values per square meter for all properties' negotiations for a given city in 2020. These values were collected from online real estate agents for the most part and, in case the data could not be found for a municipality, their index would be the same as the lowest in the autonomous region they are a part of, assuming that their lack of relevance is associated with low financial capacity. For the determination of those indexes, it is presumed that the discrepancy between the reconstruction costs from city to city can be correlated to the discrepancy between property values. The regional index (RI), as a fraction of Barcelona (the unit), was then acquired by incorporating the official property values determined by the Spanish Registrar Chartered Institute (Martínez-Gomariz et al., 2020).

For the incorporation of the time scale in the depth-damage curves, the OECD's (Organization for Economic Co-operation and Development) long-term estimation of the Spanish GDP was taken into consideration. In Martínez-Gomariz et al.'s (2020) article, Barcelona's GDP in 2020 is considered as the unit, and temporal adjustment indices (TI) are decimal fractions of this value, for the next years until 2060 (Figure 13). In that way, the research expects to better estimate future damage costs (Martínez-Gomariz et al., 2020).

The total adjustment index (TAI), which comprises both the regional index (RI) and the temporal one (TI), is the result of the multiplication  $RI \times TI$  and can be used to achieve the depth-damage curve for a city for a specific year. That could be done by multiplying the city's TAI by Barcelona's monetized depth-damage curve in 2020 (Martínez-Gomariz et al., 2020).

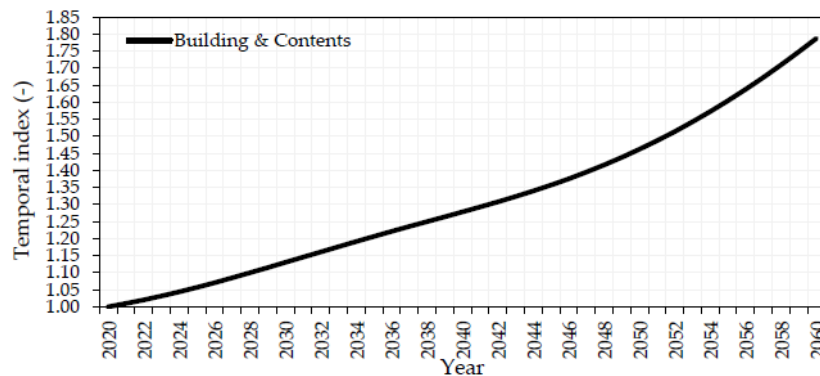


Figure 13: Temporal adjustment indices until the year 2060 (Martínez-Gomariz et al., 2020)

When analyzing results, Martínez-Gomariz et al. (2020) concluded that the curve shape is considered to change the most according to building typology, which is expected to not vary much throughout Spain. Additionally, it was recommended to consult experts whenever the correlation between depth and damage is found to be low. Regarding the time scale, the need for price updating according to the economic growth forecast was identified as a limitation.

Another research dedicated to developing depth-damage curves, in this case, according to the construction type and material of the asset, was the one carried out by Enghard et al. (2019). This paper created an approach for the large-scale evaluation of flood damage and risk that takes the vulnerability and exposure of buildings into consideration. Besides the development of depth-damage curves, the

work also aimed to create a method to assess flood risk in urban and rural regions utilizing data from ImageCat to represent exposure. The approach is notably suitable for developing countries since they present a big diversity among building types and materials.

The scope of the study conducted by Englhard et al. (2019), presented in detail in , started with a large literature review that supported the development of construction and material-based depth-damage curves. Thereafter, data from ImageCat was used to categorize building stock and identify its exposure. The third step was the obtention of maximum damage values for each of the object classes using data from ImageCat and JRC construction costs per country. Finally, the total flood risk was determined through the combination of the hazard information with the vulnerability and exposure values previously obtained (Englhard et al., 2019).

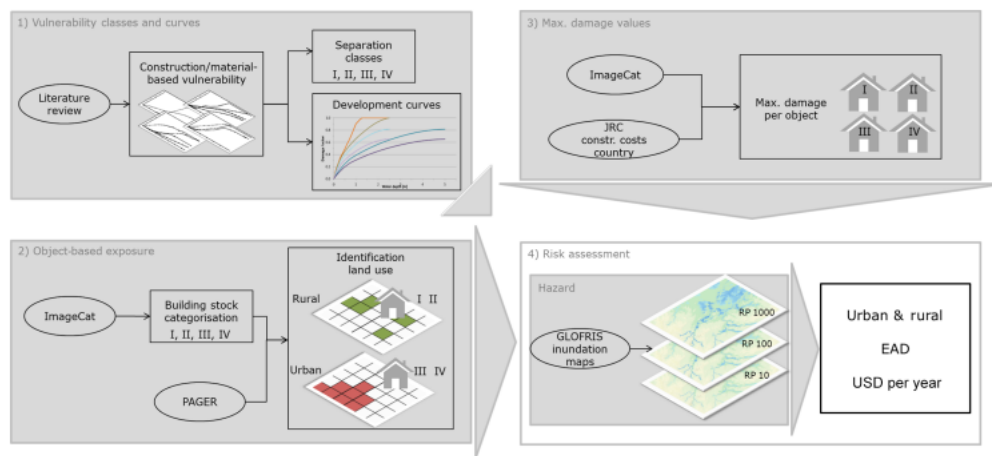


Figure 14: Flowchart for flood risk assessment with a building-material-based vulnerability approach (Englhard et al., 2019)

To define the classes and curves, researches from different locations that considered the vulnerability of specific construction types or building materials were analyzed, prioritizing studies that used actual event data. Four vulnerability classes were derived from the literature review, according to the similarities between construction types and materials and the degree of damage, they present when subjected to flood events. The classes, presented in , are (I) non-engineered construction composed with traditional materials obtained in the natural environment (such as compacted mud and adobe blocks) or informal constructions; (II) wooden buildings; (III) unreinforced stone, and masonry or concrete buildings with walls composed by burnt bricks, stones or concrete blocks; and (IV) reinforced masonry or concrete and steel buildings (c).

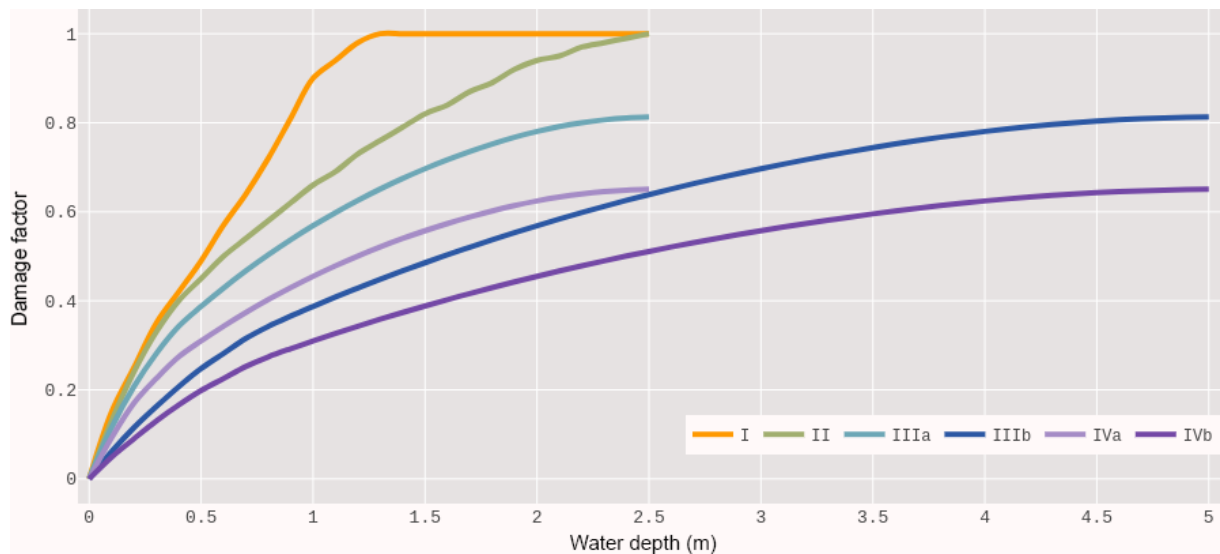


Figure 15: Stage-damage curves for four building-material-based vulnerability classes. For classes III and IV the one- and two-floor curves are denoted by (a) and (b)

For the second step, referring to the identification of the building's exposure, the objects present in the ImageCat database are categorized according to the 4 classes determined in step one and whether they are located in urban and rural areas. In this step, the hypothesis that, in developing countries, the percentage of buildings categorized in class I and II is higher in rural areas than in urban ones is presented. That hypothesis is based on the fact that in these countries the economic capacity and, consequently, living standards would be a lot lower in rural spaces when compared to urban ones (Englhard et al., 2019).

To verify this hypothesis, the PAGER dataset was used. This dataset is a nationwide building inventory that supplies data on the construction types that compose the urban and rural building stock. Initially, the PAGER dataset was grouped to conform to the 4 vulnerability classes chosen for the study and, subsequently, the percentage of the building stock that are part of classes I and II for rural and urban areas was computed (for high, upper-middle, lower-middle and low-income countries). After the computation, the hypothesis was confirmed (Englhard et al., 2019).

Besides checking the previously mentioned hypothesis, in step 2, the study also evaluated the performance of urban-rural classification of cells by comparing the performance of multiple land-use datasets: ImageCat, GHS-SMOD, GRUMP, MOD500, GUF, and HBASE. To compute the accuracy of those products, the metrics utilized to assess the overall accuracy were the kappa coefficient, producer's, and user's accuracy (Englhard et al., 2019).

For step 3, maximum damage values for the 4 vulnerability classes are established. The chosen input values were the depreciated structural maximum damage per area and country presented in the JRC report of Huizinga et al. (2017). In the report, residential construction costs are determined according to equations that relate construction costs and the GDP per capita of a specific country. To compute the maximum damage for the 4 vulnerability classes, the values presented in the JRC (structural maximum damage per area for a determined country) are multiplied by “the number of buildings that belong to a specific vulnerability class for a given cell, the building footprint (area and number of floors)

of each vulnerability class for a given cell and a maximum damage adjustment factor for each vulnerability class” (Englhard et al., 2019).

The final step of the process is the computation of damage from the combination of the exposure and vulnerability previously calculated in the study with hazard maps obtained with the GLORIS global flood risk model (WRI, 2018). In this study, flood risk is represented by the expected annual damage or EAD and is calculated by integrating the flood damage curve over all exceedance probabilities (2, 5, 10, 25, 50, 100, 500, 250, and 1000-year return periods) (Englhard et al., 2019).

In the results, the expected annual damage was categorized into four vulnerability classes and two land-use classes (rural and urban). It was observed that most of the damage comes from urban areas and, while in rural environments damage comes from classes I, II, and III, relevant damage in urban areas is a result of losses in buildings of classes III and IV (Englhard et al., 2019).

## **2.6 Slovenian and European Policies, Guidelines, and Projects for The Protection and Conservation of Cultural Heritage**

Documents that mentioned the importance of the protection and conservation of cultural heritage in Europe exist since 1974 with the “Recommendation from the Commission to the Member States of the European Union on the protection of the architectural and natural heritage” (EEC, 1975). Throughout the years, the documents concerning the protection of these assets multiplied and gradually became stricter, with instructions, requirements, and restrictions that needed to be considered when managing such invaluable sites. One example of such a document is the “European Parliament and Council's Directive 2007/60/EC on the assessment and management of flood risks that required the minimizing and controlling of flood risk to cultural heritage”. In the past decades, Europe has developed several agendas, guidelines, policies, and projects that aimed to preserve cultural heritage. Some of these initiatives are further described in this subchapter.

One of the first notable EU projects regarding the protection of cultural heritage was Noah's Arc, launched in 2007. The project aimed to identify the meteorological variables and changes that affect cultural heritage the most; to study, forecast and describe climate change impacts on cultural heritage; to create plans to mitigate climate change and adapt the most endangered historic buildings, sites, monuments, and materials; to provide heritage managers with electronic information sources and tools, such as web-based Climate Risk Maps and a Vulnerability Atlas; and to guide lawmakers and policymakers with the aid of the project's Policy Advisory Panel. The Climate Risk Maps and Vulnerability Atlas would allow heritage managers to evaluate climate change risk to cultural heritage under different future climate scenarios and the effectiveness of different measures to mitigate this risk (CNR-ISAC, 2007; UCL, 2007).

The research conducted throughout the project was compiled and organized according to four primary topics: “Rainwater and drainage infrastructure, Effects on structures, Effects on materials, and Indoor-outdoor interactions for Guidelines preparation” (CNR-ISAC, 2007). Most of the work has been devoted to mapping out the locations in Europe that are more or less likely to experience material deterioration based on the results from the first two years of research. The Vulnerability Atlas translates climate data and meteorological information into potential risk and damage to cultural heritage. The Guidelines provide methods for managing cultural heritage in the face of climate change (CNR-ISAC, 2007; UCL, 2007).

From 2009 until 2014, the European Commission financed the Climate for Culture (CfC) project. This project focuses on predicting climate change's effects on cultural heritage buildings' structure and contents in Europe and the Mediterranean. These predictions allow the determination of the damage potential of assets exposed to the highest risk, along with the social-economic consequences of this damage. In this way, it would be possible to create more targeted, effective, and efficient adaptation and mitigation measures against climate change. Ideally, those measures would be developed and supported by policymakers and reports such as the IPCC (Climateforculture.eu, 2014).

With the aid of simulation and modeling tools, the project delivered a forecast of the influence of climate change outside and inside cultural heritage buildings (including its contents) until 2100 in multiple climate zones. High-resolution Regional Climate Models or RCMs were created and combined with building simulations, to assess climate impacts on very small scales (Climateforculture.eu, 2014).

Additionally, for exceptional buildings, more comprehensive assessments were performed to obtain information such as conservation status, details regarding indoor climate conditions, and prerequisites to perform preventive conservation. Many buildings were analyzed, with different typologies, ages, and locations, to understand the impact of climate change and the type of use in their performance. The objective of the in-depth assessments was the comprehension of the climatic behavior and energetic demands of cultural heritage buildings when facing climate change and, in that way, assist the creation of solutions that help preserve the asset's exterior and interior (Climateforculture.eu, 2014).

The report "Towards an integrated approach to cultural heritage for Europe" (Diaconu, 2015) was developed in 2014 according to other cultural heritage policy documents issued in the same year ("Council conclusions on cultural heritage as a strategic resource for a sustainable Europe", "Council conclusions of on participatory governance of cultural heritage", "Committee of the Regions' opinion on Towards an integrated approach to cultural heritage for Europe" etc.). This report summarized the main discussion topics regarding cultural heritage at the time, including the results of the public hearing "An integrated approach to cultural heritage in Europe: State of play and perspectives" and insights from experts and stakeholders on the biggest obstacles faced by the sector. Thus, it was possible to propose effective solutions to overcome these obstacles (Diaconu, 2015).

The primary recommended strategies to overcome the identified obstacles presented by the report were putting the integrated approach to cultural heritage into action, translating the challenges into possibilities, recognizing the economic benefits of cultural heritage, and integrating policies that are directly related to cultural heritage, such as tourism and scientific research (Diaconu, 2015). Additionally, the report suggests promoting the modernization of the sector, encouraging research and innovation in the area while ensuring the dissemination of the obtained knowledge, taking advantage of digitization to involve a larger and younger public in the cultural heritage agenda, and maximizing the engagement of the private sector and civil society in heritage matters, to better tailor them to the current state of the EU (European Commission, 2014).

Forget Heritage is an INTERREG project launched in 2016 and with a duration of 3 years. The project's primary goal was to foster collaboration between European cities to find creative, reproducible, and sustainable public-private partnership models to manage cultural heritage sites by establishing Cultural and Creative industries. The project sought to offer guidance on how to expand cultural heritage's potential to improve the quality of life for its residents and for those working in the cultural and creative industries by providing them with job possibilities and opportunities to develop management skills (Interreg CENTRAL EUROPE, 2018a).

Forget Heritage delivered a management manual, a report containing project results, a policy handbook, a transnational training model (based on the pilot actions implemented), guidelines for citizen involvement, and a strategy for the management of cultural heritage using Cultural and Creative Industries (CCIs). Additionally, among the project outputs were the identification of buildings with untapped potential (which could be dedicated to culture), suggestions for the adaptation of the countries' policies, and enhancement of management models (Interreg CENTRAL EUROPE, 2018a).

The policy handbook presented an overview of the pertinent cultural heritage conservation laws and regulations in force in the project's partner countries, at a local, regional, and national level. It gives suggestions on how to implement them and assists the development of new initiatives by sharing acquired experience (recommendations of which actors to involve, opportunities to explore, and means of financial support). Other Forget Heritage's output is the management manual that seeks to provide orientation for policymakers and to serve as a guide for renovation projects and managers, by presenting the best management practices identified among the partners. It highlights stakeholder participation, creativity, social integration, environmental sustainability, tourism, and technology as simultaneous challenges and opportunities (Interreg CENTRAL EUROPE, 2018b; Interreg CENTRAL EUROPE, 2018c).

Another INTERREG project with more recent results is ForHeritage, a six-year-long project, finished in 2020, that fostered public participation, assisted resource mobilization, and supported the development of skills to better safeguard and manage cultural heritage in Europe. ForHeritage's objective was to enhance the impact of information and experience obtained in past EU-funded cultural heritage management initiatives, by analyzing, improving, assessing, and verifying this knowledge. To attain this goal, the project delivered a manual with detailed instructions on how to enhance cultural heritage management, workshops in the participating nations (Poland, Slovenia, Croatia, and Italy), regional implementation of cultural policies, and on-site testing (Interreg CENTRAL EUROPE, 2014).

The initiative produced documents regarding financial schemes and tools for cultural heritage, participatory governance in the sector, useful knowledge from pilot projects, impact assessment of cultural heritage projects, public-private partnerships to support heritage revitalization, and training to ameliorate cultural heritage management. It is worth highlighting the two pilot projects developed in Slovenia, a financial model to promote cultural heritage in Ljubljana's urban region, and a viability study of the potential use of private funding sources for Vodnik Homestead. The financial model presents possibilities that owners and operators of cultural heritage entities can explore and use to create their custom model, according to the cultural heritage's dimension, background, and content. For the viability study, the tool "Financial Instruments and Innovative Schemes for Cultural Heritage" assisted in the decision to pursue new financial sources for the site's maintenance (Interreg CENTRAL EUROPE, 2014; Interreg CENTRAL EUROPE, 2022a; Interreg CENTRAL EUROPE, 2022b).

The 2018 European Framework for Action on Cultural Heritage, published in 2019, intends to use the results of the European Year of Cultural Heritage 2018 and translate them into tangible measures. It also supports the 2019's EU Work Plan for Culture and is in line with the Sendai Framework for Disaster Risk Reduction 2015-2030. The framework's goal is to align heritage-related actions in the EU, especially focusing on EU policies and programs. In addition, the framework aims to structure regions, cities, cultural heritage organizations, and networks that are interested in initiating or expanding cultural heritage activities (European Commission, Directorate-General for Education, Youth, Sport and Culture, 2019).

The framework is a result of participatory planning, with the contribution of “EU Member States, EU Council Presidencies, the European Parliament, civil society organizations, cultural operators and international organizations such as the Council of Europe and UNESCO” (European Commission, Directorate-General for Education, Youth, Sport and Culture, 2019). Its principles are: a holistic approach, mainstreaming and integrated approach, evidence-based policymaking, and multi-stakeholder cooperation. The holistic approach principle is based on interpreting cultural heritage’s tangible, intangible, and digital aspects as interdependent and interlinked and on promoting the protection, empowerment, and development of cultural heritage, encouraging synergies with contemporary and future ideas and environments. Regarding the mainstreaming and integrated approach, the framework aims to ensure the consideration of cultural heritage in EU policies in various areas: “regional, urban and rural development, education and social cohesion, digital transformation, environment (including nature conservation), tourism, accessibility, the sustainability agenda and climate change adaptation, research and innovation and external relations” (European Commission, Directorate-General for Education, Youth, Sport and Culture, 2019).

On the subject of evidence-based policymaking, the framework demands cultural heritage decision-making to be based on measures of the effects of interventions and actions on those assets, along with the enhancement and structuring of data collection to contribute to European and international statistics. Finally, the multi-stakeholder cooperation principle institutes the Cultural Heritage Forum, a tool for discussing and exchanging experiences and best practices regarding cultural heritage. The forum involves “EU Member States, EU institutions, civil society, and different European Commission services” (European Commission, Directorate-General for Education, Youth, Sport and Culture, 2019).

In 2018, the European Year of Cultural Heritage, a New European Agenda for Culture was issued, based on a decision from the European Framework for Action on Cultural Heritage. The agenda’s goals had social, economic, and external aspects. From a social point of view, the agenda strives for the enhancement of cultural power and cultural diversity through the enlargement of the availability of cultural activities and the engagement of the population in them, the support of cultural professionals’ mobility, and the preservation of cultural heritage while creating awareness of those assets’ importance to the European identity (European Commission, 2018).

From an economic perspective, the agenda aspires to promote jobs and growth by means of assisting cultural education and innovation. That would be achieved by supporting the art, culture, and inventive mindset; creating appropriate conditions for the development of cultural and creative corporations, especially providing the necessary financial support; and helping the cultural and creative sector develop digital, entrepreneurial, and specialized skills (European Commission, 2018).

Finally, regarding the external dimension, the agenda seeks to expand and reinforce international cultural relations. This objective could be attained by incentivizing intercultural exchange, fostering peace, strengthening cooperation on cultural heritage, and promoting the use of cultural heritage as a tool for propelling social and economic development (European Commission, 2018).

The idea behind the “Cultural Heritage in Action” project, which spanned from 2020 to 2023 and was also part of the European Framework for Action on Cultural Heritage of the European Commission (2018), was to create a peer-learning scheme in the cultural heritage sector in which several cities and regions in Europe display their inventive and participatory projects. In these projects, cultural heritage had to be a major factor in the solution of six issues: “social inclusion, urbanization, governance, recovery and resilience, sustainability and financing”. The “Cultural Heritage in Action” project also

aims to develop policy suggestions that would lead to sustainable and resilient cultural heritage ecosystems. Furthermore, one of the outputs of the project was a 10-step guide to adapt cultural heritage policies, which included the consideration of cultural heritage in strategic documents, the tailoring of policies to environmental and societal conditions, and the encouragement of participatory planning in which multiple stakeholders are heard (Eurocities, 2022).

One of the latest European documents concerning the empowerment of cultural heritage is EU Work Plan for Culture for 2023 to 2026, published in 2022. The plan presents 4 major concerns: assisting the development of cultural and creative sectors; expanding the role of culture in society and increasing public engagement in cultural activities; benefiting from culture's capacity to help the planet; and reinforcing EU external cultural relations. Some of the guiding principles of this plan were that culture and cultural heritage has an inherent importance and it could help solidify European identity; the recognition of the outstanding importance of cultural and linguistic diversity for the EU along with the necessity of supporting and increasing them; that culture could contribute to society by fostering equality and mutual respect; and that culture boosts "sustainable development, economic and social inclusion, and territorial cohesion". Among the actions the plan suggested, are: the regulation of the status and working conditions of cultural professionals, the provision of incentives for the digital and green transitions of cultural and creative sectors, the promotion of "climate action through culture", preserving and protecting cultural heritage from natural disasters and the anthropologic impact, and fostering culture-oriented governance (Council of the European Union, 2022).

Concerning Slovenian acts and rules that focus on cultural heritage preservation, the main act that covers the subject is the "Cultural Heritage Protection Act" and two of the primary rules that regulate the topic are the "Rules on the Registry of Types of Heritage and Protection Guidelines" and the "Rules on the Categorization of Cultural Heritage Objects". Additionally, the Slovenian cultural heritage institutional framework includes the Ministry of Culture, Cultural Heritage Directorate, Culture and Media Inspectorate, Institute for Protection of Cultural Heritage and Institute for Protection of Cultural Heritage with seven Regional Offices, Restoration Centre, Centre for Preventive Archeology and Research Institute as Institutional Constitutive Parts. At a local level, municipalities are responsible for approving municipal planning acts, determining which monuments are relevant locally, financially supporting restoration and other projects, managing local heritage, and exercising pre-emption rights when monuments of local significance are up for sale (Herein System 2014; Financial Administration of the Republic of Slovenia, 2014).

### 3 CASE STUDY – PIRAN

#### 3.1 Geographical Location

Piran is a municipality located on the Slovenian coastline, along with the municipalities of Ankaran, Koper, and Izola. The city is situated in the southwestern part of Slovenia, exposed to the Gulf of Trieste and the northern Adriatic Sea (Figure 16). This area is characterized by the contrast between low-lying coastal areas and very steep cliffs (Figure 17), with shingle beaches and human-altered areas, as part of the old harbor that was filled with earth and turned into the main city square, Tartini Square, where lie Giuseppe Tartini statue and Tartini's house. Besides that, the city's disposition on a peninsula causes it to be exposed to the sea from both the west and north limits (Alivio, 2020; Mezek and Bricelj, 2002; UNEP/MAP, 2018; Kolega, 2015).

The small area occupied by the city of Piran does not prevent it from being considered one of the most relevant municipalities in the country, due to its economic importance, cultural heritage value, marine and coastal ecosystems, and natural areas that need to be preserved (Alivio, 2020; Vahtar, 2006).



Figure 16: Geographic location of Piran, Slovenia (Alivio, 2020)

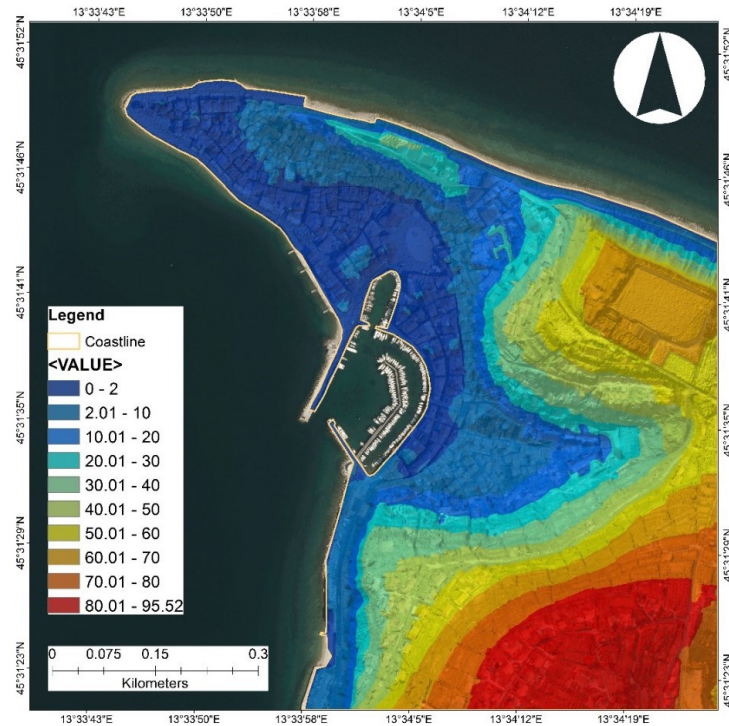


Figure 17: Elevations of Piran, Slovenia (Alivio, 2020)

### 3.2 Climate and Hydrological Context

Piran is subjected to a Mediterranean climate with dry summers and mild winters. According to the Köppen-Geiger climate classification, Piran has a Humid subtropical climate (Cfa). Its temperature ranges from a minimum of 2 degrees in February to up to 29°C in August (Figure 18) (Weatherspark.com, 2023).

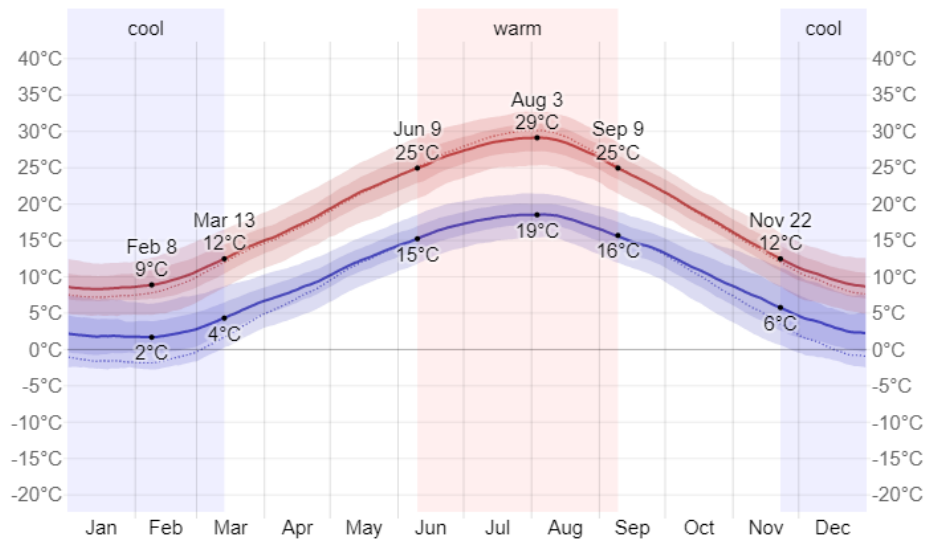


Figure 18: Temperature in Piran over the year (Weatherspark.com, 2023)

Concerning precipitation, Piran has an average of 945 mm of annual precipitation. The wettest month is September with 127 mm and the driest month is February with 46 mm of precipitation, as shown in Figure 19 (World Weather & Climate Information, 2023).

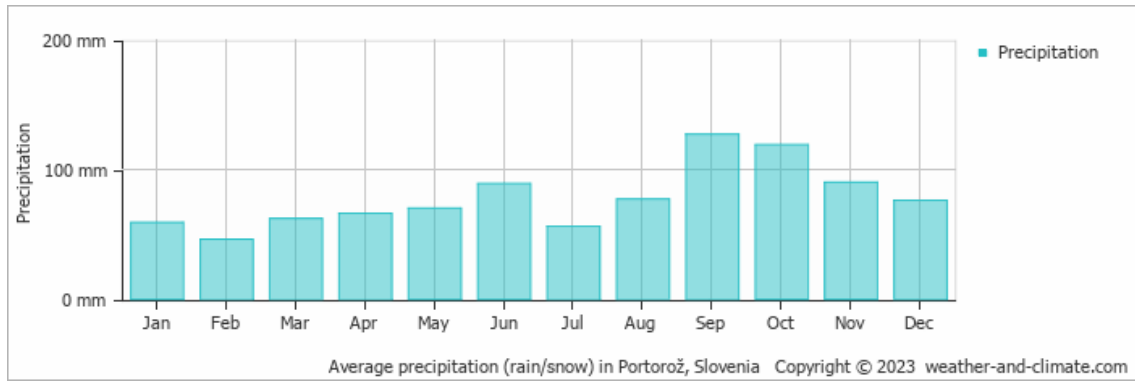


Figure 19: Precipitation in Piran over the year (World Weather & Climate Information, 2023)

The Slovenian coast hinterland area has a torrential surface water network, which results in a large amount of water being discharged into the Gulf of Trieste whenever there is rainfall. When combined with the north wind, these large discharges can cause variations in marine temperature and salinity (Bricelj, 2002).

The coastal area of Slovenia is located in the basin of the rivers Rižana, Badaševica, and Dragonja, which has a surface similar to the Gulf of Trieste's and an influence of less than 10% of the flow of the Soča/Isonzo. In general, these rivers have increased discharges in winter and almost turn dry during summer. These rivers tend to get dry in the summer due to the low precipitation rate in the area and water extraction for irrigation and water supply (Bricelj, 2002).

Regarding flood risk, Piran's location incurs its high exposure to both high tides and southerly winds. This condition results in the frequent occurrence of high tide floods especially during autumn and winter (October to December), which inundate most of the municipality's center (Kolega, 2006; Vahtar, 2006; Alivio, 2022). As in Venice, floods in Piran are complex to predict because they are a result of the combination of astronomical tides, low-pressure centers, south winds, and precipitation. When all these elements are coupled, they heighten the waves and additionally increase sea water levels (Kolega, 2006; Alivio, 2020). Even though high tides can be predicted far in advance (up to months) and with a high degree of accuracy, the movement of air pressure and winds can only be predicted a few hours before the flood event (Ntslf.org, 2019; Kne, 2020).

Concerning warning issues, a yellow alarm is issued by the Slovenian Environment Agency (Agencija Republike Slovenije za Okolje, ARSO) when the water level surpasses 300 cm (or 0.91 m according to the national altitude coordinate system (Koper tide gauge station with a mean sea level of 218cm)). Orange and red warnings are issued when the water level gets to 330 cm (1.21 m) and 350 cm (1.41 m), respectively.

Yellow warnings correspond to the point when most exposed parts of the coast start to get inundated, orange when the main square and the oldest town quarter (Punta) start to flood, and red when the main square and the oldest quarter are completely submerged. On average, a water level of 300cm is surpassed 8 times a year in Piran, with a maximum of 31 exceedances a year in 2010, resulting in huge economic loss (Ličer, 2019; Strojjan and Robič, 2016; Alivio, 2022).

### 3.3 Socio-Economic Context

According to the 2022 census, the population in Piran reached 3,802 inhabitants, distributed with a population density of 5,459 individuals per km<sup>2</sup>, the highest in Slovenia (SURS, 2022). The Slovenian

Statistical Office allows, through STAGE, a web service application, access to a cartographic tool that presents and helps disseminate national statistical data in several time and space resolutions free of charge. In STAGE, it is possible to find information regarding the population distribution in Piran, with a resolution of 100 by 100m, which is portrayed in Figure 20 (Kuza and Merc, 2015; Alivio, 2020).

Piran's economy, similar to other coastal cities, is mostly based on tourism, which has higher rates during the summer months (from June until September). Only in March 2022, 50,800 national tourists came to the city to visit cultural heritage sites, museums, and beaches (Mlakar and Zupančič, 2022). The income resultant from tourism in Piran and other coastal Slovenian cities is not only relevant to the municipalities themselves but also to the country, as it accounted for more than 12% of the gross domestic product in Slovenia and generated 110,700 jobs in 2018 (Priatelj, 2019; Alivio, 2020).

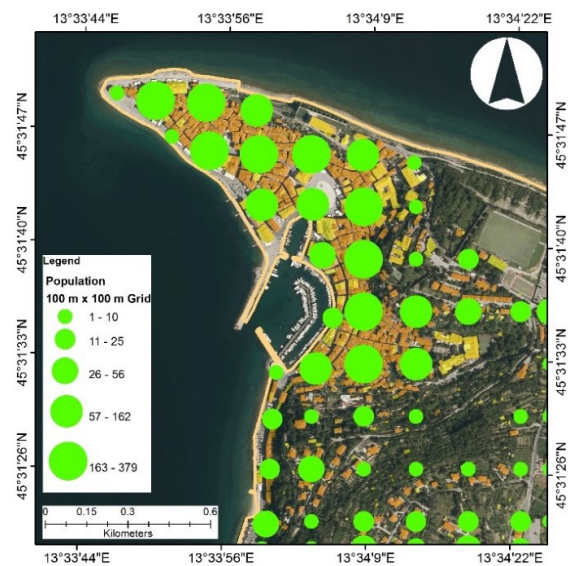


Figure 20: Population distribution in Piran (Alivio, 2020)

### 3.4 Cultural Heritage in Piran

Piran is one of the municipalities with the oldest settlements in Slovenia, having been first occupied during the pre-roman era. According to the Slovenian Tourist Board (STO), the town is one of the most authentic and photogenic on the Adriatic coast. The municipality's ancient character, analog to Venice's, is materialized in monuments and buildings closely constructed in narrow streets, which has provided it full monumental protection as an urban heritage site (Benčič, 2018).

The city's elements, such as the well-preserved medieval wall, Tartini monument, Venetian house, the town hall, baroque house, Tartini central square, and Tartini's birth house fall into the highest category of historical and cultural heritage protection. Piran is considered one of the most relevant Slovenian historic urban areas due to its diversified architecture (medieval, gothic, and renaissance), representative of its long history over the past centuries (Benčič, 2018; Benčič, 2012; Alivio, 2022; Deu, 2016).

The city's cultural heritage sites are registered in a geodatabase created by the Ministry of Culture, freely available online on their website (<https://data-mk-indok.opendata.arcgis.com/>), in which the elements are classified into the following 6 categories: archaeological sites, memorial heritage, settlement heritage, profane buildings, sacred heritage, and sacred profane buildings. The geographical location of the cultural heritage sites in Piran is presented in Figure 21 (Ministry of Culture of the Republic of Slovenia, 2018; Alivio, 2022).



Figure 21: Culture heritage locations and heritage status in Piran

## 4 RESEARCH METHODOLOGY

This chapter describes the methodology used to accomplish the main goals of the present work. In the following sections, the steps taken to execute the research are presented and detailed.

### 4.1 Methodological Framework

This research followed the steps detailed in the flowchart presented in Figure 22. Initially, a bathtub model was created in QGIS to determine the flood depths for different mean SLR scenarios at locations of the 51 cultural heritage sites analyzed. Then, a literature review on flood vulnerability indexes (FVIs) for cultural heritage directed the creation of a flood risk matrix and FVIs tailored for Piran. The data necessary to obtain the index values was collected on a field trip to Piran. In possession of flood depths for cultural heritage assets, the flood risk matrix, and FVIs adapted to Piran's cultural heritage, a qualitative flood risk assessment was performed. A superficial qualitative analysis of the long-term evolution of salt deterioration to climate change was also performed with the aid of Regional Climate Models (RCM) data on temperature and relative humidity.

For the quantitative flood risk assessment, depth-damage curves provided by the Ministry of Culture of the Republic of Slovenia along with functions found in the literature for different building types and materials were incorporated in the KR PAN model. To make the damage estimations more precise, the previously calculated FVIs also contributed to damage calculation in the model.

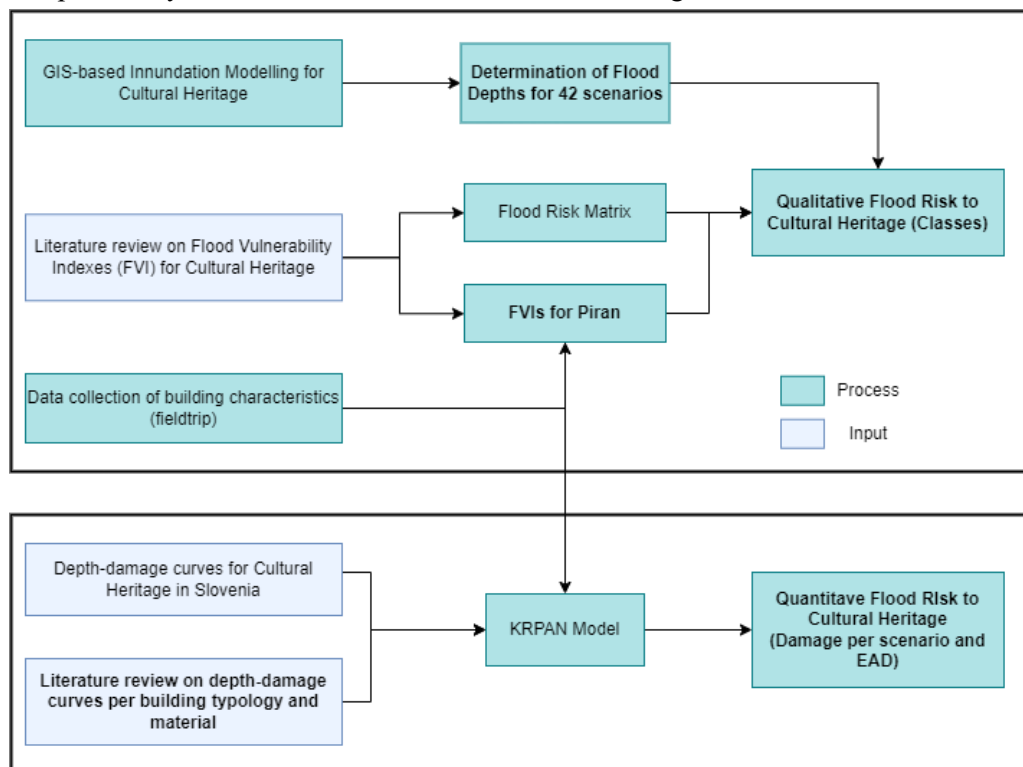


Figure 22: Methodology Flowchart

### 4.2 Data sources

The data utilized in this study was gathered from various Slovenian government agencies, which either make their data publicly available online or shared it upon request. The pertinent datasets needed to complete the study's goals are listed in Table 4, along with their sources and resolution.

Table 4: Datasets used in the study

Dataset	Data Type	Resolution/Scale	Source
LiDAR DEM	Raster	1m	Agencija Republike Slovenije za Okolje (ARSO, Slovenian Environment Agency) of the Ministry of the Environment and Spatial Planning
Orthophoto	Raster	0.25 m	Surveying and Mapping Authority of the Republic of Slovenia of the Ministry of the Environment and Spatial Planning
Registry of Buildings	Vector	1: 1000	Surveying and Mapping Authority of the Republic of Slovenia
Population	Vector	100 m by 100 m grid	Slovenian Statistical Office (SURSO)
Cultural Heritage Polygons	Vector	1: 5000	Ministry of Culture of the Republic of Slovenia
Cultural Heritage Renovation costs	Cost	Building	Ministry of Culture of the Republic of Slovenia
Projected Sea level rise	Hydrological	Global / Regional	Scientific literature
Flood depth-damage curves	Hydrological	Global / Regional	Scientific literature Ministry of Culture of the Republic of Slovenia

### 4.3 GIS Analysis

Initially, the updated cultural heritage data provided by the Ministry of Culture was collected and coupled with the LiDAR DEM provided by the Ministry of Environment and Spatial Planning for the entire country through their National Aerial Laser Scanning Project (2014 – 2015).

The chosen flood depth scenarios were the ones presented by Alivio (2020). In his work, Alivio (2020) has obtained extreme water depths associated with different return periods (T2, T5, T10, T100, and T1000) by performing a statistical analysis of 60 years of extreme historical mareographic data from Koper's station, which included testing the fit of GEV and Gumbel distributions (Table 5). Eventually, the Gumbel distribution was considered the most adequate to fit the data.

In addition, Alivio (2020) has established 7 scenarios of climate change with crescent values of sea level rise from 0.1 to 1.46m. The lack of availability of sea level rise projections on account of climate change for Slovenian's coast led the chosen scenarios to be oriented by North Adriatic Sea projections. After reviewing the North Adriatic Sea accessible literature, Alivio (2020) considered sea level rise scenarios from 10 to 50 cm with 10 cm steps suitable to allow a broad understanding of the impacts of the increase in sea level in the coming decades. This step choice was a reflection of the 8 cm RMSE of the LiDAR DEM (Mlasko, 2011) and the 10 cm sea level rise that occurred on the Slovenian coast in the last decades (Strojan and Robič, 2016). For the second most extreme sea level scenario, the RCP8.5, the worst scenario presented by the Intergovernmental Panel on Climate Change (IPCC) in 2019, was considered, with a value of 0.84m. And finally, for the most extreme scenario, the sea level rise projection of Kopp et al. (2017) was taken into account, with an increase of 1.46m. Table 6 summarizes the sea level rise scenarios created by Alivio (2020).

Table 5: Extreme sea level elevations for various return periods using GEV and Gumbel distribution models  
(Alivio, 2020)

Return Period	Sea Level Elevations (cm)	
	GEV	Gumbel
2 year	326	328
5 year	342	343
10 year	355	353
100 year	401	384
500 year	442	405
1000 year	463	414

\*300cm is considered to be the elevation at which the Adriatic Sea starts to flood the most exposed areas

Table 6: Sea level rise scenarios (Alivio, 2020)

Scenario	Sea level rise (cm)
S1	10
S2	20
S3	30
S4	40
S5	50
S6	84
S7	146

In order to estimate flood depths to the cultural heritage sites in Piran, a bathtub model was used. 42 flood depths were computed as a result of the combination between the 6 return periods and 7 mean sea level rise scenarios. Initially, terrain elevations were assigned to each one of the 51 cultural heritage assets. Once each of the objects had heights associated with it, the sea level elevation per return period with sea level rise was subtracted by the terrain heights. The final value after the subtraction corresponds to the average flood depth in the area of the cultural heritage site's ground floor plan.

It is important to highlight that, in this work, the dynamic influence of the sea (e.g. waves actions) was not taken into consideration, even though, as Piran is a coastal municipality, it is known that the wave's length and height play an important role in the extent and impact of floods. In addition, the buildings are considered as one entity with only one terrain height and flood depth, which is an acceptable approximation since the sizes of the cultural heritage sites are rather small.

#### 4.4 Flood Vulnerability Index (FVI)

Many of the studies that aimed to estimate flood risk in cultural heritage sites, especially Miranda and Ferreira (2019) and Stephenson and D'Ayala (2013), suggested the development of a Flood Vulnerability Index or FVI to describe the exposure and sensitivity of those sites. Miranda and Ferreira (2019) created an FVI based on 5 sensitivity parameters: material, condition (presence of cracking, moisture, settlements, and deformations), number of stories (1 to 4 stories), age (from before the 14th century until the 21st) and heritage status (building classification and its sphere of interest) and one exposure parameter, wall orientation (degree of exposition to flow and presence of openings). Those parameters were categorized into classes from A to D, with A being the least vulnerable and D being the most fragile. According to the created classes, the most vulnerable buildings would be the ones fully exposed to flow with openings (wall orientation), made of earth structures (material), with expressive cracking and serious material decay (condition), with 4 stories or more (number of stories) and constructed until the 14th century (age). A building with more stories is considered to be more vulnerable because it is supposed that the construction has a superficial foundation. In that case, classes

A, B, C, and D are associated with values of 10, 40, 70, and 100, respectively (Figure 23) (Miranda and Ferreira, 2019).

Thereafter, the FVI is calculated by multiplying the sum of the sensitivity parameters (varying from 50 to 500) by the exposure one (10 to 100), resulting in indexes with values from 500 to 50000. For the previously mentioned example of the most vulnerable buildings, all 5 sensitivity components would be assigned to class D and a value of 10. The sum of the 5 parameters would be 50 and that value would be multiplied by the exposure component of 10 (class D, since the asset is highly exposed) (Miranda and Ferreira, 2019).

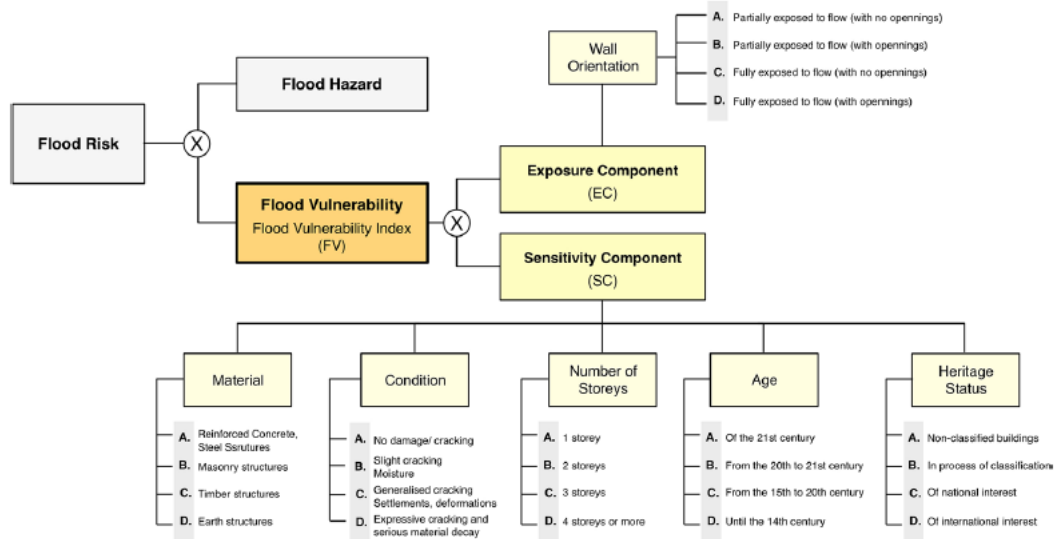


Figure 23: Framework for simplified flood vulnerability assessment (Miranda and Ferreira, 2019)

On the other hand, even though Stephenson and D'Ayala (2013) chose most of the same parameters to calculate a vulnerability index, their work does not consider an exposure term, and, for each parameter, 3 to 5 attributes were chosen and rated from 10 to 100, divided equally by the number of attributes. Stephenson and D'Ayala's (2013) work has collected data at the city, street, and building levels, and, subsequently, the cumulative vulnerability index of cities was compared.

Statistical analyses were applied in both pieces of research. In Miranda and Ferreira (2019), the distribution of the flood vulnerability indexes from all the buildings was presented in a histogram and the best fit normal curve was applied to it. In turn, Stephenson and D'Ayala (2013) created a cumulative log-normal distribution of the vulnerability indexes for each parameter.

In the current work, the following 8 sensitivity parameters were chosen to calculate flood vulnerability indexes: (1) heritage status (exceptional or regular), (2) number of stories (1, 2, 3, or 4 stories or more), (3) material (flysch, sandstone masonry, exposed masonry or limestone and other vulnerable materials), (4) presence of ornaments, (5) presence of limestone base, (6) condition (well preserved, slightly damaged or damaged), (7) recent renovation (in case there was one) and (8) age (until the 15th century or from the 16th to the 20th century). Concerning exposure, the buildings were rated depending on their location (elevated area, low-lying area not exposed to the sea, and low-lying area exposed to the sea).

The parameters were rated with values of 10, 40, 70, and 100 and classified into A, B, C, and D according to Table 7:

Table 7: Sensitivity and Exposure parameters with their class and rating

Class	Rating	Heritage status (1)	n° Stories (2)	Material (3)	Ornaments (4)	Limestone base (5)	Condition (6)	Recently renovated (7)	Age (8)	Exposure
A	10		1	Flysch	No	Yes	Well preserved	Yes		Elevated area
B	40	Regular	2	Sandstone Masonry			Slightly damaged		From 16th to 20th	
C	70		3	Exposed Masonry or limestone			Damaged			Low-lying areas NOT exposed to the sea
D	100	Exceptional	4 stories or more	Other vulnerable materials	Yes	No		No	Until 15th century	The low-lying areas exposed to the sea

To obtain FVI values, the sum of the 8 sensitivity parameters was multiplied by the exposure parameter and the resultant index ranged from 800 to 80000. An FVI of 800 would then correspond to the least vulnerable asset and 80000 to the most vulnerable one.

Once the parameters were defined, fieldwork was conducted in the city of Piran to obtain the necessary information. The fieldwork was assisted by flood-related professors from the University of Ljubljana (UL) and one of the engineers responsible for calculating disaster damage in the Ministry of Culture. The collected data was inserted into Excel where values were assigned to each of the 8 parameters for the 51 buildings considered and FVIs were calculated. Further, the FVI values were normalized according to the maximum possible value of FVI, 80000, obtaining results from 6.25 to 77.5 out of 100. The normalized indexes were statistically distributed on account of the percentage of buildings that fell into FVI intervals of 5%. In Figure 24 the values are presented in a histogram and, in Figure 25 a cumulative curve.

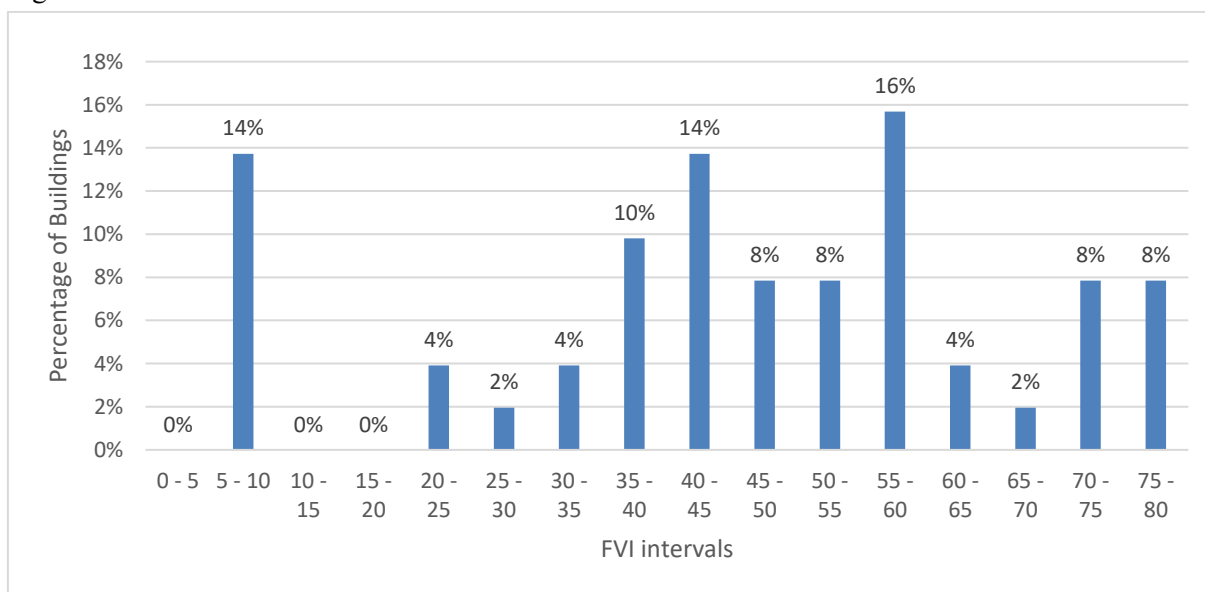


Figure 24: Frequency of Flood Vulnerability Indexes

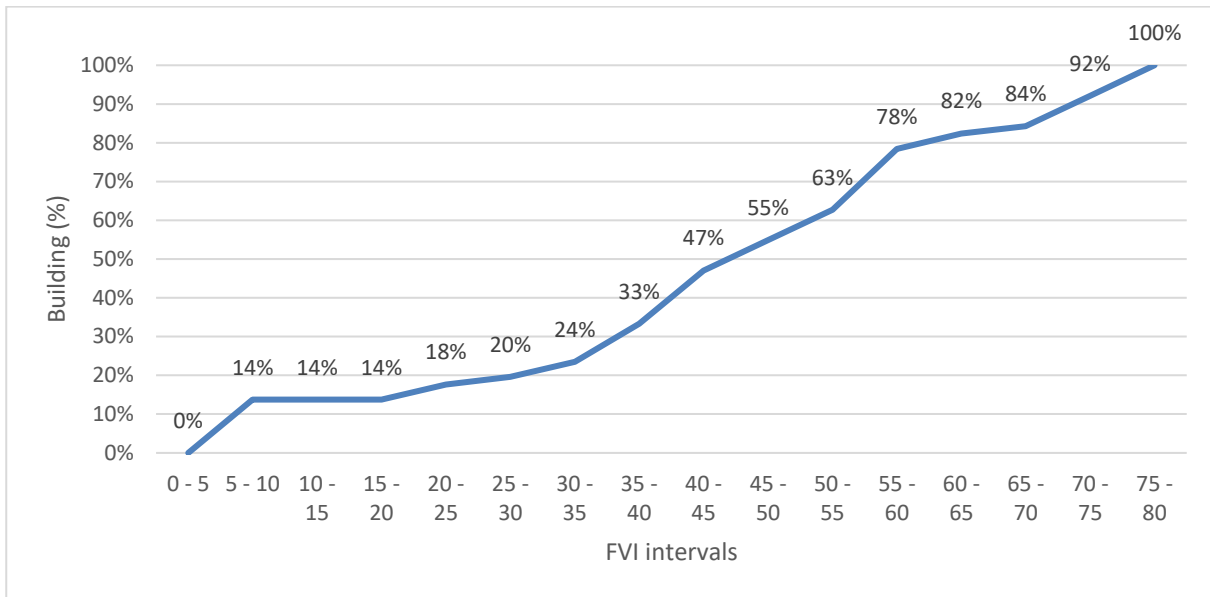


Figure 25: Cumulative distribution of Flood Vulnerability Indexes

The mean value of the 51 Flood Vulnerability Indexes assigned to analyzed cultural heritage sites was 40 with a standard deviation of 23. According to the cumulative frequency curve, it is possible to see that a very small number of them present FVIs lower than 20 (less than 20%), and most of the buildings present a flood vulnerability index from 20 to 60 (approximately 65%).

Subsequently, the information associated with each of the parameters was exported to ArcGIS, where vulnerability maps referring to the 9 attributes were created. The maps related to sensitivity and exposure parameters of the 51 buildings are presented from Figure 29 to Figure 36. In addition, a flood vulnerability index ranking and a map with the most vulnerable buildings (Table 8 and Figure 27) were produced.

Table 8: Ranking of the most vulnerable buildings

Ranking	Item	FVI	FVI Normalized
1	Mary of Health’s Church/ Cerkev Marije Zdravja	62000	77.50
2	St. Peter’s Church /Cervek Sv. Petra	62000	77.50
3	Pallazzo Bartole Fonda	62000	77.50
4	Part of the wall/Resslova ulica 1	62000	77.50
5	Sergej Mašera Maritime Museum Pomorski/ Musej Sergej Masera	59000	73.75
6	Piran’s Post Office /Posta Piran - Palazzo Bartoli Ventrella	56000	70.00
7	Punta/Piranski svetilnik	56000	70.00
8	Cliff/Natural heritage	56000	70.00
9	Palazzo Barbojo Trevisini	53000	66.25
10	Ulica IX. korpusa 2/ Piranske soline Piran (Benečanka)	50000	62.50

According to this ranking, the most vulnerable buildings among the 51 cultural sites analyzed are Mary of Health's Church (Figure 26), St. Peter's Church, Pallazzo Bartole Fonda, and part of the wall in Resslerova ulica 1, with a flood vulnerability index of 77.5 out of 100.



Figure 26: Mary of Health's Church/ Cerkev Marije Zdravja – One of the four buildings with the highest FVI



Figure 27: 10 most vulnerable buildings in Piran according to FVI

A map with the FVI class of all analyzed buildings is presented in Figure 28. The normalized FVIs were categorized as Low (0 - 25), Moderate (25 - 50), High (50 - 75), and Extreme (75 - 100). It can be seen that the buildings that belong to low vulnerability classes are mostly the ones in less exposed (elevated) areas, such as hilltops. Additionally, the most vulnerable assets are the ones in Punta, surrounding Tartini Square, and by the port.



Figure 28: Flood Vulnerability Index classes in Piran

Concerning building age, Figure 29 shows the cultural heritage buildings in Piran categorized by construction period. During the field survey, two classes of buildings' age could be distinguished: (1) buildings built until the 15th century and (2) buildings built from the 16th until the 20th century. Those categories were defined because there was no more detailed register available where all the buildings were included. For a few buildings, it was possible to know the exact year they were erected, for others, the century and, in some cases, the only information available was the style of the building (that usually refers to a century or a couple of centuries). In the city of Piran, most of the 51 buildings analyzed (41 or 80%) have been constructed between the 16th and 20th centuries. Most of the buildings that were constructed until the 15th century are parts of the wall, gates, and the church in Punta.

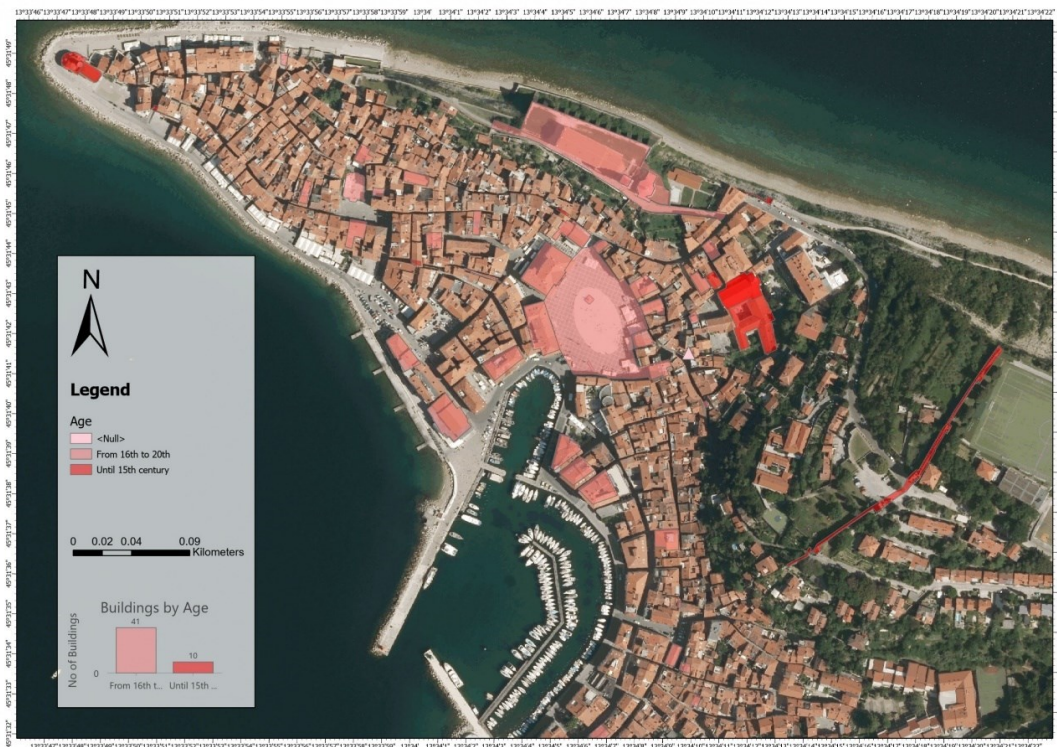


Figure 29: Age of cultural heritage buildings in Piran

Figure 30 presents the 3 categories defined to classify the condition of cultural heritage buildings: well-preserved, slightly damaged, and damaged. While well-preserved buildings are the ones in which it is not possible to see any significant sign of damage, slightly damaged buildings have signs of moisture, small cracks, superficial issues with painting, or limited surface recession (in the case of medieval constructions as the wall). The most extreme deterioration degree identified in Piran is one the of damaged buildings, with generalized cracking, exposed structure, presence of settlements and deformations, and intense surface recession. The map in Figure 21 shows that most of the heritage assets in Piran are in a slightly damaged condition, accounting for 47% of the buildings, followed by the well-preserved group with 33% and 20% of damaged buildings.



Figure 30: Condition of cultural heritage buildings in Piran

The 3 different categories chosen to express exposure are shown in Figure 31. Those categories are based on the geographical location of the cultural assets in the site in question: elevated areas, low-lying areas not exposed to the sea, and low-lying areas exposed to the sea. The low-lying areas exposed to the sea would be the ones with the highest degree of vulnerability and, in Piran's case, the ones with the highest density of cultural heritage buildings, with 23 assets or 45% of the sample. In addition, 41% of the constructions are located in low-lying areas not exposed to the sea and only 13% are located in elevated areas.



Figure 31: Exposure of cultural heritage buildings in Piran

Generally, The Ministry of Culture of the Republic of Slovenia defines 2 types of cultural heritage: exceptional or monument and regular or ordinary. Monuments would be buildings that present ornaments, frescoes (in churches, for example), or rich finishings. Regular buildings, despite having cultural significance, are not that elaborate. Most of the buildings studied are considered exceptional, summing up to 40 assets or 78% of the total (Figure 32).

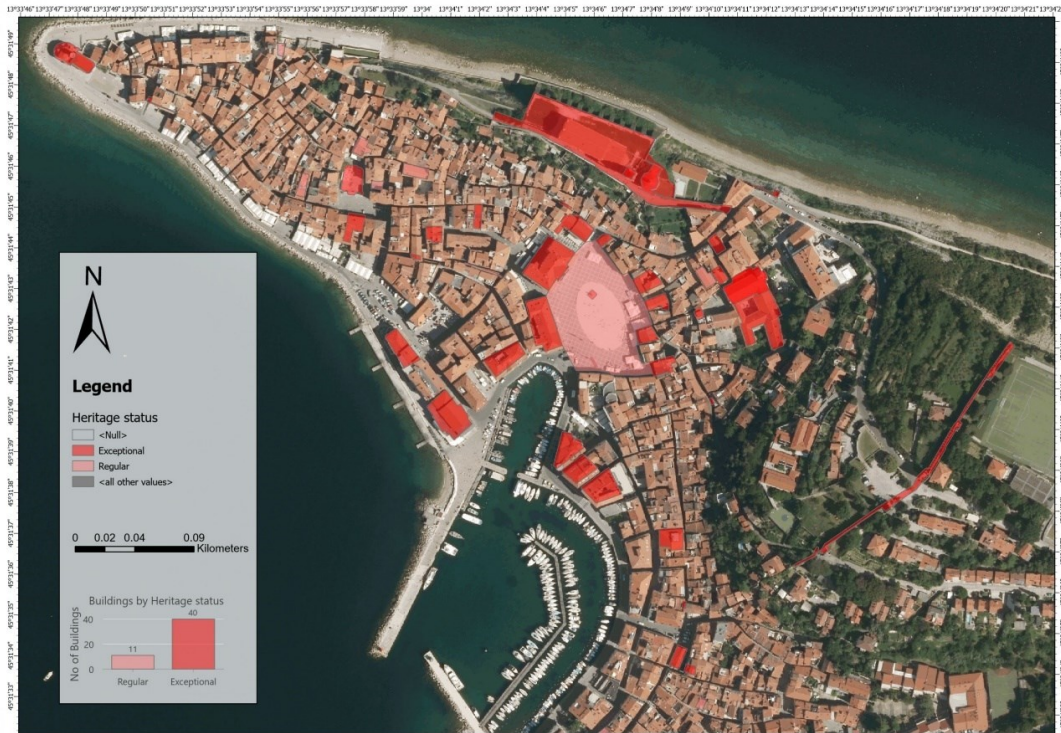


Figure 32: Heritage Status of cultural heritage buildings in Piran

During the field trip, particularity in the cultural heritage buildings in Piran was noticed and pointed out by the professors and the Ministry of Culture engineer. This particularity is the presence of a limestone base in the inferior part of the building façade (up to 50 cm) of many buildings, intending to protect the building construction and facade from floods and the negative effects of seawater. The geographical distribution of the presence of this base is presented in Figure 33. 35% of the analyzed buildings (or 18 constructions) were found to have a limestone base.



Figure 33: Presence of limestone base on cultural heritage buildings in Piran

As portrayed in other examples of calculations of FVIs, the number of stories is an important factor to consider when determining the vulnerability of a building. Assuming that the constructions have superficial foundations, the more floors a building has, the more vulnerable it would be to floods. In Figure 34 it can be seen that most of the assets considered have up to 3 floors and the ones that have more than 4 floors are exceptions such as church towers.



Figure 34: Numbers of stories of cultural heritage buildings in Piran

Figure 35 shows the buildings that have ornaments on their exterior or interior. Buildings with ornamental elements have a higher value and are, thus, considered to be more vulnerable to direct contact with seawater or other meteorological factors. Most of the constructions in Piran have these elements, accounting for 31 buildings or 58% of the sites.



Figure 35: Presence of ornaments on cultural heritage buildings in Piran

In Figure 36, it is possible to see which cultural heritage buildings were recently renovated in the city of Piran. Even if it may seem counterintuitive, some of the buildings that were recently renovated are not well-preserved ones. Part of the buildings that were subjected to interventions in the past few years may already have issues with painting or moisture. In Piran, 14 of the 51 buildings analyzed, or 27% are recently renovated constructions.



Figure 36: Occurrence of recent renovation on cultural heritage buildings in Piran

**4.4.1 Coastal City Flood Vulnerability Index (CCFVI)**

Hoping to contribute to future research regarding the threat of climate change in coastal cities on a global scale and for the country of Slovenia, 15 of the 19 CCFVI indicators proposed by Balica et al. (2012) were estimated for the city of Piran and presented in Table 9:

Table 9: CCFVI indicators for the city of Piran

No	Name	Abb.	Factor of	Unit	Definition	Piran
1	Sea-level rise	SLR	Exposure	mm/year	How much is the level of the sea is increasing in 1 year	1.7
2	Storm surge	SS	Exposure	m	A storm surge is the rapid rise in the water level surface produced by onshore hurricane winds and falling barometric pressure. Higher storm surge	3.76 or 0.76 above the mareographic zero
3	Foreshore slope	FS	Exposure	%	Foreshore Slope and depth of the sea near the coast,	0.16

					can change a lot and often. The average slope of the foreshore beach	
4	Coastal line	CL	Exposure	km	Kilometers of coastal line along the city	2.96
5	Cultural heritage	CH	Exposure	#	Number of historical buildings, museums, etc., in danger when coastal flood occurs	51
6	Population close to coastline	PCL	Exposure	#	Number of people exposed to coastal hazard	3787
7	Growing coastal population	GCP	Exposure	%	% of the growth of population in urban areas in the last 10 years	-7.26
8	Shelters	S	Susceptibility	#	Number of shelters per km <sup>2</sup> , including hospitals	24
9	Awareness and preparedness	A/P	Resilience		Are the coastal people aware and prepared for floods? Did they experience any floods in the last 10 years? (Scaled)	9
10	Recovery time	RT	Resilience	days	Amount of time needed by the city to recover to a functional operation after coastal flood events	14
11	km of drainage	Drain	Resilience	km	km of canalization in the city	5.198
12	Flood hazard maps	FRP	Susceptibility	-	Flood Hazard Mapping is a vital component for appropriate land use planning in flood-prone areas.	8
13	Institutional organizations	IO	Resilience	#	Existence of IO	4
14	Uncontrolled planning zone	UP	Exposure	%	% of the surrounding coastal area (10 km from the shoreline) is uncontrolled	0
15	Flood Protection	FP	Resilience	-	The existence of structural measures that physically prevent floods from entering the city (Storage capacity)	0

\* 4 of the 19 indicators were not presented due to the lack of data availability or applicability to the studied area

To obtain these indicators, the main sources were ARSO, the Slovenian Environment Agency of the Ministry of the Environment and Spatial Planning, the Surveying and Mapping Authority of the

Republic of Slovenia, the Slovenian Statistical Office (SURs), and documents provided by professors of the University of Ljubljana, such as reports of projects to increase the flood safety in Piran.

Concerning the presented information, it must be highlighted that Piran has a reasonably high awareness and preparedness indicator due to the high frequency of floods in the area (almost yearly) and the consequences of the last major flood event in 2019. After that flood event, the issuing of flood forecasts, installation of mobile barriers, and enhancement of the population's understanding of flood adaptation measures improved considerably. In addition, even though the shoreline is reinforced by ripraps installed 20 years ago in Piran, aiming to protect the seafront from waves, their effect is minimal, and, throughout the years, the materials have severely receded.

#### 4.5 Depth-Damage Curves

Once the spatial data was adapted for its insertion in KR PAN (Cumulative Calculation of Flood Damage and Analyses model), superposing of databases of the Ministry of Culture and KrpaP, the model was modified to incorporate the specificities of the cultural heritage sites in Piran, through the inclusion of the FVIs. Subsequently, to better describe the damage to cultural heritage, three depth damage curves were included in the model, one provided by the Ministry of Culture and two found in the literature, related to specific construction materials or building typologies. The depth-damage curves that were inserted in the model are described below and the studies that led to their obtention were previously presented in section 2.5. It must be highlighted that, as previously mentioned in the literature review, the influence of salt intrusion could not be accounted more in detail for when adapting or developing new depth-damage curves, due to the lack of available data, adequate time, equipment, and labor, despite the relevant effects of sea floods in Piran.

The depth-damage curve provided by the Ministry of Culture considered the most suitable for this work was the one regarding the first floor of cultural heritage buildings. The one-story curve is fundamental because many times, it is only required to perform renovations on the first story, which is usually the most damaged story in the building.

For the present research, the most significant piece of information presented by Martínez-Gomariz et al. (2020) was considered to be the church and singular building depth-damage curve. Nevertheless, the methodology created to allow the transferability of depth-damage curves was described as it could be applied in the future as a way of increasing the accuracy of depth-damage curves for all municipalities in Slovenia.

The depth-damage curve presented by Englhard et al., (2019) considered relevant for the development of the present work is the one referring to class III a (unreinforced stone or stone masonry buildings with one floor). Concerning its vulnerability, class III buildings are considered to be less resistant than reinforced buildings because they are less capable of withstanding floodwater pressure on their walls. Nevertheless, stones are sturdier than materials such as wood and earth and, therefore, would be less prone to disintegration, surface recession, and substitution after a flood event (Englhard et al., 2019).

Finally, the three depth damage curves selected for the present work are presented in Figure 37: one provided by the Ministry of Culture for buildings with one floor (blue), one referring to churches and singular buildings from Martínez-Gomariz et al. (2020) (red) and one for stone buildings with one floor, presented in Englhard et al.'s (2019) article (green). Those 3 curves were incorporated into the KR PAN software and there, 2 simulations were performed: the first with all damage calculated based

on the curve provided by the Ministry of Culture (curve 12); and the second with the sandstone masonry buildings associated with the depth-damage curve from Martínez-Gomariz et al. (2020) (curve 14) and with buildings made of raw stone or more vulnerable materials linked with the Enghard et al.'s (2019) curve (curve 13). This correspondence is clarified in Table 10 below:

Table 10: Explanation of the 2 simulations executed in KRPAN

		Type of Building	Depth-damage curve (Source)	Curve ID
Simulation	Simulation 1	All buildings	Ministry of Culture	12
	Simulation 2	Sandstone masonry buildings	Martínez-Gomariz et al. (2020)	13
		Buildings made of raw stone and more fragile materials	Enghard et al. (2019)	14

The reason behind those curves' choices (curves 13 and 14) was the fact that they describe structure types that are similar to the cultural heritage buildings located in Piran, especially regarding their construction material. In this way, it would be possible to incorporate the building material type into the calculation of damage to cultural heritage assets. The results from the curves obtained from the literature review would then be compared with the damage values acquired when only the Ministry of Culture's curve (curve 12) is considered, assuming that, as this curve is a result of a local study (for cultural heritage in the country of Slovenia), it should be the one that reflects the most consistently the impact of floods on the cultural heritage buildings in Piran.

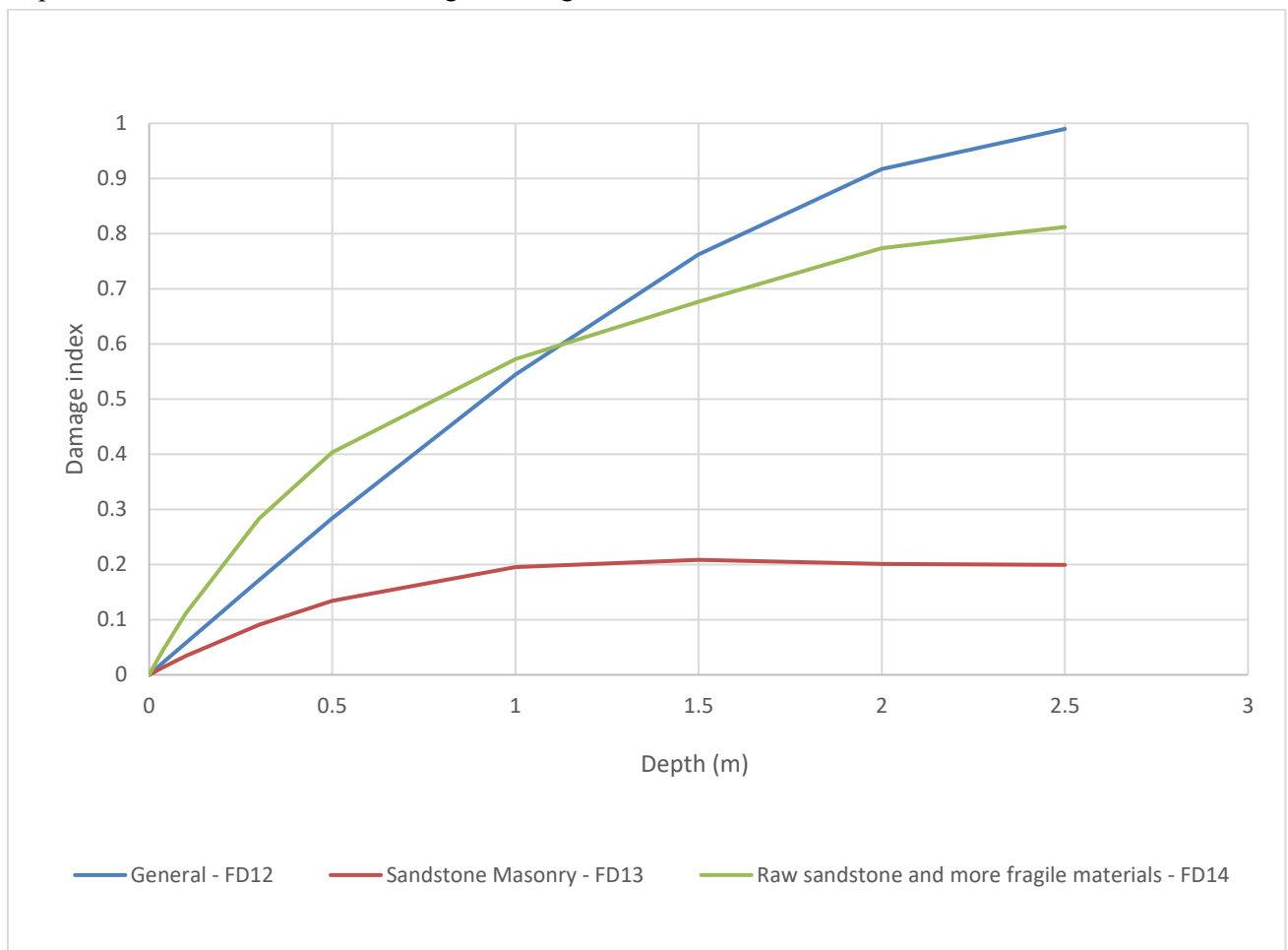


Figure 37: Depth-damage curves selected for the present work. General (blue), raw sandstone, more fragile materials (green), and sandstone masonry (red).

#### 4.6 Evolution of the number of salt transition cycles

Multiple articles presented in section 2.3 point out the increase in the number of salt transition cycles as one of the causes of cultural heritage deterioration due to climate change. That would be because the climate alterations would allow the salts present in the building materials or introduced by precipitation or capillarity to precipitate more often inside the materials' pores and, in that way, create fractures and weaken them. Based on the work of Ciantelli et al. (2018), which estimated the impact of climate change, and more specifically, salt weathering, on UNESCO cultural heritage sites in coastal areas, the present research performed a superficial assessment of the gradual long-term impact of salt deterioration in the future caused by climate change.

Ciantelli et al. (2018) compared the number of past and future salt transition cycles predicted by diverse regional climate models (RCM) for each month of the year. On the other hand, the present work aimed to see the evolution of the number of salt dissolution–crystallization cycles year by year and, to assess that, the number of salt transition cycles forecasted until 2100 was obtained. Such data is provided by RCM, that, in this case, was assembled in the CORDEX experiment. The CORDEX experiment comprises RCM simulations portraying various future socio-economic scenarios (Copernicus.eu, 2023).

Following the methodology of Ciantelli et al. (2018), the number of times in a year that the average daily relative humidity crossed the threshold of 75.3% when decreasing and the temperature was equal to or higher than 25°C was computed (assuming the analyzed salt to be NaCl). The number of times that the average daily relative humidity crossed the threshold when decreasing is computed because that would be when the salts go from a liquid to a solid state. This data was collected in the CORDEX Site (Domain EUR 11), and two variables were collected, near-surface relative humidity (hurs) and temperature of air surface (tas). For both variables, daily predicted data from a rcp4.5 scenario from 2023 to 2100 were downloaded. The rcp4.5 scenario was chosen because it is an IPCC intermediate scenario, that presents neither optimistic nor pessimistic predictions.

To treat the data, an R code was utilized, to transform .nc files into time series and apply the data to the municipality of Piran. The analysis and visualization of the data were performed in Excel and are further presented in the results section.

## 5 RESULTS

This chapter deals presents the results of the qualitative and quantitative evaluation of flood damage to cultural heritage under a series of mean sea level rise scenarios. Additionally, it displays the results of a superficial assessment of the gradual long-term effect of salt transition cycles in cultural heritage assets.

### 5.1 Qualitative Flood Risk

Similar to the studies presented in section 2.2, the present work performed a qualitative flood risk assessment of cultural heritage buildings in Piran. For this assessment, the vulnerability, represented by the FVIs previously calculated was intersected with hazard levels, translated in flood depths, to classify the 51 analyzed buildings in 3 flood risk classes: low, high, and moderate. The vulnerability and hazard were intersected according to a flood risk matrix.

Based on this qualitative assessment of flood risk by Davis et al. (2023), which also calculated FVIs, a similar flood risk matrix was created for our study which is adapted to flood hazard classes in Slovenian legislation and is presented in Table 11:

Table 11: Flood risk matrix – present work. H is water height in m.

Flood Risk	Hazard Level		
	Low	Moderate	High
Flood Vulnerability Index	H<0.5	0.5<H<1.5	H>1.5
Extreme (>75)	High	High	High
High (50 – 75)	Moderate	High	High
Moderate (25 – 50)	Moderate	Moderate	High
Low (<25)	Low	Moderate	Moderate

The basic differences between the flood risk matrix created by Davis et al. (2023) and the one adapted to the present study are the non-existence of a class of negligible flood risk, a division of the flood vulnerability index that is independent of the mean and the standard deviation of the sample and the selection of only three hazard levels, with values of water depth equal and above 1.5 m being considered high. Based on the flood risk matrix presented in Table 11, the buildings were categorized into three flood risk classes for return periods of 10 and 100 years and mean sea level rise scenarios S0 (no sea level rise considered), S3 (most probable, with a mean SLR of 0.3m) and S7 (most extreme, with a mean SLR of 1.46m).

Figure 38 presents the flood risk class distribution of the 51 buildings for the 6 scenarios. The graph shows that the 10-year return period is the one that presents the highest shift between the flood risk classes when the sea level rise scenarios change. Besides that, the smallest shift occurs when the buildings are exposed to the same mean sea level rise scenario of 1.46m and the return periods are changed from 10-year to 100-year. Furthermore, for all scenarios the percentage of buildings included in the low-risk flood class is very similar, ranging from 16 to 18%. The buildings present in that class are mostly the ones located in elevated areas. The smaller percentage of the buildings in the low-risk class (16%) is associated with the most extreme sea level rise scenario (S7).

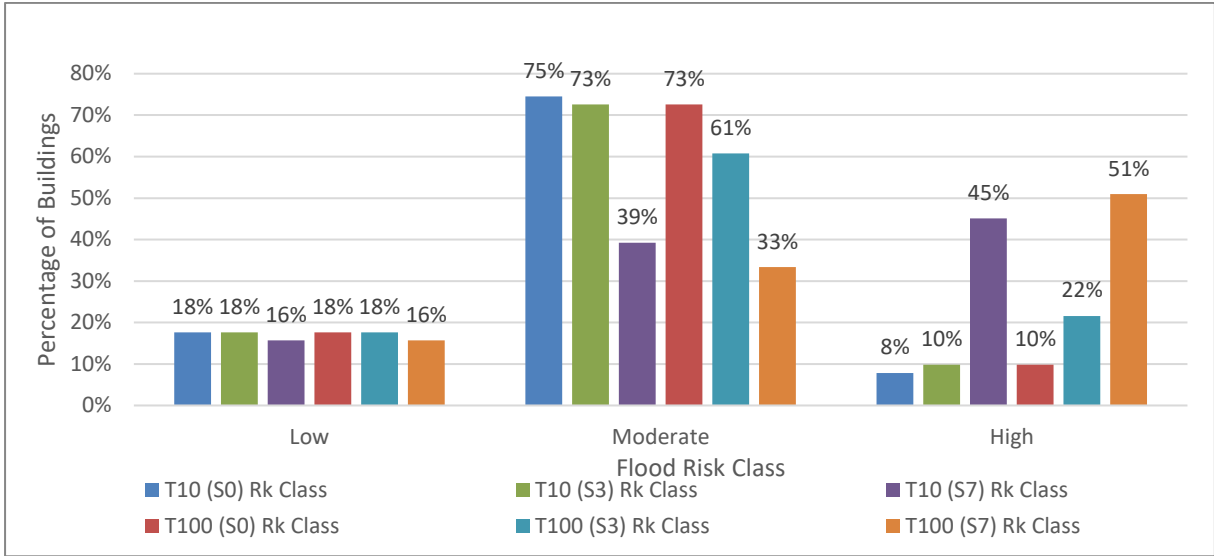


Figure 38: Flood Risk Distribution for the cultural heritage buildings in Piran

To better visualize the flood risk class of each building, flood risk maps were created in GIS and are presented from Figure 39 to Figure 44.

Under a 10-year return period scenario with no sea level rise (Figure 39), the majority of the buildings (73%) were included in the moderate risk class, followed by 9 of the 51 assets in the low-risk class and 4 in the high-risk one. The constructions positioned at higher elevation account for the biggest part of the low-risk class. The buildings considered to be under high risk are in very exposed locations, such as in Punta, in contact with the port, and in direct contact with Tartini Square.

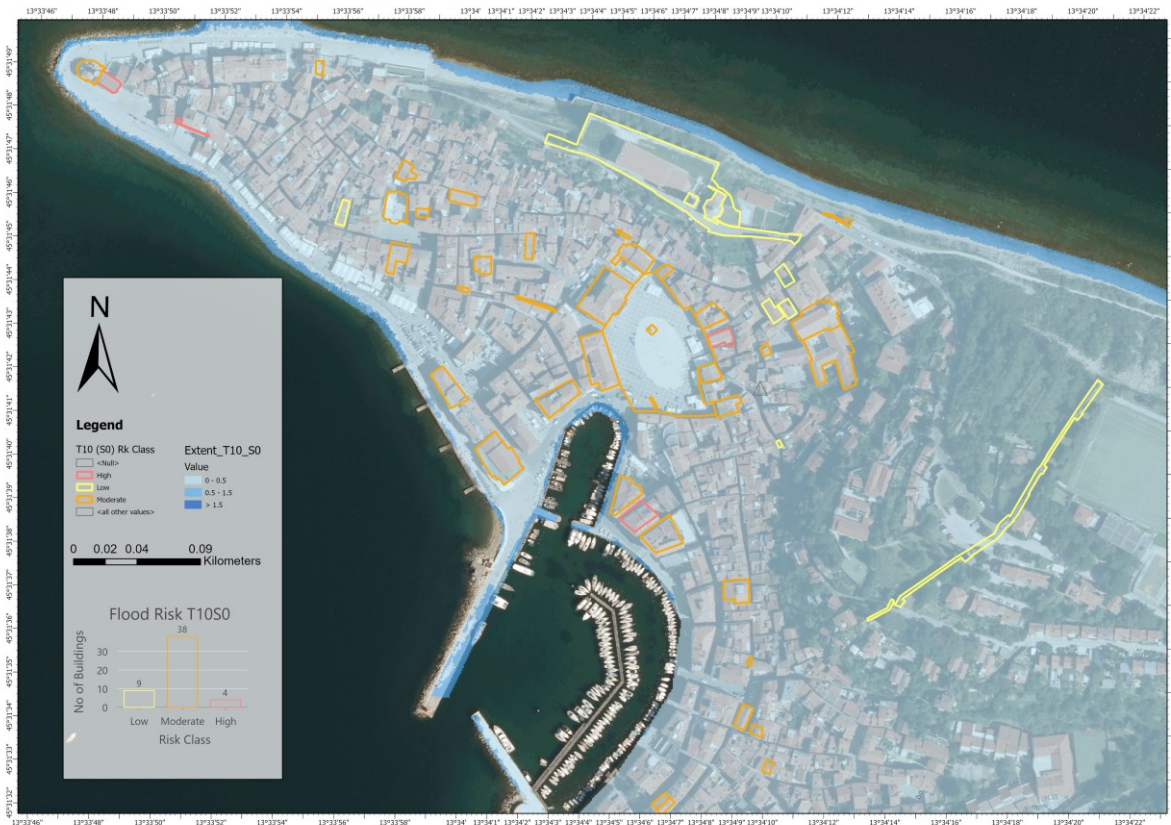


Figure 39: Risk Classes for the 10-year return period and no sea level rise (S0).

For a 10-year return period and 0.3m mean sea level rise (Figure 40), the distribution of the flood class risk of the buildings is only slightly altered in comparison with the scenario with no sea level rise. The number of buildings present in the low-risk class remains the same and one of the buildings under a moderate flow risk when SLR is not taken into consideration shifts to the high-risk class. to the constructions positioned at higher elevation account for the biggest part of the low-risk class. The asset that shifted flood risk classes was the lion statue in Tartini Square called “Leone di San Marco”.

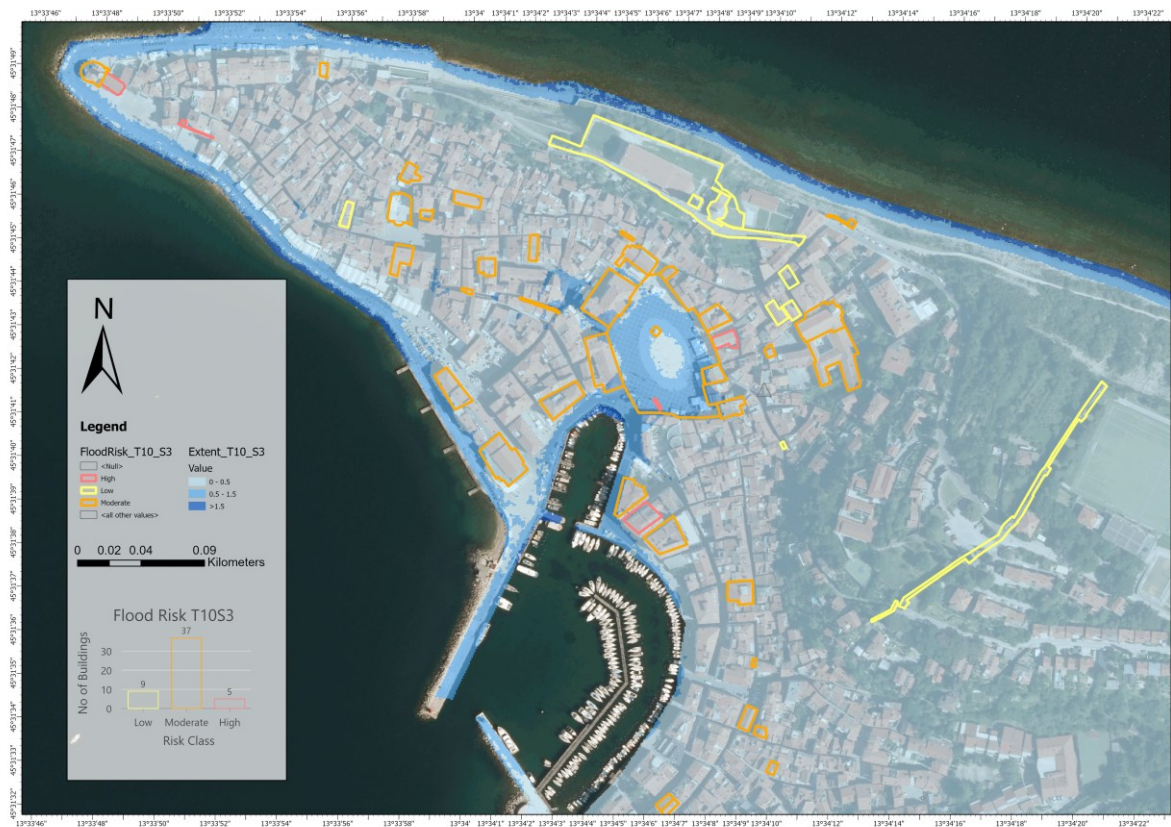


Figure 40: Risk Classes for the 10-year return period for a 0.3m mean sea level rise (S3).

Under a 10-year return period scenario with an elevated mean sea level rise of 1.46m (Figure 41), the majority of the buildings (45%) are included in the high-risk class. When compared with the most expected sea level rise (0.3m) it can be seen that 18 buildings (or 35%) increased their risk category from moderate to high. Additionally, most of the buildings present in the low-risk category for a 0.3m mean sea level rise are maintained in that category even when subjected to a mean sea level rise of 1.46m, only one out of nine buildings went from low to moderately endangered.



Figure 41: Risk Classes for the 10-year return period for a 1.46m mean sea level rise (S7).

Under a 100-year return period scenario with no sea level rise (Figure 42), the buildings have the same distribution as in the 10-year return period scenario and most expected mean sea level rise (0.3m). 73% of the assets are under a moderate flood risk, 9 are in the low flood risk class, and 5 are in the high-risk one. When compared with a 10-year return period scenario with no sea level rise. One asset changed categories from moderate to high-risk class, the Leone di San Marco located in Tartini Square.

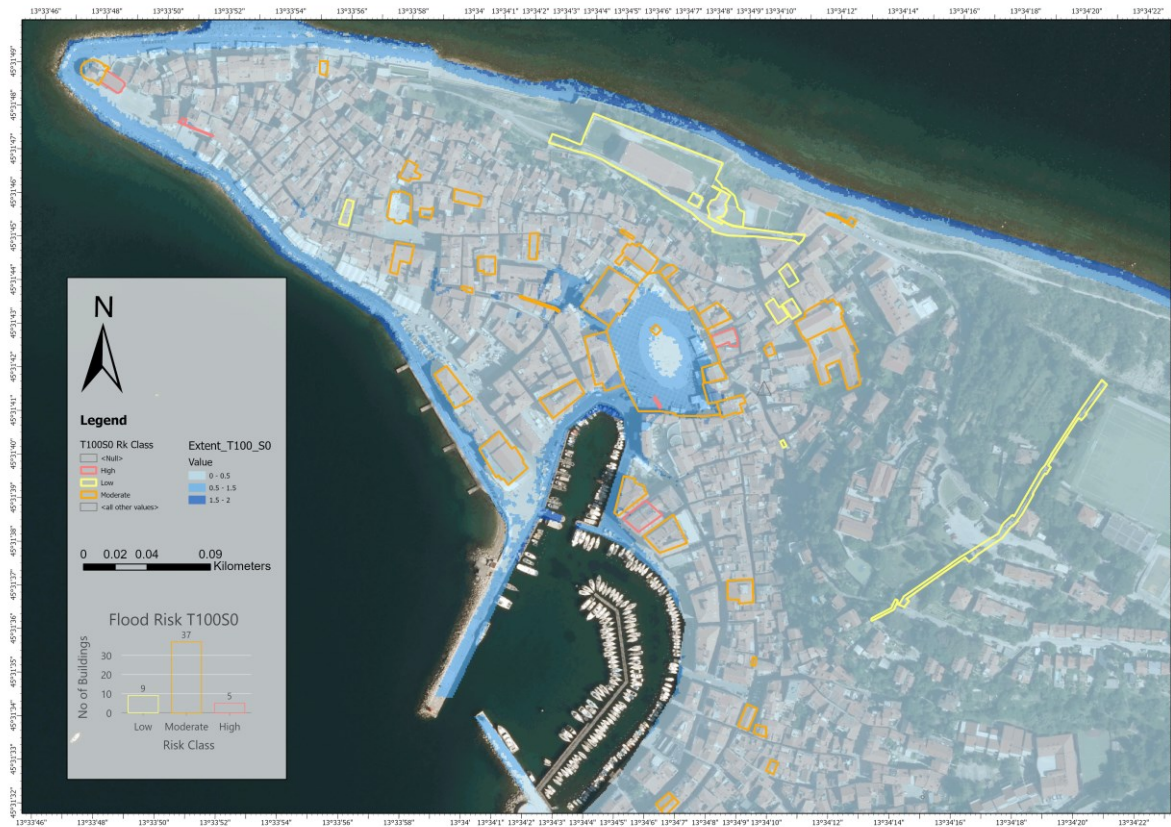


Figure 42: Risk Classes for the 100-year return period and no sea level rise (S0).

Considering a 100-year flood scenario with the impact of 0.3m mean sea level rise (Figure 43), 61% of the assets are under moderate flood risk. Comparing this state with a 10-year return period one with the same sea level rise, it is possible to see that the same number of buildings remain in the low-risk category and 6 of the buildings (12 %) are transferred from the moderate class to the high-risk one. That means that the influence of the sea level rise variation from expected to extreme is bigger than the impact of the change from a 10-year to a 100-year return period. This could be attributed to the fact that the difference in flood height between the two return periods (T10 and T100) is smaller than the difference between the SLR scenarios (S0, S3, and S7). Regarding the 100-year flood scenario with no sea level rise, 6 buildings shift from the moderate risk class to the high-risk one.

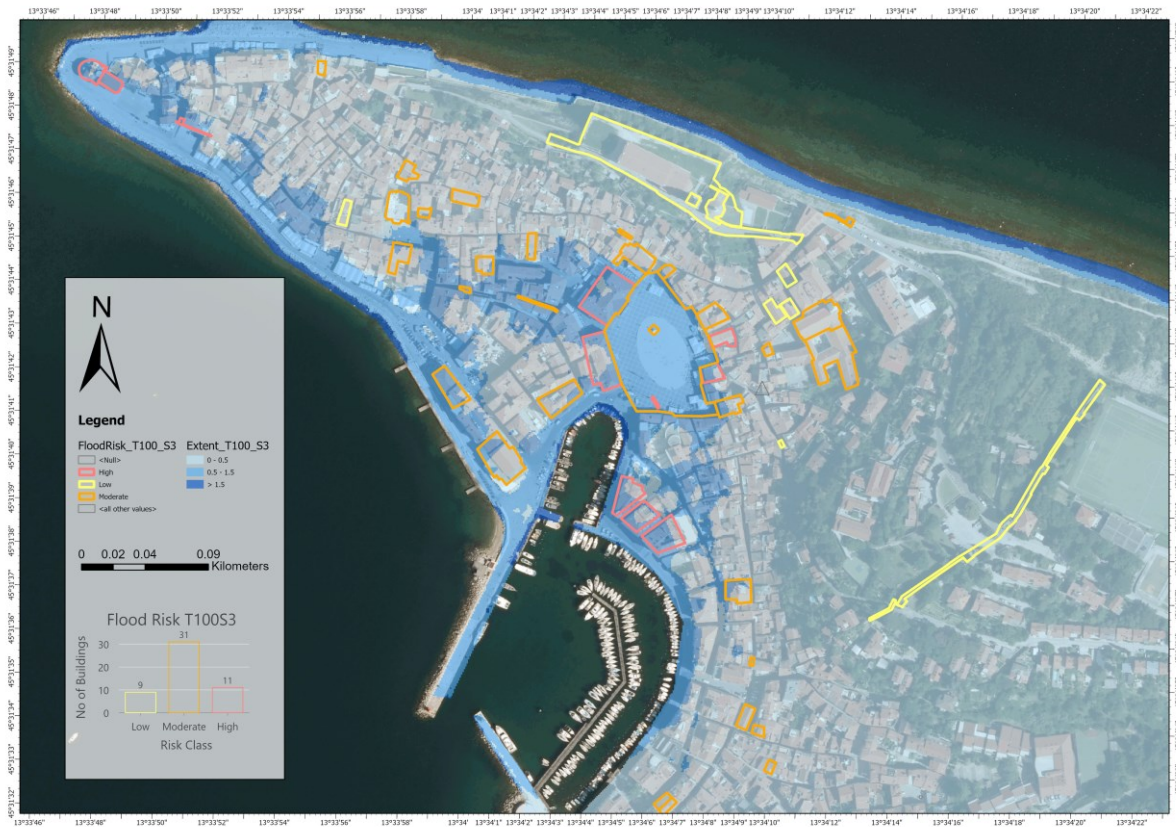


Figure 43: Risk Classes for the 100-year return period for a 0.3m mean sea level rise.

In the most extreme case considered for the qualitative flood risk, 100-year return period and 1.46m mean sea level rise, the largest part of the cultural sites (51%) is under high risk. In Figure 44 it can be seen that the 8 buildings under the low-risk class, located in higher areas, will not be affected by floods even under the worst flood scenario considered. The buildings that do not belong to the high-risk class are mostly located in more sheltered somewhat elevated areas further from the coast. In addition, in comparison to the distribution of risk for the same return period and less important sea level rise, 13 buildings (25%) shifted from a moderate risk category to a high one.

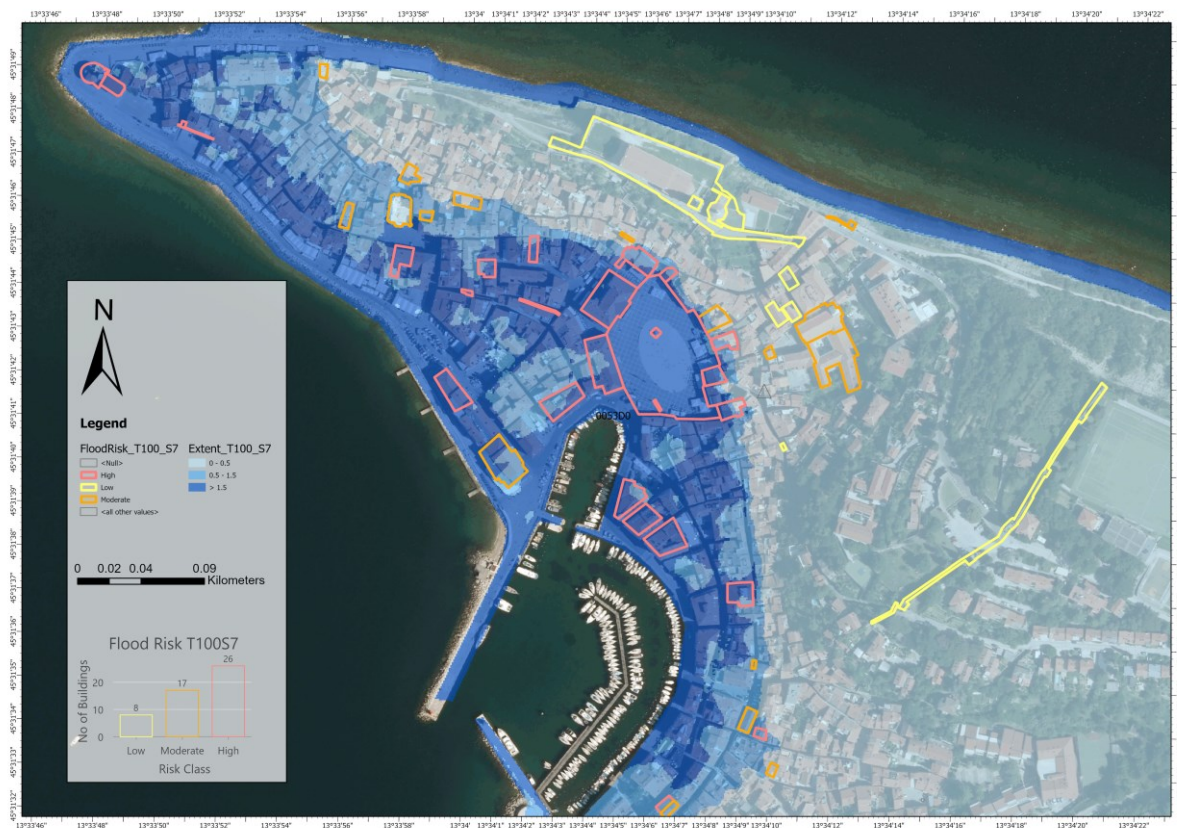


Figure 44: Risk Classes for the 100-year return period for a 1.46m mean sea level rise.

## 5.2 Quantitative Flood Risk

The quantitative flood risk assessment of cultural heritage performed in the present work was executed through the implementation of the KR PAN model (the Cumulative Calculation of Flood Damage and Analyses for the Slovenia territory). The model contains historical damage data that were coupled with the three selected depth-damage curves (two selected from the literature and one created by the Ministry of Culture of Slovenia (Figure 37)), and the previously calculated FVIs to deliver damage costs for each of the 51 buildings analyzes along with the shapes of the affected area.

When comparing the 6 climate change scenarios and the 3 flood scenarios not considering sea level rise (S0), it can be seen that only for the 3 most mild scenarios (current state for 10 and 100-year return periods and 0.3m mean sea level rise (S3) for 10-year return period) the damage cost of FD13+FD14 surpasses the cost of FD12. As the scenarios become more extreme, the cost difference between the two combinations of curves gets larger and, for the flood scenario referring to a 1000-year return period with a mean sea level rise of 1.46m, this difference reaches more than 2 million euros, and the expected damage costs estimated with FD12 are almost double the costs estimated with FD13+14. It can also be observed that, when FD12 is applied, the difference in damage costs for different mean SLR scenarios is larger than when using FD13+FD14.

In every case, FD13 has the lowest damage cost associated with it, both because it is associated with less vulnerable buildings and also because the minority of the sample is linked to that curve. These characteristics are also reflected in the shape of the curve presented in . When compared with FD12 and FD13, FD14 ascends more mildly and only reaches a damage index of approximately 0.2, while FD13 gets to 1 and FD14 to more than 0.8.

Regarding the influence of different sea level rise scenarios, it is possible to see that the damage values for a mean sea level rise of 1.46m are much larger than for a 0.3m meter one, reaching a 529% increase for a 10-year return period (using FD12). When compared to the damage costs of a no sea level rise scenario, the values for the most extreme sea level rise and a 10-year return period are more than 25 times higher (also considering FD12). This return period is the one that presents the largest difference between the damage costs for a no sea level rise scenario and the most extreme one (as the return period gets larger the increase in sea level rise causes a smaller impact). As an example, considering FD12, comparing the no sea level rise scenario with the 1.46m mean sea level rise one, for a 10-year return period the costs of the most extreme SLR scenario are 25 times higher than the no SLR, for a 100-year return period, 6 times higher and for a 1000-year return period only 3 times higher.

For all scenarios, the increase in sea level rise affects the costs calculated with curve FD12 the most, followed by the costs obtained with curve FD13 and with curve FD14. The simulation that uses curves FD13+FD14 is also less affected by sea level rise for any return period scenario when compared with the one using FD12. As an example, comparing 10-year return period scenarios, one with no sea level rise and the other with 1.46m mean sea level rise, FD12 shows values 25 higher for the most extreme scenario, FD13 values are 21 times larger, FD14 values 9 times higher and FD13+14 have values 10 times larger.

Furthermore, it can be seen that the number of buildings affected by the 6 climate change scenarios does not change much, ranging from 28 for a 10-year return period and no SLR to 39 for a 1000-year return period and 1.46m mean SLR. That occurs because, due to the municipality's topology, the buildings located in high elevations are never affected by floods.

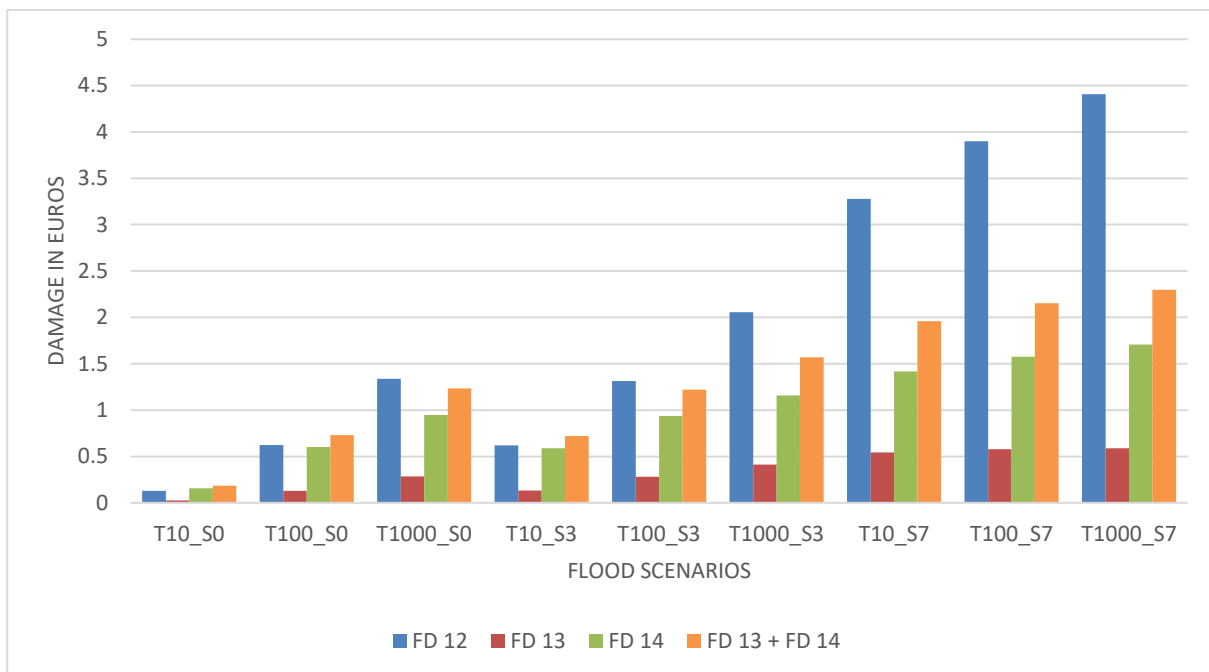


Figure 45: Damage per flood scenario and depth-damage curve

Concerning the uncertainty of the damage costs calculated in this work, the use of three different depth-damage curves (FD12, FD13, and FD14) accounted for particularities that cultural heritage buildings might have. Since FD12 and FD14 show a behavior significantly different from FD13 (Figure 46) it is expected that the damage in the buildings analyzed is described by depth-damage curves that

could fit in the uncertainty band (marked with purple stripes) delimited by the three curves. The simulation that considers the combination of curves FD13 and FD14 would better account for such uncertainties since it would give more importance to the differences in typology and material among buildings. Such information could help direct further studies when upgrading or tailoring depth-damage curves to better predict damage costs.

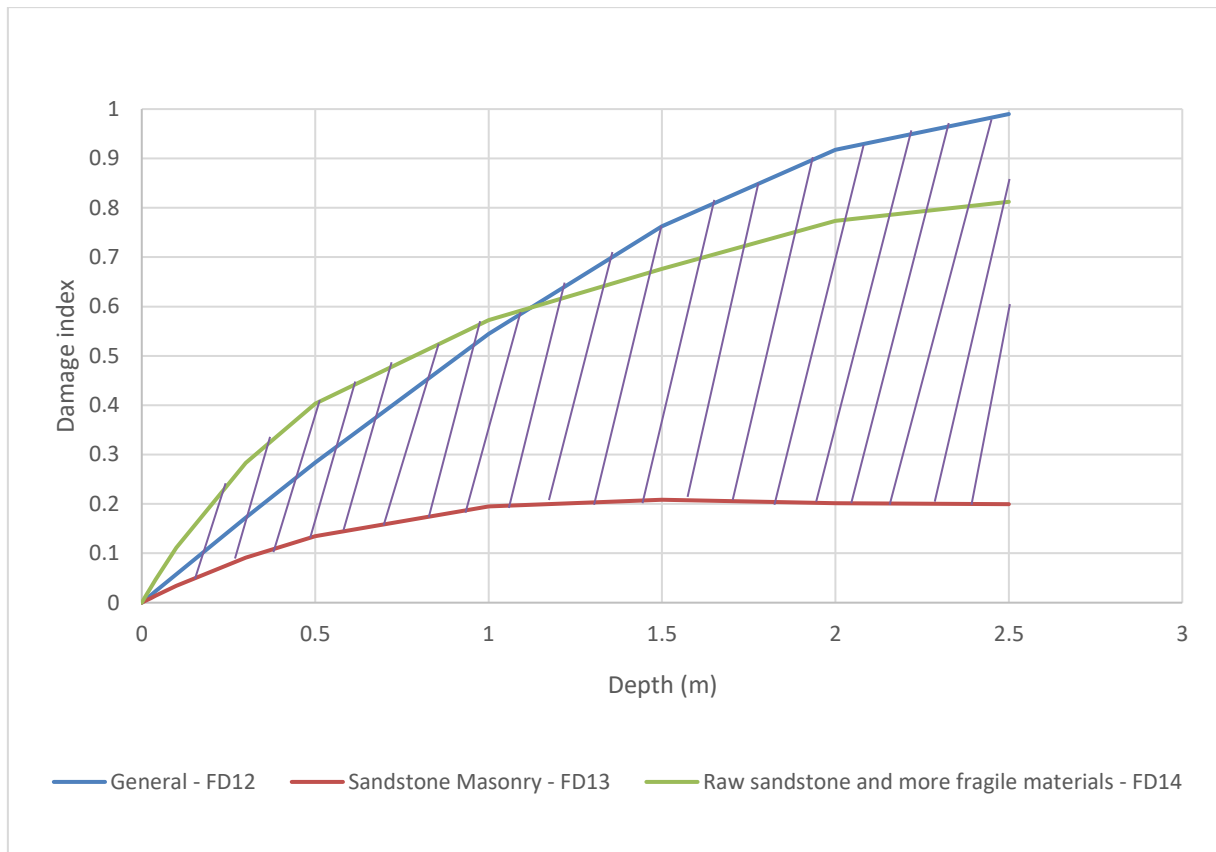


Figure 46: Damage per flood scenario and depth-damage curve with uncertainty bands (purple stripes)

Furthermore, analyzing the uncertainty bands in view of flood scenarios with different return periods and sea level rise projections, for less extreme scenarios (especially for the 10 and 100-year return periods) the difference in total damage cost to cultural heritage in Piran is not very large, reaching a maximum of a million euros for T100 (S0) (Figure 47). Nevertheless, as the mean SLR scenarios get more severe and the return periods larger, the damage costs estimated by the curve gradually diverge more. This span of the simulated scenarios would account for the uncertainty associated with these estimations as it covers many different future outcomes. This knowledge is highly relevant for decision-makers responsible for cultural heritage preservation and protection.

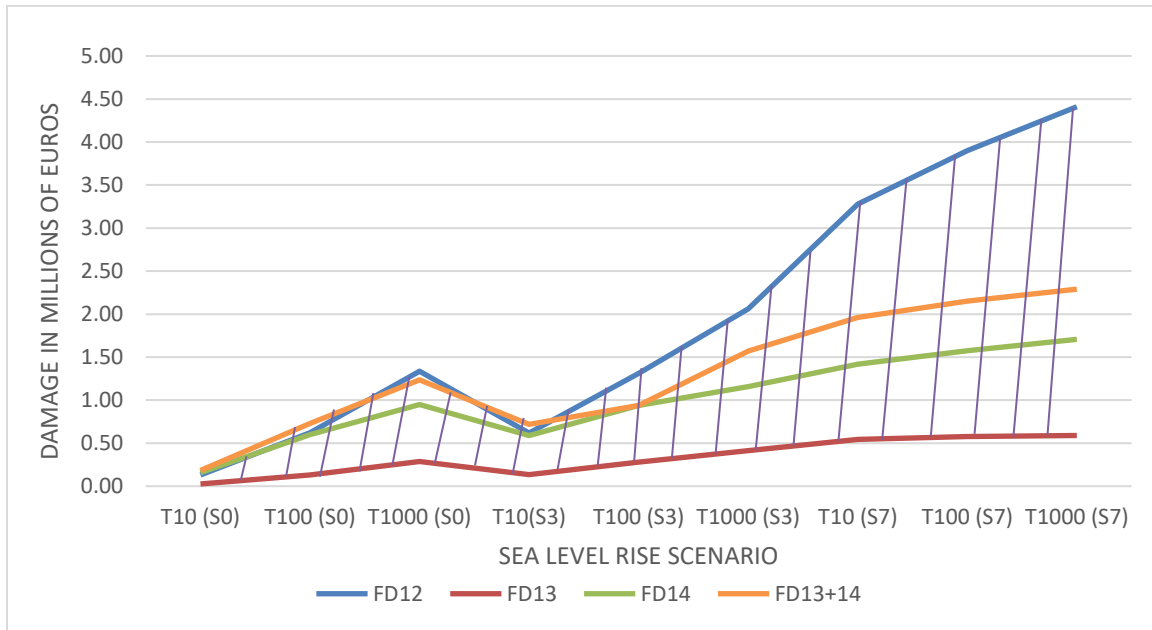
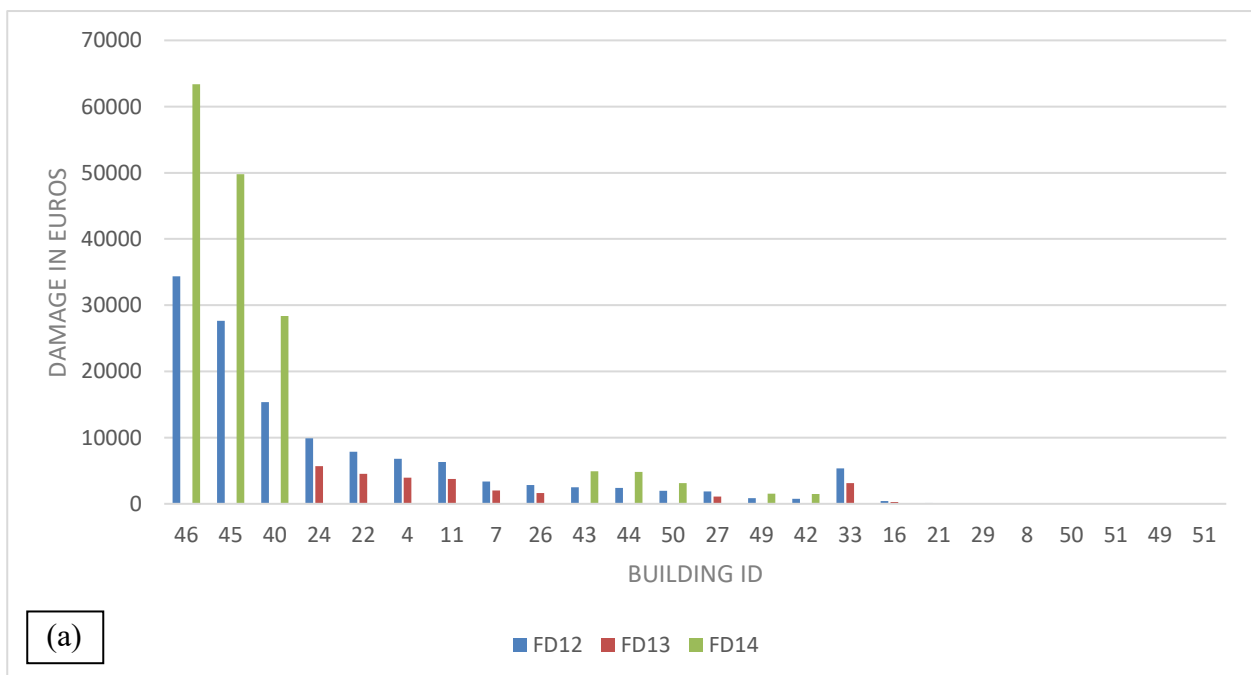


Figure 47: Comparison between damage estimates: Damage per flood scenario (in millions of euros) and depth-damage curve with uncertainty bands (purple stripes)

For a 10-year return period flood scenario with no sea level rise (Figure 48), it is possible to observe that the damage costs vary from 63,380 (FD14) for Tartini Square 2 to less than 100 euros (FD13) for Tartinijev trg 3/Mestna Kavarna. Furthermore, 21 of the 51 assets (41%) present flood damage. Concerning the application of the 3 depth-damage curves to estimate the damage costs, the combination of curves FD13 and FD14 (curves found in the literature) shows higher damage costs than the FD12, curve provided by the Ministry of Culture of Slovenia.



(a)

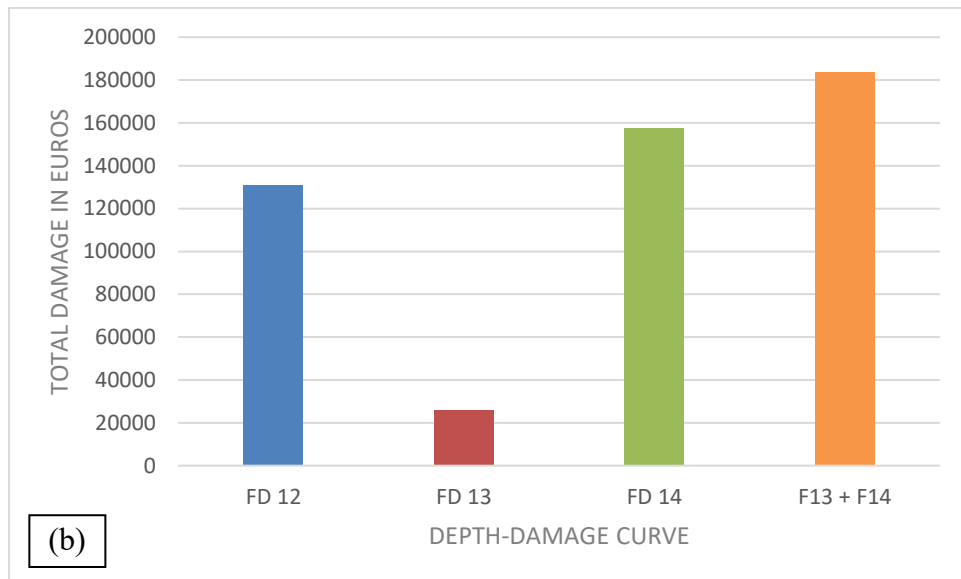
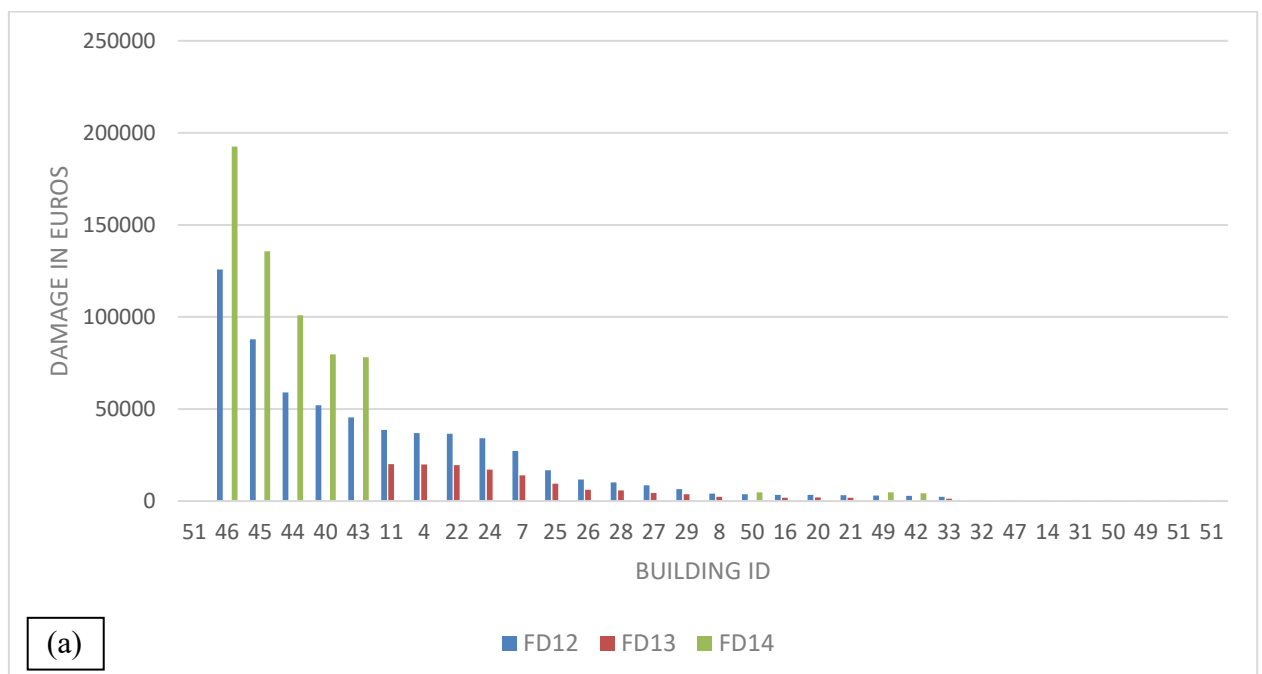


Figure 48: Damage per (a) building and (b) curve for a 10-year period and no sea level rise

For a 100-year return period flood scenario with no sea level rise (Figure 49), it is possible to observe that the damage costs vary from 192,607 (FD14) for Tartini Square 2 to less than 100 euros (FD13) for Church Prvomajski trg. Furthermore, 28 of the 51 assets (55%) present flood damage. Concerning the application of the 3 depth-damage curves to estimate the damage costs, the combination of curves FD13 and FD14 (curves found in the literature) shows higher damage costs than the FD12, curve provided by the Ministry of Culture of Slovenia.



(a)

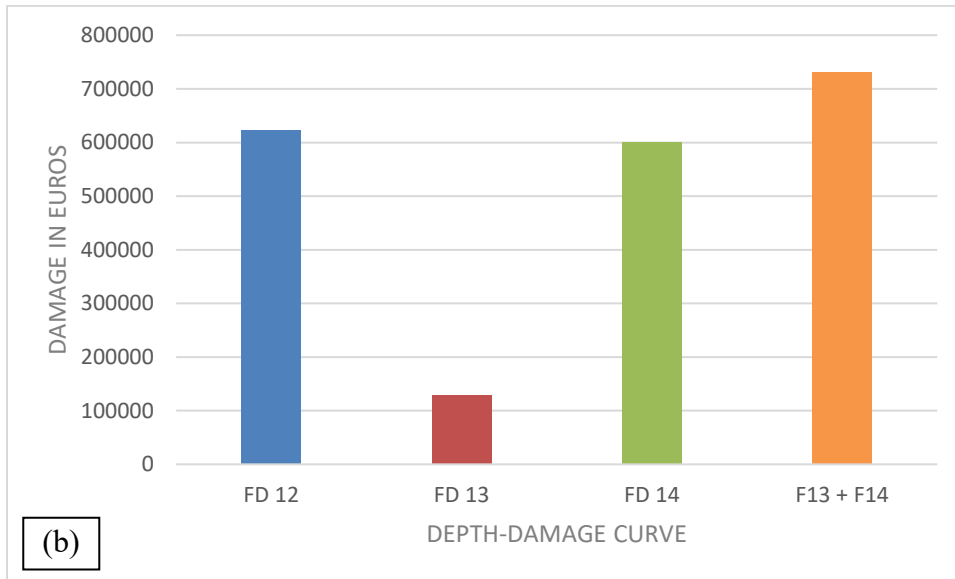
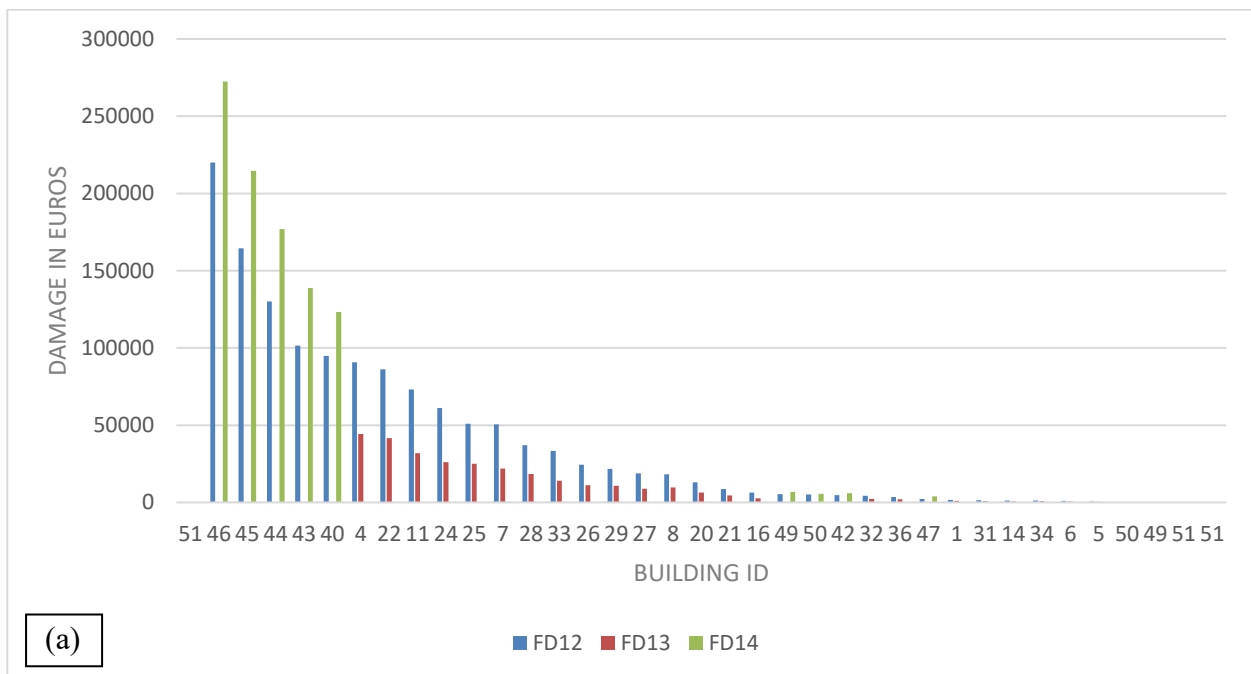


Figure 49: Damage per (a) building and (b) curve for a 100-year period and no sea level rise

For a 1000-year return period flood scenario with no sea level rise (Figure 50), it is possible to observe that the damage costs vary from 272,379 (FD14) for Tartini Square 2 to 600 euros (FD13) for Pecarstvo Andrej Turk s.p.. Furthermore, 28 of the 51 assets (55%) present flood damage. Concerning the application of the 3 depth-damage curves to estimate the damage costs, the combination of curves FD13 and FD14 (curves found in the literature) shows higher damage costs than FD12, a curve provided by the Ministry of Culture of Slovenia.



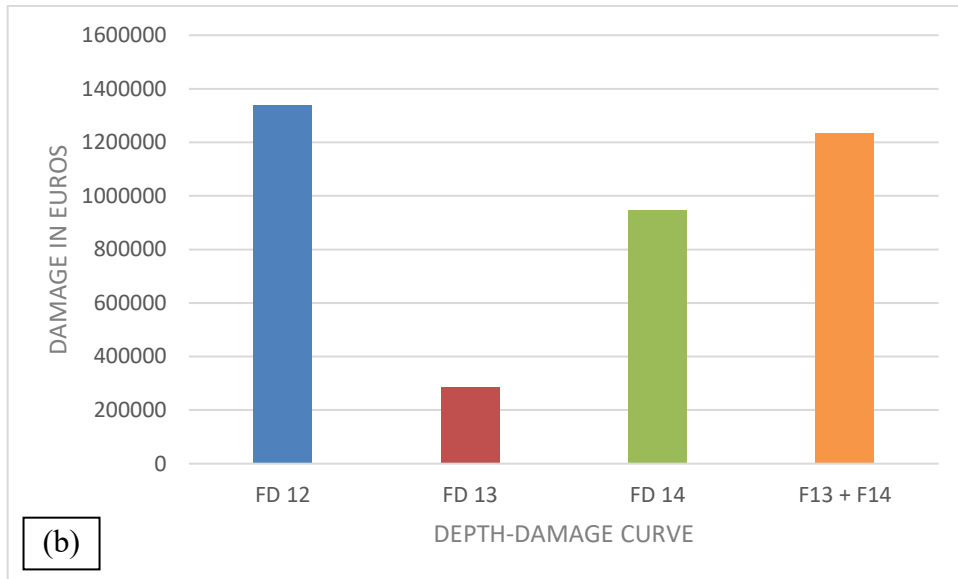
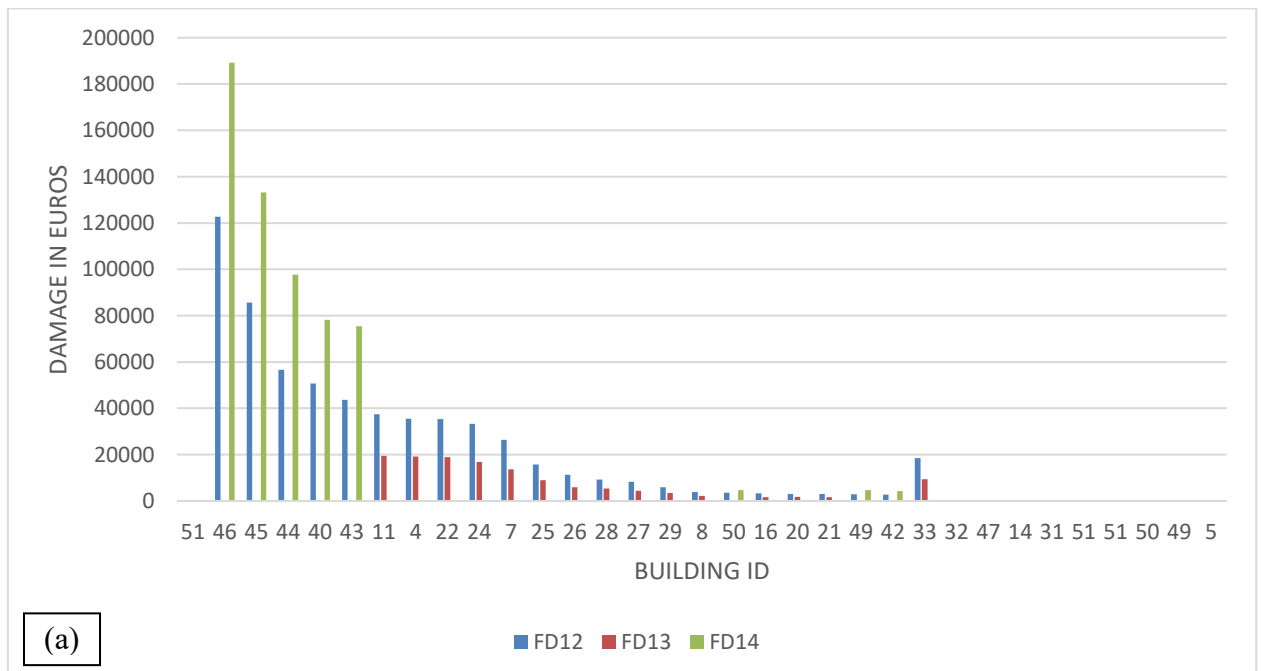


Figure 50: Damage per (a) building and (b) curve for a 1000-year period and no sea level rise

For a 10-year return period flood scenario with a 0.3 mean sea level rise (Figure 51), it is possible to observe that the damage costs vary from 189,200 euros (FD14) for Tartini Square 2 to less than 100 euros (FD13) for the Church in Prvomajski trg. Furthermore, 32 of the 51 assets (63%) present flood damage. Concerning the application of the 3 depth-damage curves to estimate the damage costs, the combination of curves FD13 and FD14 (curves found in the literature) shows higher damage costs than the FD12, curve provided by the Ministry of Culture of Slovenia.



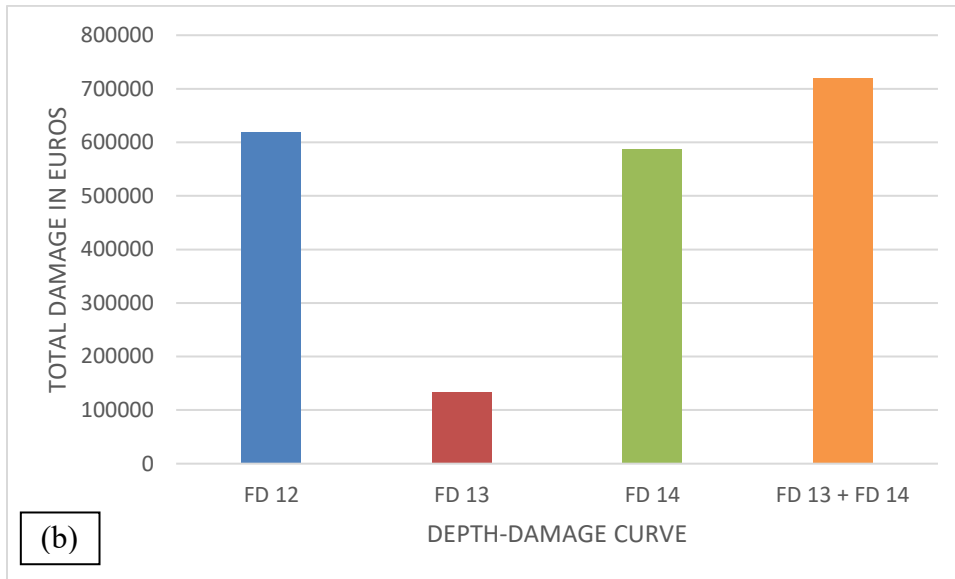
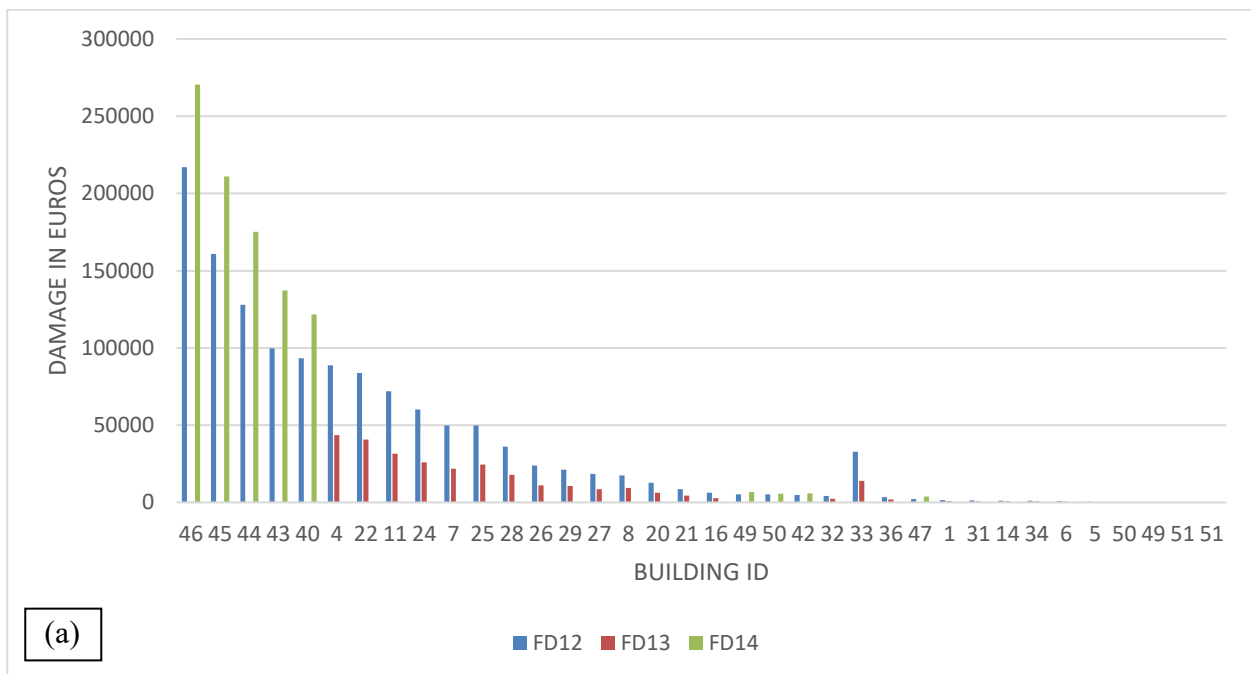


Figure 51: Damage per (a) building and (b) curve for a 10-year period and 0.3m mean sea level rise

Considering a 100-year return period flood scenario with a 0.3m mean sea level rise (Figure 52), it is possible to observe that the damage costs vary from 270,400 euros (FD14) for Tartini Square 2 to 300 euros (FD13) for Casa Tartini. In addition, 35 of the 51 assets (69%) are affected by this flood scenario. Regarding the application of the 3 depth-damage curves to estimate the damage costs, the combination of curves FD13 and FD14 (curves found in the literature) shows lower damage costs than the FD12, curve provided by the Ministry of Culture of Slovenia.



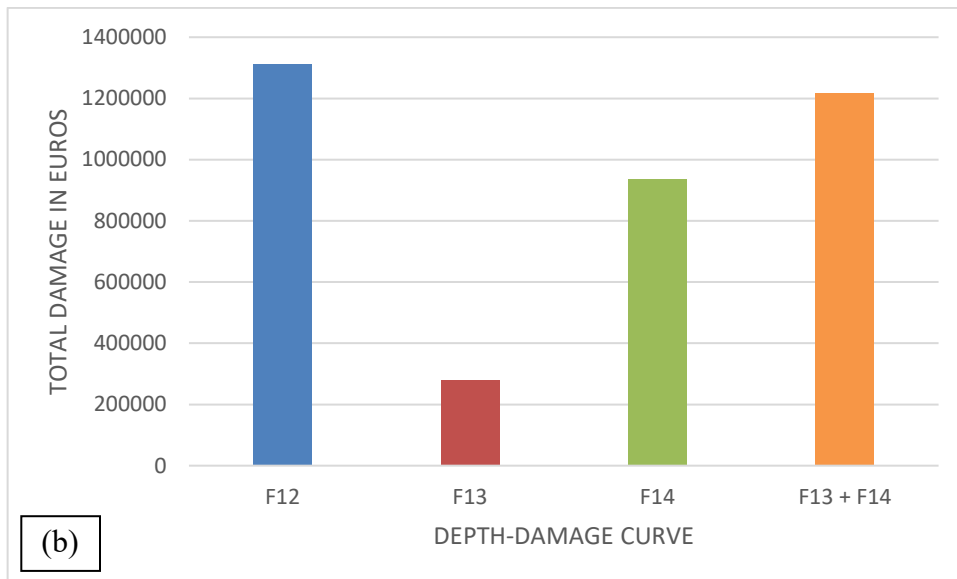
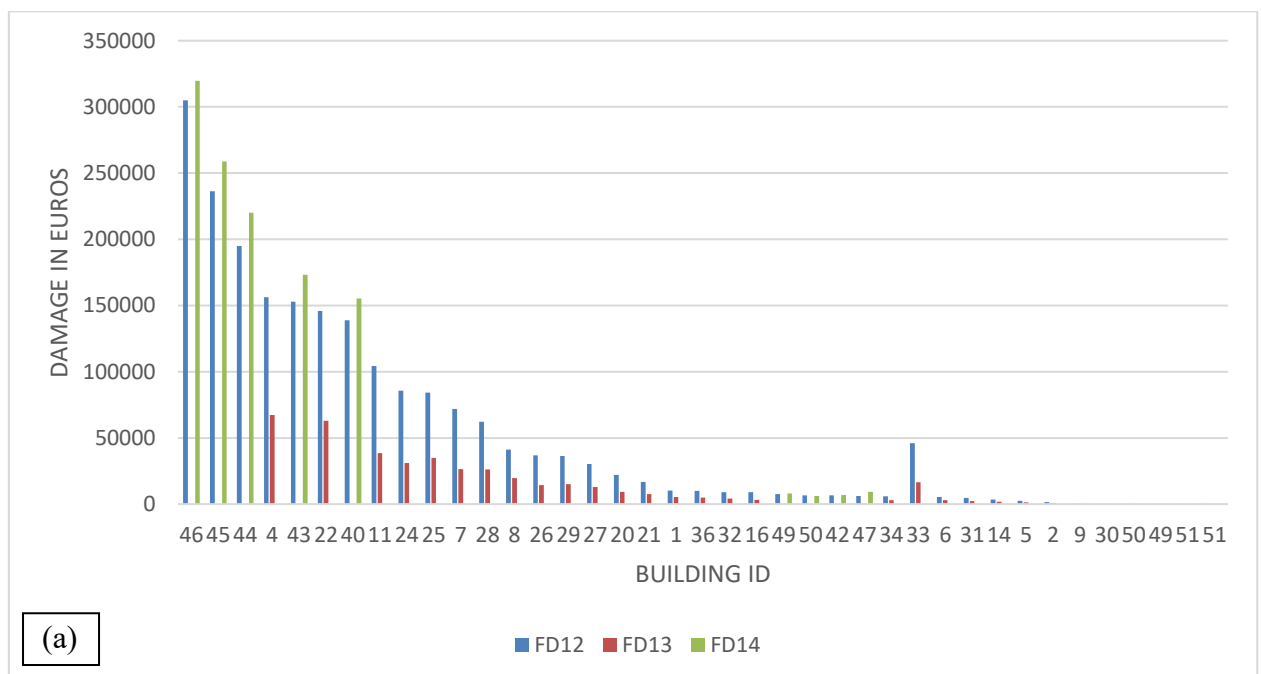


Figure 52: Damage per (a) building and (b) curve for a 100-year period and 0.3m mean sea level rise

In the case of a 1000-year return period flood scenario with a 0.3m mean sea level rise (Figure 53), it is possible to observe that the damage costs vary from 319,600 euros (FD14) for Tartini Square 2 to less than 100 euros (FD13) for Pecarstvo Andrej Turk s.p.. Additionally, 36 of the 51 assets (71%) are endangered by this scenario. Concerning the application of the 3 depth-damage curves to estimate the damage costs, the combination of curves FD13 and FD14 (curves found in the literature) shows lower damage costs than FD12, a curve provided by the Ministry of Culture of Slovenia.



(a)

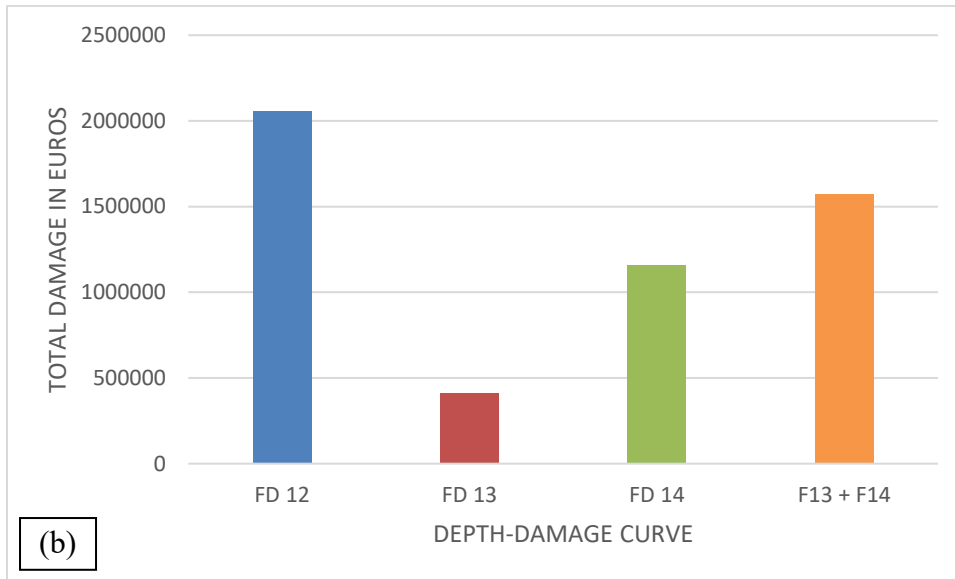
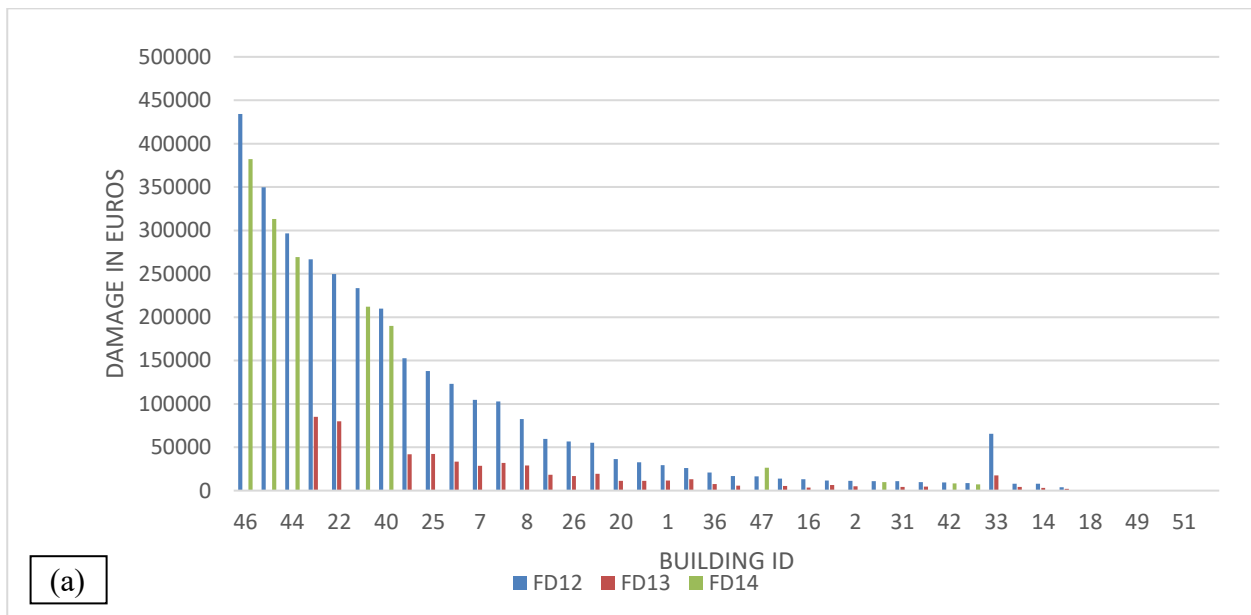


Figure 53: Damage per (a) building and (b) curve for a 1000-year return period and 0.3m mean sea level rise

When accounting for a 10-year return period flood scenario with a 1.46m mean sea level rise (Figure 54), it is possible to observe that the damage costs vary from 434,200 euros (FD12) for Tartini Square 2 to less than 100 euros (FD13) for Alma Vivoda ulica 13-15. Besides that, 38 of the 51 assets (74%) are endangered by this scenario. Concerning the application of the 3 depth-damage curves to estimate the damage costs, the combination of curves FD13 and FD14 (curves found in the literature) shows lower damage costs than the FD12, curve provided by the Ministry of Culture of Slovenia.



(a)

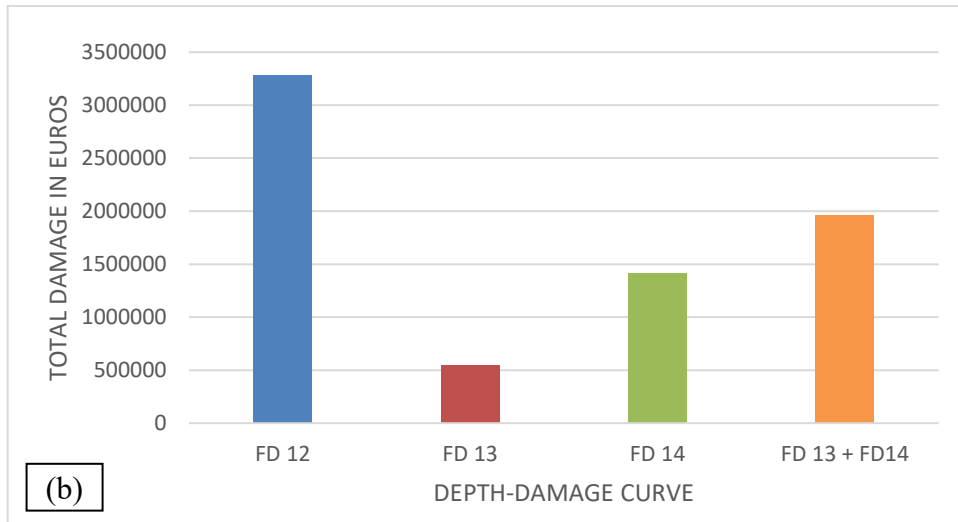
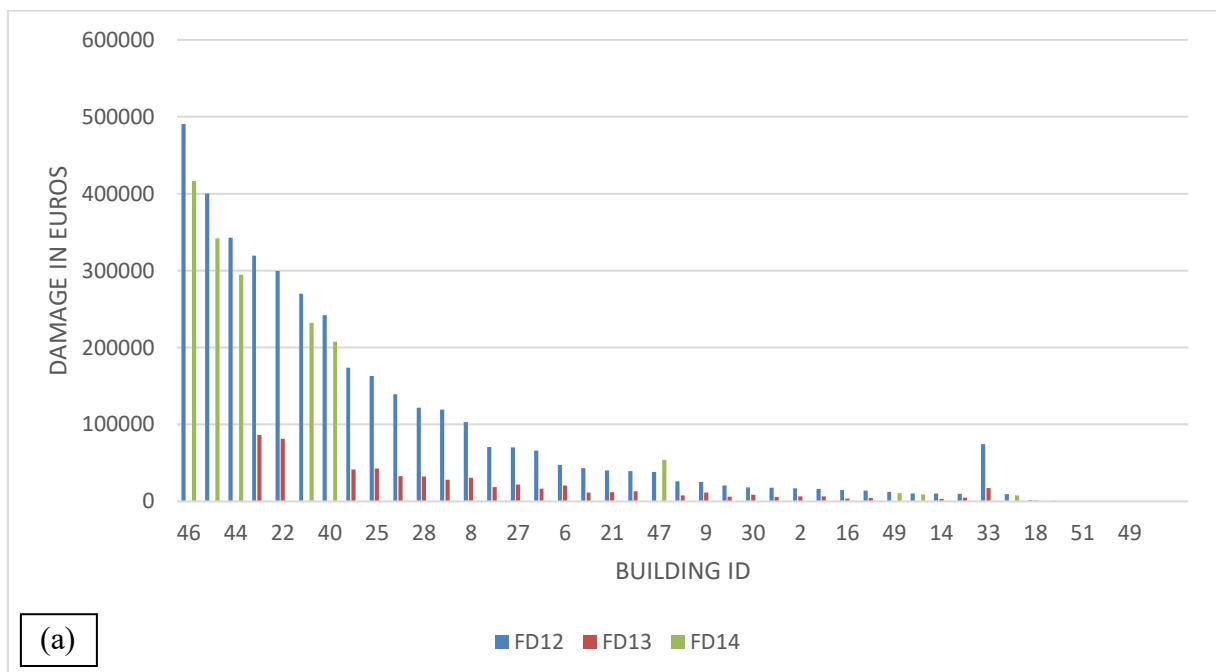


Figure 54: Damage per (a) building and (b) curve for a 10-year return period and 1.46m sea level rise

Taking into consideration a 100-year return period flood scenario with a 1.46m sea level rise (Figure 55), it is possible to observe that the damage costs vary from 490,400 euros (FD12) for Tartini Square 2 to 300 euros (FD13) for Trubarjeva ulica bridge/Passage under the building. It can also be noted that 39 of the 51 assets (76%) have damage costs associated with this scenario. Concerning the application of the 3 depth-damage curves to estimate the damage costs, the combination of curves FD13 and FD14 (curves found in the literature) shows lower damage costs than the FD12, curve provided by the Ministry of Culture of Slovenia.



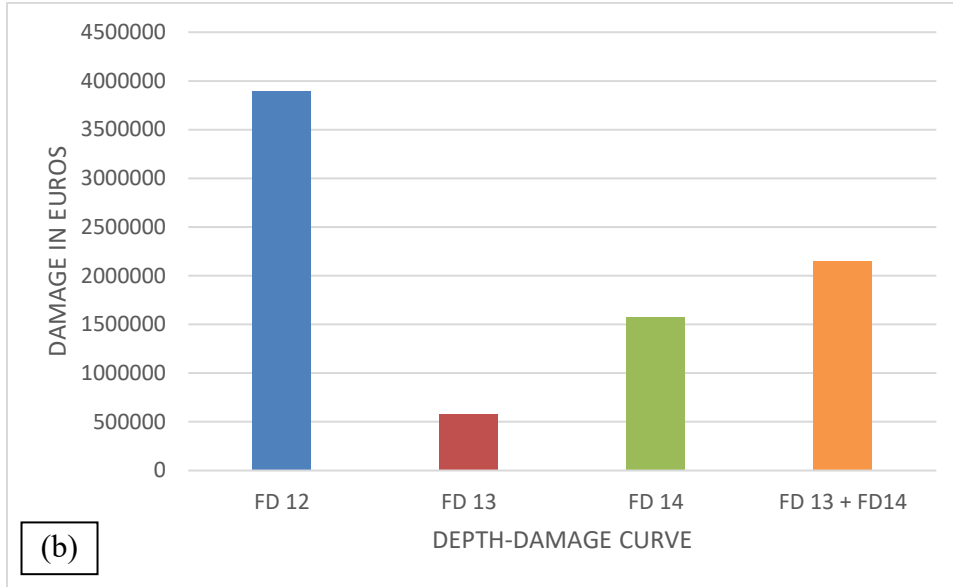
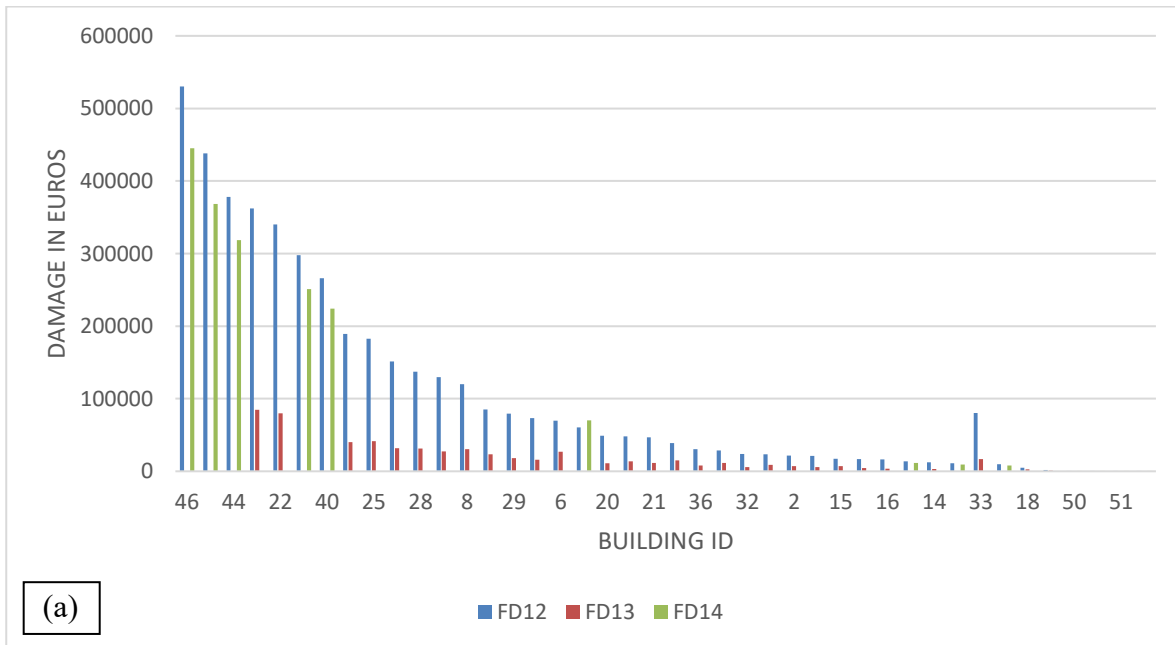


Figure 55: Damage per (a) building and (b) curve for a 100-year return period and 1.46m mean sea level rise

For a 1000-year return period flood scenario with a 1.46m mean sea level rise (Figure 56), it is possible to observe that the damage costs vary from 530,200 for Tartini Square 2 to 1000 euros (FD13) for Trubarjeva ulica bridge/Passage under the building. It can also be highlighted that, similar to the 100-year flood scenario with the same mean sea level rise, 39 of the 51 assets (76%) have damage costs associated with this scenario. Concerning the application of the 3 depth-damage curves to estimate the damage costs, the combination of curves FD13 and FD14 (curves found in the literature) shows lower damage costs than FD12, a curve provided by the Ministry of Culture of Slovenia.



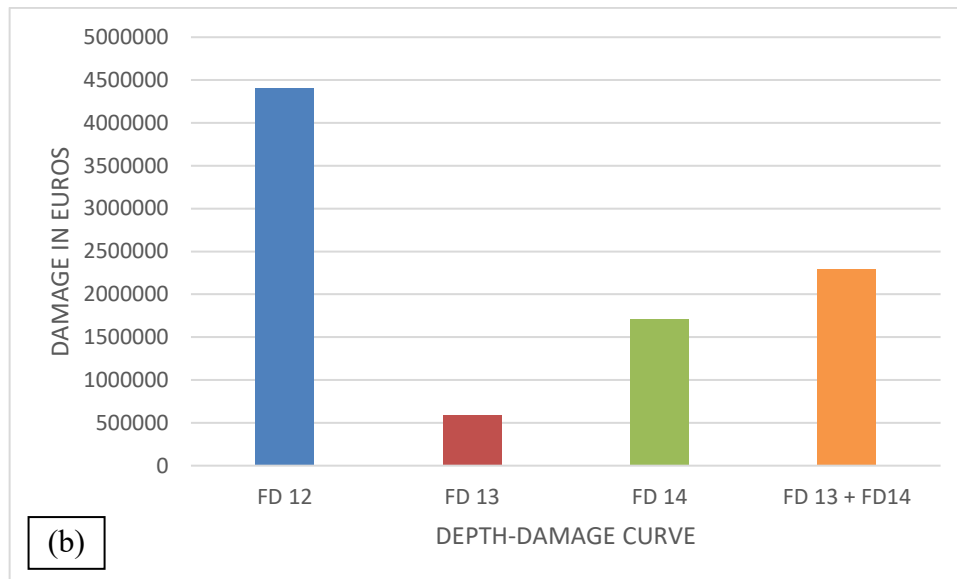


Figure 56: Damage per (a) building and (b) curve for a 1000-year return period and 1.46m mean sea level rise

### 5.2.1 Comparison with Previous Studies in Piran

In Alivio's (2020) flood risk assessment of Piran, the contribution of each sector (cultural heritage, public infrastructure, residential, etc.) to the total damage incurred by floods (percentage) and the total damage cost for seven mean sea level scenarios (0.1, 0.2, 0.3, 0.4, 0.5, 0.84 and 1.46m) and six return periods (2, 5, 10, 100, 500 and 1000-year) were computed. This subchapter aims to compare the cultural heritage damage costs calculated in Alivio's (2020) work with the costs from the present research for three return periods (10,100 and 1000) and two mean sea level rise scenarios (0.3 and 1.46m). Such comparison could provide important insights into how damage costs to cultural heritage can be underestimated when only general depth-damage curves from FEMA (2014) are utilized and specific characteristics of cultural heritage buildings are not considered.

Initially, the percentage of share of cultural heritage to the total flood damage is collected for 10,100 and 1000-year return periods (Figure 57). In Figure 57, the sectors presented are cultural heritage (blue), public infrastructures (orange), residential (gray), business (yellow), cleaning and temporary residence (purple), and others (green). Thereafter, the total cost of damage for cultural buildings for probabilities of 0.1, 0.01, and 0.001 for SLR3 and SLR7 are obtained from damage-probability curves from Piran (Figure 58). The results of the damage costs for cultural heritage for the 6 flood scenarios are presented in Table 12.

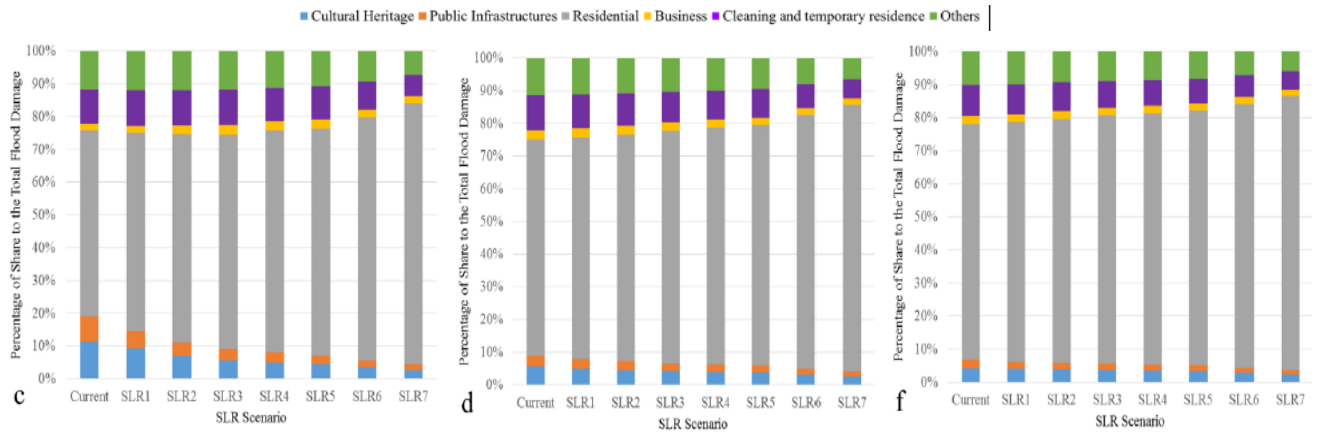


Figure 57: Shares of flood damages by sectors (cultural heritage sector in blue) for façade 10-year; (d) 100-year; and (f) 1000-year recurrence intervals at varying SLR scenarios (Alivio, 2020)

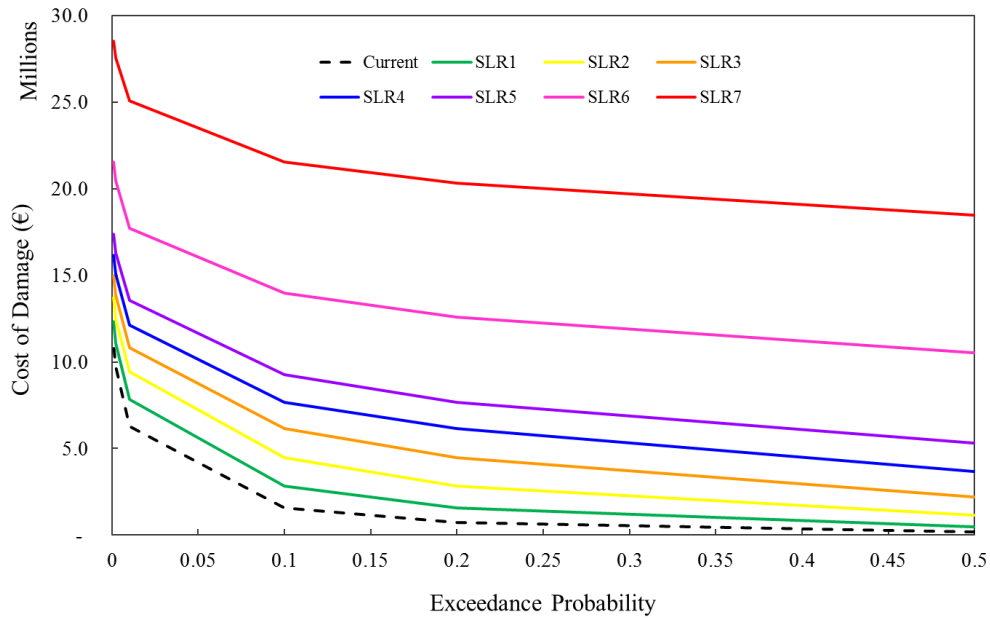


Figure 58: Damage-probability curves for Piran according to different SLR scenarios (Alivio, 2020)

Table 12: Cost of damage to cultural heritage (Alivio, 2020)

	Flood Scenario								
	T10 (S0)	T100 (S0)	T1000 (S0)	T10 (S3)	T100 (S3)	T1000 (S3)	T10 (S7)	T100 (S7)	T1000 (S7)
Percentage of damage referring to cultural heritage	11.27	5.32	4.04	5.53	4.04	3.62	2.55	2.34	2.34
Cost of the total damage (Millions of Euros)	1.56	6.28	9.2	6	10.72	13.88	21.44	24.96	27.36
Cost of damage to cultural heritage (Millions of Euros)	0.18	0.33	0.37	0.34	0.43	0.50	0.55	0.59	0.61

After the flood damage costs of cultural heritage were calculated according to Alivio (2020), the obtained values were compared with the values computed in the present work (Table 13 and Figure 59).

Table 13: Comparison between costs of damage to cultural heritage in Alivio (2020) and the present work

		Flood Scenario								
		T10 (S0)	T100 (S0)	T1000 (S0)	T10 (S3)	T100 (S3)	T1000 (S3)	T10 (S7)	T100 (S7)	T1000 (S7)
Cost of damage to cultural heritage (Millions of euros) (Alivio, 2020)		0.18	0.33	0.37	0.34	0.43	0.50	0.55	0.59	0.61
Cost of damage to cultural heritage (Millions of euros) (Present work)	FD 12	0.13	0.62	1.34	0.62	1.28	1.31	3.28	3.90	4.41
	FD 13+14	0.18	0.73	1.23	0.72	0.94	1.22	1.96	2.15	2.29

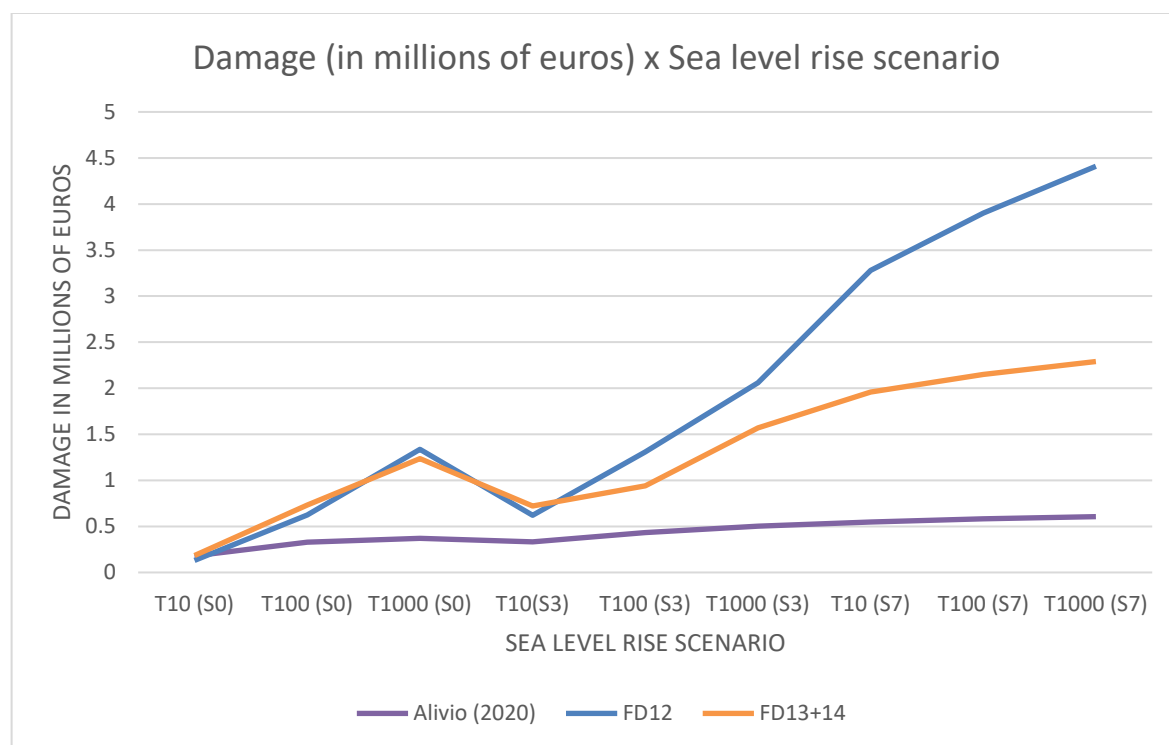


Figure 59: Comparison between depth-damage curves for cultural heritage: Alivio (2020) – blue, FD12 – red, and FD13+FD14 – green.

Table 13 and Figure 59 show that the damage costs from Alivio (2020) and the present study are very different, especially when the costs are calculated using FD12 (the curve provided by the Ministry of Culture of Slovenia). The values calculated in the present work range from being smaller than (FD12) and similar (FD13+14) to Alivio's (2020), for a 10-year return period and no sea level rise

(independently of the curve used), to 3.8 and 7.3 times Alivio's (2020) cost, respectively for FD13+FD14 and FD12. Comparing the curves that plot damage per sea level rise scenario, the 2 curves chosen from the present study portray a general concave tendency, even though they disperse for more extreme scenarios. However, the behavior presented by Alivio's (2020) curve is linear, very different from the other 2 curves.

The part of the curve that refers to a no sea level rise scenario differs considerably from the rest of it for FD12 and FD13+14. The no-sea level rise portion of the curve is a lot steeper than the rest of the curve. While, for a no sea level rise scenario, the 1000-year return period cost is up to 10 times higher than the 10-year one, for a 0.3 mean SLR this value goes down to 2 times and for a 1.46m mean SLR the costs are 1.5 times lower. That could mean that the impact of the sea level rise hinders the effect of the change of return period, making all cost values more similar.

It can also be seen that the damage costs for a 100-year return period and no sea level rise scenario are similar to the costs for a 10-year and 0.3m mean sea level rise scenario. Nevertheless, Alivio's (2020) curve has a consistent linear behavior when progressively increasing return periods and mean sea level rise scenarios.

Despite the big discrepancy between the results found in those 2 studies, it was expected that the cost estimation of damage based on FEMA curves conceived for residential buildings would be inaccurate, around 3 times smaller than the expected value. This difference of 300% is a rough approximation of experts from the Ministry of Culture of Slovenia when the damage costs comparing ordinary to exceptional assets. This approximation was based on expert knowledge and the estimation of renovation costs. In that way, the use of the curves FD13 and FD14 shows acceptable results.

Additionally, to compute the expected annual damage or EAD for the present study and compare them with Alivio's (2020), damage probability curves for cultural heritage were derived from Figure 57 and Figure 58. Table 14 and Figure 60 display a comparison between the expected annual damage to cultural heritage in Alivio's (2020) work and the present study.

Table 14: Comparison between EAD to cultural heritage in Alivio (2020) and the present work

EAD (Expected Annual Damage) (Millions of euros)				
	Alivio (2020)		Present work	
	General	Cultural Heritage	F12	F13+F14
S7 (1.46m)	10.208	0.284	1.537	0.949
S3 (0.3m)	2.374	0.148	0.243	0.279
S0 (no SLR)	0.660	0.057	0.062	0.078

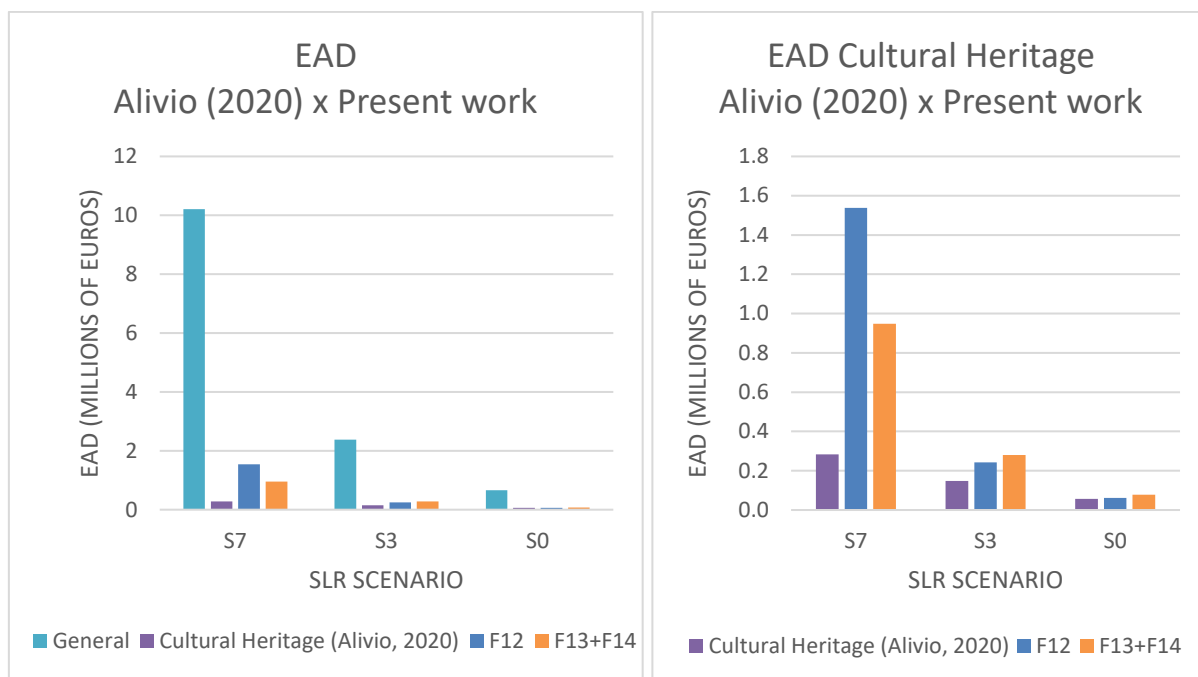


Figure 60: Expected Annual Damage (General and Cultural Heritage) in Piran according to different mean SLR scenarios (Alivio, 2020)

Table 14 and Figure 50 show that the relevance of the cultural heritage's EAD in the total EAD in Alivio's (2020) work decreases as the sea level rise scenarios get more extreme, from 9.1% (S0) to 2.7% (S7). In addition, following the same trend as observed before, the EAD calculated in the present work is considerably higher than the one calculated by Alivio (2020), with an augmentation of the discrepancy as the sea level rise scenarios get more extreme (up to 541% increase for S7). The values for the current state, with no sea level rise, are, in reality, very similar to the ones calculated by Alivio (2020). Considering that the values computed in the present work were expected to be approximately 3 times higher than Alivio's (2020), due to its increase in accuracy, the recommended curves to estimate cultural heritage's EAD would be FD13 and FD14, which reach a maximum of 334% of the values obtained by Alivio (2020) for the most extreme sea level rise scenario.

### 5.2.2 Comparison with Renovation Costs

The Ministry of Culture provided renovation reports for two types of cultural heritage in Piran: regular and exceptional constructions. The renovation reports are usually prepared after flood events to obtain a tangible estimate of the foreseen renovation costs. Regular constructions are buildings that are considered to have cultural value due to their construction system and date as far back as the 17th century. On the other hand, exceptional buildings are the ones made with more sophisticated materials and building techniques, some of the examples are present in Tartini square, such as the town hall and the courthouse. The reports include a description of the building materials, an assessment of the general condition of the buildings, a list of the interventions considered necessary to bring the building back to its original state, or as near as possible to it, and the financial breakdown of the proposed interventions. Figure 61 presents the condition of the two buildings analyzed in the reports when subjected to 0.4m of flood depth (Institute for the Protection of the Cultural Heritage of Slovenia, 2020).



Figure 61: Condition of buildings after the impact caused by the sea flood in November 2019 (0.4m flood depth):  
(a) Obzidina ulica 2; (b) Tartini Square 2;

Both renovation projects were based on the inundation event of November 2019, which impacted both buildings with a flood height of 0.4m. This inundation resulted in the soaking of the walls and damage to plaster, stone elements, and joinery. Besides that, the renovation projects for the two buildings include the following general interventions: repair of stone elements; removal of old damaged lime façade plaster; repair and painting of joinery; and production of new lime façade with final painting of the façade. The main difference between the renovation works applied to monuments and ordinary buildings is the replacement of elements, which tends to not be executed for monuments. In addition, the costs of the planned works in monuments are considerably higher than in ordinary buildings, as portrayed in Table 15, which presents examples of the interventions to be executed (Institute for the Protection of the Cultural Heritage of Slovenia, 2020).

Table 15: Comparison between renovation interventions costs for exceptional and ordinary buildings (Institute for the Protection of the Cultural Heritage of Slovenia, 2020)

Work	Cost/Dimension Exceptional	Cost/Dimension Ordinary building	Cost Exceptional /Ordinary building
Production façade scaffolding up to 10 m high, plinth installation, assembly, and disassembly, and all auxiliary work on the construction site, billing per square meter;	12.40 EUR/m <sup>2</sup>	9.10 EUR/m <sup>2</sup>	1.36
Refaçade of facade plasters and removal to the permanent construction material depot, removal of plasters at a height of h = 1.20m above the ground; billing per m <sup>2</sup> .	10.60 EUR/m <sup>2</sup>	7.40 EUR/m <sup>2</sup>	1,43
Carpentry repair, cleaning, and painting windows, with painting of fittings in the color according to the instructions of the monument protection service.	280.00 EUR/piece	165.00 EUR /piece	1.69
Repair, and remodeling of the stone façade of the facade with a final protective coating.	94.60 EUR/m <sup>2</sup>	87.70 EUR/m <sup>2</sup>	1.08
Painting the facade with secco lime paint according to the instructions of the monument protection service, all auxiliary works included, calculation per m <sup>2</sup>	28.70 EUR/m <sup>2</sup>	12.80 EUR/m <sup>2</sup>	2.24

In Table 15 it can be seen that the price of the interventions executed in exceptional buildings can go as high as 224% of the value of the interventions for ordinary ones. The main reasons behind the more expensive costs of those interventions are the lack of specialized labor (Slovenian companies and workers that have experience in renovating cultural heritage buildings), the high price of the materials used in the construction of the original buildings due to their high quality (e.g. high-quality stones or painting) and difficulty to be found, as they are not currently utilized (at times it is even impossible to find the same materials with specific characteristics).

To perform a cost-benefit analysis of the renovation works that were proposed, the damage costs of the two analyzed buildings estimated in the present work were compared to their renovation costs in Table 16, for a similar floodwater depth. As the report considered a flood depth of 0.4m, a flood scenario with the most expected sea level rise (S3, with 0.3m) and in which the buildings presented approximately the same flood depth was chosen. The flood scenario that matched the previous description was a 10-year return period flood, with an estimated flood depth of 0.38m for both considered buildings. To be able to compare the renovation and damage costs for the two assets, the three buildings in Obzidina ulica were combined, thus having a similar area as the town hall in Tartini Square 2.

Table 16: Comparison between damage and renovation costs for the buildings analyzed in the Ministry of Culture report (Institute for the Protection of the Cultural Heritage of Slovenia, 2020)

	Type of Building	Flood depth that caused the renovation (m)	Renovation costs (euros)	Correspondent flood scenario	Damage costs (euros)	Difference damage – renovation costs (euros)
Tartini Square 2	Exceptional	0.4	63.428,84	T10_S3 (0.38m)	122.681,75 (F12)	59.252,91
					189.219,99 (F14)	12.5791,15
Obzidina ulica 2,4 and 8	Ordinary	0.4	20.954,71	T10_S3 (0.38m)	18.496,48 (F12)	-2.458,23
					9.333,91 (F13)	-9.162,57

After comparing the damage and renovation costs for the buildings in Tartini Square 2 and Obzidina ulica 2,4 and 8 it could be seen that, for Tartini Square 2 (an exceptional building), the implementation renovation works would bring a positive financial balance, by utilizing FD12 or FD14 to estimate damage costs. Nevertheless, for Obzidina ulica 2,4, and 8 (ordinary buildings), renovation interventions would result in a negative financial balance, as the renovation costs would be higher than the estimated damage, independently of the depth-damage curve used to estimate costs. It should be considered that economic benefits should not be the only benefits considered when deciding whether renovation interventions should be implemented in cultural heritage buildings. The cultural and social values these buildings embrace should be recognized and protected to support the identification that citizens feel towards them now and in the future. Additionally, independently of the resultant financial balance, this type of cost-benefit analysis could be beneficial, as it assists decision-makers to develop better renovation and protection plans for cultural heritage.

According to (Bogaards, 2008) the development of cost benefit analysis in the cultural heritage sector would allow decision makers to conclude that the benefits outweigh the costs of conservation and

therefore push for additional conservation efforts. A cost-benefit analysis would help prioritize the cultural heritage assets to intervene on and better plan the financial scheme of these renovations, especially when the resources are limited.

### 5.3 Evolution of the number of salt transition cycles

After intersecting the relative humidity and temperature data according to the thresholds established by Ciantelli et al. (2018), the following graph was created, presenting the estimation of the yearly evolution of the number of salt crystallization cycles of the city of Piran from 2023 until 2100.

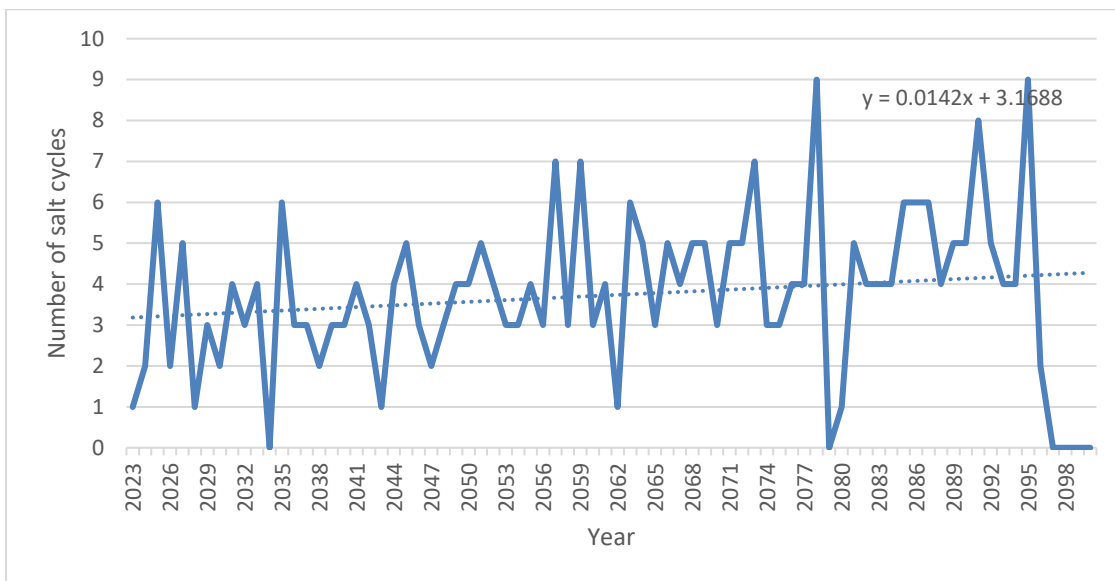


Figure 62: Yearly evolution of the number of salt crystallization cycles

In Figure 62 it can be seen that there is a positive trend in the number of salt crystallization cycles to increase over the next 77 years. According to the trendline, this increase is small, adding up to 1.4% per year to a mean of approximately 3 cycles per year. Therefore, by 2100, the number of cycles is expected to have a new mean of approximately 4 cycles. Figure 62 shows that this data could be divided into bands of a maximum number of salt cycles: from 2023 to 2056, with a maximum of 6 cycles, and 2057 to 2100 with a maximum of 9 cycles.

It should be noted that, for salt weathering processes to cause severe deterioration, it is not necessary to have a high number of salt crystallization cycles every year. A year with a high maximum, especially when accompanied by other deterioration factors such as biological degradation and erosion caused by the sea, could cause irreparable and invaluable damage to cultural heritage buildings.

Supposing a direct relationship between the number of cycles and losses, the percentage growth in the number of crystallization cycles would be transferred to the damage costs incurred to cultural heritage. It is expected that the increase in the number of salt transition cycles along with the increase in sea level rise and flood frequency resulting from climate change will lead to the augmentation of cultural heritage losses.

## 6 DISCUSSION

### 6.1 Second-Tier Flood Vulnerability and Risk Assessment

Figueiredo et al (2021) developed a synthetic, component-based modeling framework to assess the flood vulnerability and risk of individual cultural heritage assets. The research created building-specific depth-damage functions according to their flood susceptibility (derived from its material and building technique) and the relative value of the building components. In possession of those curves, a semi-quantitative probabilistic estimation of flood risk was performed (Figueiredo R. et al., 2021).

The study proposes the in-depth vulnerability analysis and data collection of particular assets that have already been identified as highly endangered in a preliminary flood risk assessment. This refined analysis would be directed to only a few selected buildings due to the large number of resources (time, qualified personnel, and financial support) it demands, which is usually not provided for cultural heritage studies. The article highlights the risk of using exclusively first-tier flood risk assessments to make decisions concerning flood adaptation strategies due to its high degree of uncertainty (Figueiredo R. et al., 2021).

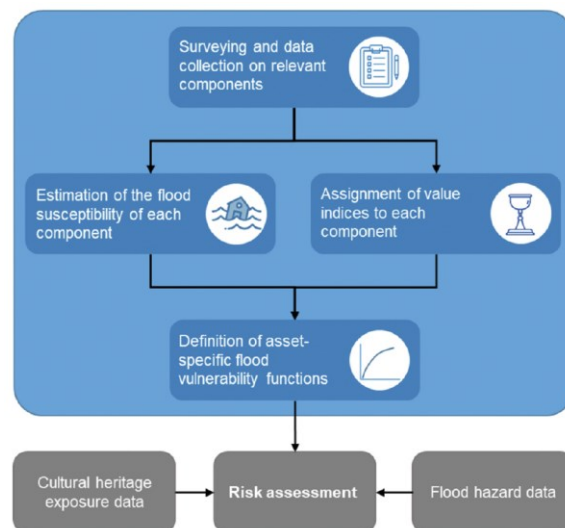


Figure 63: Workflow of the proposed flood vulnerability modeling approach for cultural heritage buildings, in blue. Grey boxes represent the other components of a flood risk assessment (Figueiredo R. et al, 2021)

Figure 63 presented the workflow of the research conducted by Figueiredo R. et al (2021). Figueiredo R. et al.'s (2021) workflow is similar to the methodology defined for the present work. Both studies include the survey and data collection of building characteristics, the estimation of flood vulnerability, the definition of flood vulnerability function according to the asset's characteristics and, finally, the assessment of risk after the incorporation of flood hazard data. Nevertheless, for the present work, only data on the building exterior was collected, values were not assigned to any of the assets, or its components, and the depth-damage functions were applied to groups of buildings and not individual constructions.

The first stage of Figueiredo R. et al.'s (2021) work comprises the data collection on relevant components present in cultural heritage assets (classified as part of the building – group 1 or content – group 2) through a field survey and the identification of the components' relative cultural value when

compared with the entire building. The most relevant collected data for Figueiredo R. et al.'s (2021) study were the material, building technique, and height of the component (Figueiredo R. et al., 2021).

Thereafter, the flood susceptibility, or level of impact caused by flooding, of each component was estimated. To perform that estimation, a literature review on the impact of floodwater on various materials and components built with different techniques was conducted. The information collected was classified into two categories, the first associated with the most predictable damage that floodwater causes to multiple materials/techniques, and the second related to the factors that may intensify or reduce the most expected damage (such as ease of drying and efficiency of the response measures). The described information was analyzed, and five degrees of susceptibility were determined and transferred into a scale of susceptibility indices (Table 17). Then, these indices were designated to the different types of material or techniques with bands, resulting from the damage influencing factors (Figure 64). When no further information is available, the base index should be chosen and, if several materials compose an element, the susceptibility index of the element will be the same as the one of the most susceptible material (Figueiredo R. et al., 2021).

Table 17: Scale of susceptibility indices (Figueiredo R. et al., 2021)

Level	Description	Susceptibility index
Very high	Extensive damage is expected in the short term. Affected components will likely not be recoverable.	5
High	Significant damage is expected in the short term. Affected components will likely be only partially recoverable.	4
Intermediate	Some damage is expected in the short-medium term, although affected components will likely be fully recoverable.	3
Low	Some damage is expected in the medium-long term, particularly if components are subjected to continuous exposure to water.	2
Very low	The occurrence of damage is not expected. Components may require unspecialized cleaning and/or drying.	1

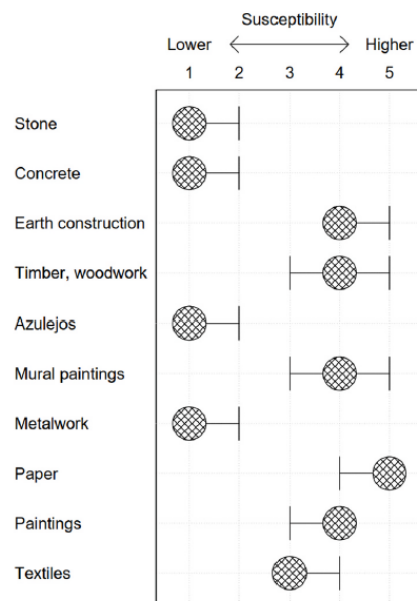


Figure 64: Susceptibility index per building type (Figueiredo R. et al., 2021)

At the same stage as the estimation of susceptibility, value indexes were associated with each building component. These indexes describe the value of the component itself and its importance for the total asset value. Value indexes were assigned to components according to the scale presented in Table 18 (Figueiredo R. et al, 2021).

Table 18: Three-level scale to score the value of each component (Figueiredo R. et al., 2021)

Level	Description	Value index
High	Unique components with exceptional cultural value, which are determinant for the global cultural value of the asset	10
Intermediate	Unique components that have significant cultural value	3
Low	Components that are not unique and that contribute in a limited manner to the overall cultural value of the asset	1

The third step of this methodology was the creation of a depth-damage function for singular cultural heritage buildings. The damage was calculated according to a step-by-step simulation of the inundation of a specific asset (each step corresponds to a single water depth). To account for very different materials, such as walls (considering all walls as a single element) and statues, weights were assigned to each component (Figueiredo R. et al, 2021). In addition, to compute damage both susceptibility and value indexes were normalized, as shown in the equation below for a single step:

$$D = \frac{\sum_i^{n_1} g(x) \cdot v_i \cdot s_i}{\sum_i^{n_1} v_i \cdot 5} w_1 + \frac{\sum_i^{n_2} g(x) \cdot v_i \cdot s_i}{\sum_i^{n_2} v_i \cdot 5} w_2$$

$$g(x) = 1 \text{ if } x \geq h_i$$

$$g(x) = 0 \text{ if } x < h_i$$

"where x is the water depth of each simulated step,  $n_1$ ,  $w_1$ ,  $n_2$ , and  $w_2$  refer to the number of components in groups 1 and 2 and their weights, respectively,  $h_i$  is the height at which the base of the  $i$ th component of a given group is located above a reference level (typically the external ground level, from which the water depth is also measured), and  $v_i$  and  $s_i$  are the value and susceptibility indices of the  $i$ th component of the same group"(Figueiredo R. et al, 2021).

Finally, overlaying these curves with exposure and hazard data, flood risk indexes (HFR) for the selected assets were determined according to the equation below:

$$HFR = V \sum_{i=1}^{n-1} (P_{i+1} - P_i) \frac{D_{i+1} - D_i}{2}$$

"where n is the number of adopted hazard scenarios,  $P_i$  is the annual probability of occurrence of the  $i$ th hazard scenario (which is assumed to be equal to the inverse of its return period),  $D_i$  is the damage index calculated using the developed vulnerability functions presented in the previous subsection, and V is the index of the global value of the cultural heritage assets, which is defined based on their listed status (Figueiredo R. et al, 2021). "

In the results section it was presented that although higher flood depths were found in one of the buildings, its damage was not the highest due to the elevation of the rooms and the height of the building

components. That helps justify the implementation of such higher-tier vulnerability analysis for priority buildings (Figueiredo R. et al, 2021).

It would be valuable to perform such second-tier assessments in the municipality of Piran since a general assessment of the most endangered buildings was already executed. The same methodology, scale, and equations could be applied to obtain further knowledge of the impact of floods of the 10 most vulnerable floods identified in the present work (Table 8 and Figure 27), for example. To do that, the methodology of the present work could be updated to include data collection on the building contents and the definition of values for buildings components (movable and unmovable). The time and effort invested in the extensive identification and cataloging of the buildings' structure and elements would allow the development of specific depth-damage curves for the most vulnerable buildings. These curves' higher precision would allow a more accurate and effective assessment of potential flood risk management measures.

## 6.2 Evaluation of Flood Adaptation Strategies

Davis et al. (2023), besides performing a qualitative flood risk assessment, evaluated flood risk reduction strategies on the building scale, including retrofitting with replastering, door and windows replacement, reduction of the number of openings, and drainage network enhancement, among others. The two assessed strategies differentiated on the number of buildings affected by interventions. For the first one, only the most endangered buildings were adapted (most vulnerable class, D), and, for the second, more buildings were included in the retrofitting plan (two most vulnerable classes, C and D).

The flood risk reduction with the implementation of the two strategies was assessed qualitatively and quantitatively. Qualitatively, the flood vulnerability index and flood classes for the whole sample were compared before and after the interventions. On the other hand, quantitatively, the retrofitting costs for the two strategies were compared with the total damage cost previously calculated using adapted depth-damage curves (Davis et al., 2023).

Davis et al. (2023) adapted the depth damage curves presented in Martínez-Gomariz et al. (2020) according to the FVIs of the analyzed buildings. The FVIs are translated into factors, these factors are derived from the percentage of buildings existent in each category. The low category accommodates the largest percentage of buildings (51%) and, therefore, it is associated with a factor of 1 (Table 19). The curves are then multiplied by the adjustment factor to find damage costs that reflect the vulnerability of the assets (Davis et al., 2023).

Table 19: Average level of flood risk for depth damage curve and adjustment factors (Davis et al., 2023)

Flood risk level	Average level of flood risk	Adjustment factor
Negligible	13%	0.5
Low	51%	1
Moderate	19%	1.25
High	11%	1.5
Extreme	6%	1.75

In addition, the original damage was examined in contrast with the damages after executing the two flood mitigation strategies (after positively changing the FVIs). The two flood mitigation strategies would change the FVIs and cause the buildings to be reclassified in terms of flood risk class. The change

in flood class altered the adjustment factor applied to each building and the total damage cost of the sample. With the new damage values in hand, the old and new damage costs could be compared (Davis et al., 2023).

In the present work, a comparison between damage and retrofitting costs was also calculated. The most relevant difference between the analysis performed in the current work and by Davis et al. (2023) is their scale. For this study, the renovation data available comprised only 2 buildings. On the other hand, Davis et al. (2023) estimated damage costs for interventions in over 500 buildings, which allows the authors to further assess the benefits of a measure that could be applied to many assets or a region. Nevertheless, the 2 sample analyses performed in the present work could be extended to other similar cultural heritage buildings. It was identified that 8 buildings are similar to Tartini Square 2 (made of stone with a lot of finishings, mostly located in the main square) and 4 have characteristics that resemble the buildings in Obzidina ulica (residential buildings made of stone masonry with no outstanding details). Furthermore, Davis et al. (2023) included flood protection measures in their retrofitting plan, such as the additional layer of render, brick or facing, and the installation of flood-resistant doors, flood skirts, and automatic flood guards, while the present work mostly considers the repair and replacement of building materials.

To elevate the present research, it would be beneficial to further investigate more in detail the building materials, building elements, and renovation costs of all cultural heritage buildings in the area and enhance the renovation plans with the inclusion of flood protection measures that could be applied on a building scale. In that way, it would be possible to estimate the benefits of the renovation for the entire city, the impact of such measures in the flood risk class the assets belong to, and the reduction in damage costs after such buildings are adapted (and FVIs are reduced).

### **6.3 Flood Risk Reduction Measures Proposed for Piran**

Due to its endangered state, Piran has been the subject of multiple flood mitigation and reduction studies that analyzed several structural and non-structural measures, such as the installation of mobile elements. As part of the initiative “Creative Path to Knowledge” co-financed by the EU, UL water engineering, environmental engineering, and architecture students developed POPKLIMAS, a project designed to increase flood safety in the coastal area of Piran due to global climate change. Initially, to dimension flood solution measures, current and future (next 50 to 70 years) wave heights were estimated according to the method of Darbyshire & Draper monograms (Bolčič et al., 2020; Kne, 2020).

Thereafter, an assessment of the current sewage system was performed, and a rearrangement of the system was proposed. The current sewage system in Piran is mixed, directing waste and discharging stormwater toward the Piran KČN. Besides that, the system is outdated and not watertight, allowing improper discharges of mixed water into the sea and seawater intrusion. That scenario results in system overload when subjected to heavy rainfall or high tides, which allows mixed water to reach street surfaces through road gullies. The system proposed in POPKILMAS is a vacuum sewer, that provides the essential waterproofing for the network (Bolčič et al., 2020; Kne, 2020).

Another coastal safety measure envisioned for Piran is the enhancement of the breakwaters. To project this measure, the stone weight, average diameter, and size of the rocks for the head of the structure are calculated in POPKILMAS. In addition to this measure, to protect the port, a gate similar to the one proposed by the MOSE project in Venice was conceived for Piran (Figure 65), connecting

both piers and relieving the traffic burden of the current route to inner Mandrač (Bolčič et al., 2020; Kne, 2020).

Considering structural measures, besides the installation of the gate, three main flood protection interventions were suggested for Piran. The first is the creation of a park across the entire coast of Piran, increasing urban green space and including pedestrian ramps for access to the beach (Figure 66 and Figure 67). The second is the development of a promenade, where the idea is to break the element of the wall into several smaller linear elements or several levels at different heights, which adds various utilities (such as accessing the beach, restaurants, and exercising) (Figure 68 and Figure 69). Finally, the third suggested intervention was the construction of a high wall that goes from the captain's office to the end of the embankment on the north side of the peninsula, to protect the city from more extreme sea level rise scenarios. For this measure, restaurants and other businesses would be moved to old, abandoned buildings or roofs to revive inner streets. In addition to the wall, floating temporary platforms could be installed to carry out specific activities, such as sports and music events (Figure 70 and Figure 71) (Bolčič et al., 2020; Kne, 2020).

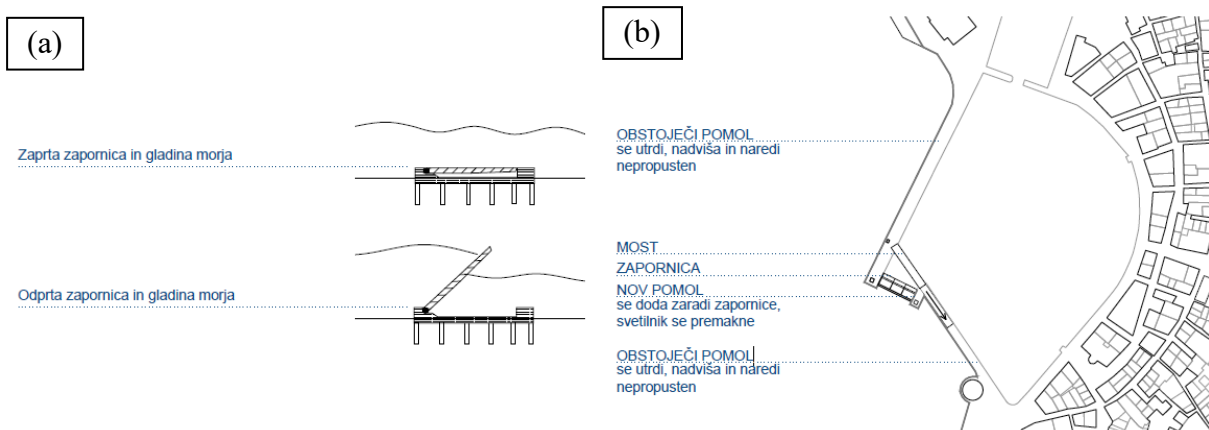


Figure 65: Structural measures proposed to Piran – (1) Gate: (a) section view, (b) top view



Figure 66: Structural measures proposed to Piran – (2a) Park – top-side view

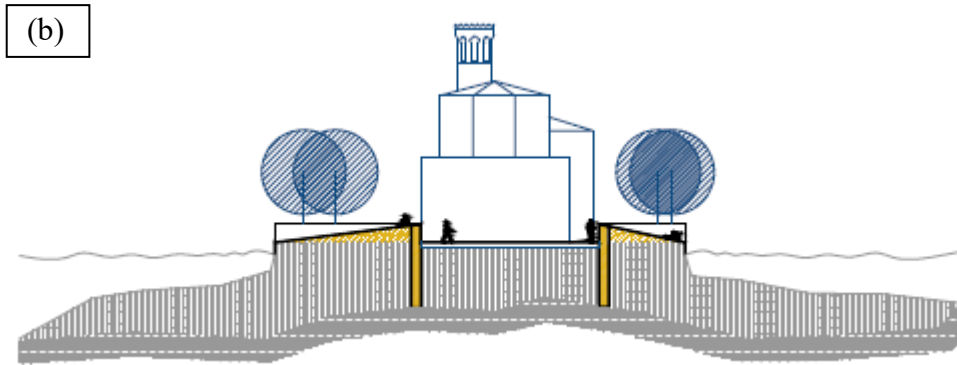


Figure 67: Structural measures proposed to Piran – (2b) Park–section C-C

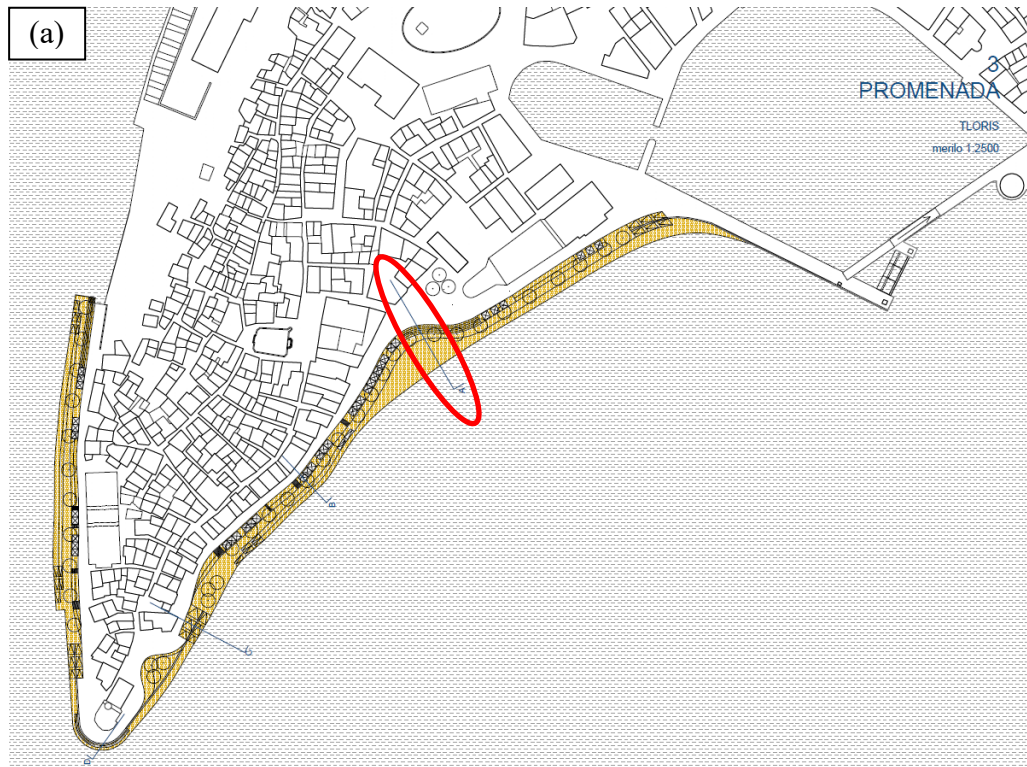


Figure 68: Structural measures proposed to Piran – (3a) Promenade – top view

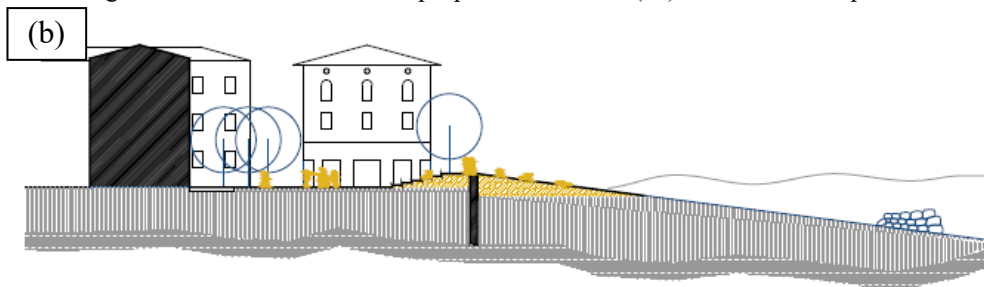


Figure 69: Structural measures proposed to Piran – (3b) Promenade – section A

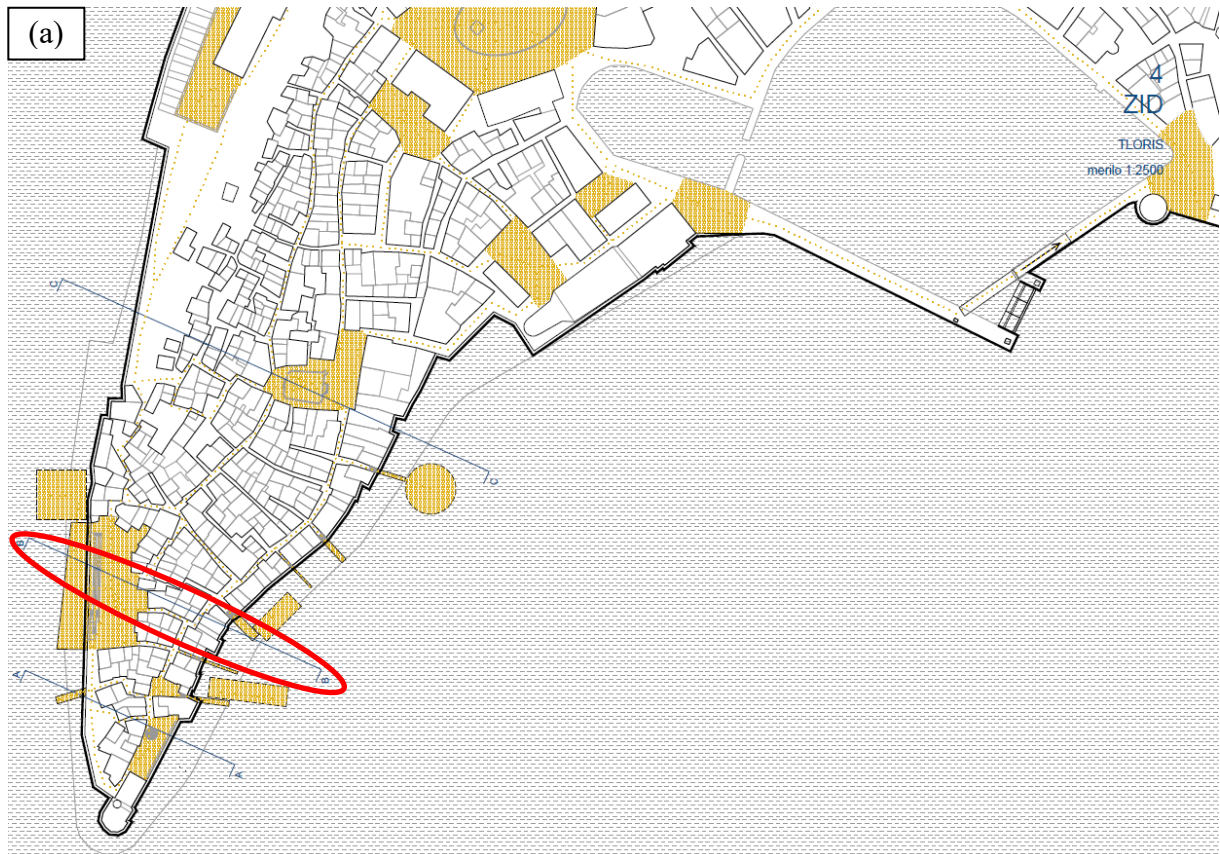


Figure 70: Structural measures proposed to Piran – (4a) Wall-top view

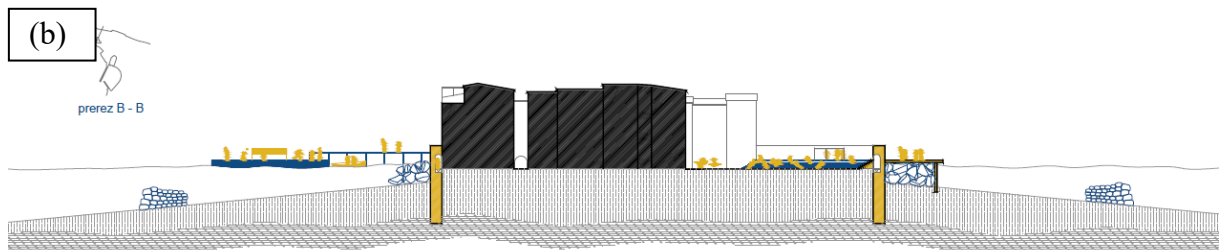


Figure 71: Structural measures proposed to Piran – (4b) Wall-section B-B

Besides the proposition of structural interventions, the flood safety project encourages the implementation of non-structural measures, such as effective notification, warning systems, public alarms, and civil protection organization in case of exceptional flood events. Another relevant non-structural measure is the installation of protective panels and sandbags, which can be quickly placed in such a way as to protect the most endangered areas or assets (Bolčič et al., 2020; Kne, 2020).

#### 6.4 Damage Assessment of Saltwater Floods

Despite the relevance of salt weathering to the durability of cultural heritage in Piran, due to the municipality's exposure to the sea and the forecasted increase in the intensity and frequency of coastal floods in the area, the impact of salt presence was not considered in detail for the calculation of flood damage costs. That exclusion is justified by the lack of data on the composition of the building materials,

on the saltwater present in the surroundings of the city, and the impossibility of obtaining that data through extensive chemical analysis of the materials.

The literature review performed in the present work leads to the conclusion that, to fully assess salt weathering damage to cultural heritage buildings, it would be necessary to extract samples of the assets and perform several tests, such as stereomicroscope observations, polarized light microscopy observations, and X-ray powder diffraction analysis. After the tests allow the characterization of the material in porosity, texture, and structure and the identification of deterioration patterns, the depreciation caused by such deterioration would have to be determined, and the renovation interventions necessary to retrofit the buildings estimated, along with its costs.

Such analysis demand overcoming administrative requirements regarding intervening in cultural heritage, the availability of controlled environments (laboratories) with access to specific equipment to perform the necessary tests, and qualified labor of experts that could validate the entire process. This entire operation is reasonably challenging, considering the amount of time and financial resources needed to execute it. These are some of the reasons why most of the published studies on the subject of salt's impact on cultural heritage assets only consider one or a few buildings in a specific location. No assessments that delivered equations that describe the influence of salts on cultural heritage damage globally or regionally were identified.

An option to predict future salt deterioration due to the gradual consequences of climate change is the estimation of the number of crystallization cycles utilizing meteorological data from climate models, such as temperature and relative humidity. Assuming the presence of a specific salt in the cultural heritage building materials, it is possible to determine the temperature and relative humidity limits for its precipitation. This work analyzed the evolution of the number of salt transition cycles in Piran for NaCl in section 5.3 and identified an increasing trend of the number of occurrences of such processes until 2100. The long-term evolution of the number of crystallization cycles in a certain area could help cultural heritage management authorities improve conservation strategies.

## 7 CONCLUSION

The key findings of the study are reported in this chapter along with a concise review of the work that was done for the thesis. The chapter also discusses the limitations of the research as well as the employed methodology. Additionally, applications of the findings and suggestions for the ongoing advancement of this research are included below.

### 7.1 Summary

One of the most relevant effects of climate change that threatens coastal cities is the acceleration of sea level rise and its possible consequences. This risk is particularly high for Piran, which is already frequently affected by floods and has irreplaceable cultural heritage buildings in the areas that are the most exposed to floods (such as Punta and Tartini Square). Besides the 10 cm increase in sea level recorded in the mareographic station in Koper from 1960 to 2015, Piran is expected to experience a sea level rise of at least 30 cm until 2100 (Ličer, 2019; Strojjan and Robič, 2016). The large quantity and importance of cultural heritage assets in Piran are a result of the many civilizations that have occupied the area. Those elements now shape the city's identity and help the population cultivate and propagate their culture. Slovenia recognizes the risk of flood damage to cultural heritage and thus included that type of asset in their model for Cumulative Calculation of Flood Damage and Analyses (KRPAN). Nevertheless, the functions used to estimate this damage were general, derived from FEMA (2014), and the vulnerability of cultural heritage was not determined. This research aims to deliver better estimations of damage costs to cultural heritage according to the building's characteristics.

The statistical analysis of extreme sea levels performed along with sea level rise projections found in literature and selected by Alivio (2020) allowed the determination of 42 climate change scenarios. These scenarios were associated with 6 different return periods (2, 5, 10, 100, 500, and 1000-year period) and 7 mean sea level scenarios (0.1, 0.2, 0.3, 0.4, 0.5, 0.84, and 1.46m). Flood depths for each one of the 51 buildings analyzed are estimated utilizing a bathtub model in QGIS. The depths correspond to the water level for the 42 scenarios subtracted by the mean terrain elevation of each one of the assets. For the determination of qualitative flood risk, the vulnerability of the 51 buildings is also estimated. The vulnerability in this work is represented by a flood risk index (FVI), which results from the multiplication of sensitivity and exposure factors. The factors are chosen based on the literature on the application of the same type of index in other locations. The data necessary to compute the factors and the index was collected during a field survey in Piran. As in other studies that computed FVIs, a flood risk matrix is created to describe the flood risk in a building according to its hazard (flood depth) and vulnerability (FVI). The implementation of the flood risk matrix allowed the qualitative assessment of the flood risk of 51 heritage buildings. The buildings are categorized into three flood risk classes: low, moderate, and high. The long-term gradual evolution of salt degradation in relation to climate change was also investigated. This analysis was performed obtaining the yearly number of salt transition cycles per year with the aid of RCM data on temperature and relative humidity until 2100.

The quantitative assessment of flood risk is performed by incorporating the previously obtained FVIs and depth-damage curves adapted to cultural heritage in the KPAN model. The new depth-damage curves inserted in the model came from two different sources, one is the Ministry of Culture of Slovenia, which developed a depth-damage curve for cultural heritage in Slovenia, and the other literature on depth-damage curves for singular buildings and for building materials commonly found in the cultural heritage assets in Piran. The use of three depth-damage curves allows two different damage estimations.

The first uses the curve provided by the Ministry of Culture for all 51 buildings. The second applies the curve for singular buildings to the most resistant buildings (since the singular buildings that the curve was based on are mostly made of stone masonry), and the curve for stone buildings to the less resistant buildings (made of stone or more fragile materials). That allows a more precise estimate of the costs depending on the building characteristics. KR PAN delivers the damage costs for the 51 buildings according to the 42 flood depth scenarios and for each one of the three depth-damage curves. These results are compared among one another (for different combinations of curves), to the values obtained by Alivio (2020) and to the renovation costs provided by the Ministry of Culture for two buildings, to perform a cost-benefit analysis.

## 7.2 Conclusions

The primary goal of this work is to accurately assess the impact of coastal flooding and the future damage caused by sea level rise on the cultural heritage in Piran. According to the 42 flood risk scenarios determined by Alivio (2020), flood depths are estimated for the 51 cultural heritage buildings considered. The buildings exposed to the highest flood depths are found to be the ones surrounding Tartini Square, in Punta, and buildings positioned by the port. The assets affected by the lowest flood depths are the ones that are located at higher elevations, such as the church complex on top of the hill.

The information collected to compute the flood risk vulnerability indexes allow an assessment of the characteristics of the sample. Most of the buildings analyzed have been constructed from the 16<sup>th</sup> to the 20<sup>th</sup> century, adding up to 80% of the sample. Regarding the buildings' condition, the majority are found to be in a slightly damaged condition, corresponding to 47% of the buildings, followed by the well-preserved group with 33% and 20% of damaged buildings. In terms of exposure, 45% of the buildings are located in the low-lying areas exposed to the sea, the most endangered area, 41% are located in low-lying areas not exposed to the sea and the reminiscent 13% are located in elevated areas. Concerning the heritage status, the buildings are categorized as ordinary and exceptional, and most of the assets (78%) are considered to be exceptional, due to the presence of ornaments, frescoes (in churches, for example), or rich finishings in their façade or internal area. Some of the other analyzed characteristics are the presence of a limestone base, the number of stories, the presence of ornaments, and the occurrence of a recent renovation in the building.

After collecting field data in Piran, it is possible to compute and analyze the flood vulnerability index of the buildings in Piran. The maximum and minimum values of FVI obtained are 6 and 77 out of 100, respectively. The average of the calculated FVIs is 40 with a standard deviation of 23. Most of the buildings present a flood vulnerability index from 20 to 60 (approximately 65% of the sample) and only 20% of the buildings are associated with a FVI up to 20. That distribution shows that most of the assets have a moderate (37.5%) or high (37.5%) flood vulnerability index, with moderate FVIs ranging from 25 to 50 and high FVIs from 50 to 75. This means that cultural heritage in Piran is significantly vulnerable to floods, and, with time and the consequent deterioration of the buildings, the tendency is for these assets to become even more vulnerable. Furthermore, the vulnerability ranking shows that Mary of Health's Church, St. Peter's Church, Pallazzo Bartole Fonda, and part of the wall in Resslerava ulica 1 are the most vulnerable assets, with a flood vulnerability index of 77.5 out of 100.

The qualitative flood risk results for 10 and 100-year return period floods and mean sea level rise scenarios of 0.3m (most expected) and 1.46m (most extreme) show that, under all scenarios, 8

buildings (16% of the sample) located in elevated locations are subjected to low flood risk. Analyzing the flood risk distribution of the buildings it can be concluded that the influence of the sea level rise variation (highest shift of 35%) is bigger than the impact of the change of flood return periods (highest shift of 25%). In addition, the 10-year return period is the one that presents the highest shift between flood risk classes when sea level rise scenarios change.

Regarding the assessment of the evolution of the number of salt transition cycles per year, it is expected that the number of salt crystallization cycles to increase over the next 77 years. This increase is small, adding up to 1.4% per year to a mean of approximately 3 cycles per year. Additionally, the maximum number of salt transitions is expected to increase until 2100.

For the analysis of the quantitative assessment results, damage costs for three different return periods (10, 100, and 1000-year) and three different sea level rise scenarios (no sea level rise or S0, 0.3m or S3 and 1.46m or S7) are considered. The results point to the conclusion that only for the 3 most mild scenarios (current state for 10 and 100-year return periods and 0.3m mean sea level rise for a 10-year return period) the damage cost of FD13+FD14 (curves obtained in the literature review) is higher than the cost of FD12 (curve provided by the Ministry of Culture). As the predicted flood depth increase, the difference in damage costs between FD12 (depth-damage curve for cultural heritage in Piran) and FD13+14 gets larger and, for the flood scenario referring to a 1000-year return period with a mean sea level rise of 1.46m the difference between the damage costs for the 2 combinations of curves gets to more than 200 thousand euros. Furthermore, for all scenarios, FD13 (depth-damage curve for singular buildings such as churches) has the lowest damage cost associated with it, both because it is associated with less vulnerable buildings and because the minority of the sample is linked to that curve.

The damage values increase as the sea level rise scenarios get more extreme. For a 10-year return period, values for a 1.46m mean sea level rise reach up to 529% of the costs for a 0.3m scenario and 25 times the costs for a no sea level rise scenario. Additionally, the impact of the sea level rise on the damage cost for cultural heritage buildings gets smaller as there is an increase in the number of years of the return period. It should be noted that in every scenario, the building located in Tartini Square 2 is the one that contributed the most to total damage, with damage costs up to 530 thousand euros for a 1000-year return period and a 1.46m mean sea level rise.

Comparing the obtained damage costs with the costs computed by Alivio (2020), it is concluded that the costs presented in the present work are significantly higher than the ones presented by Alivio (2020). The values calculated in the present work range from being approximately double Alivio's (2020), for a 10-year return period and 0.3 mean sea level rise (independently of the curve used), to around 4- and 7-times Alivio's (2020) cost, respectively for FD13+FD14 and FD12. These results are expected, since the damage costs for residential buildings, estimated with FEMA (2014) curves, tend to be considerably lower than the costs of cultural heritage damage, due to its more expensive and rare building materials and the presence of ornaments and frescoes. According to experts' estimates, the average damage values obtained in this work are expected to be approximately 3 times higher than the ones calculated with FEMA (2014) curves. That would lead to the conclusion that the curves applied in the present work are more suitable for estimating flood damage in cultural heritage.

Performing a cost-benefit analysis of the renovation costs for the 2 buildings for which the Ministry of Culture provided reports, it is concluded that it would be financially beneficial to execute the renovation of the exceptional building located in Tartini Square 2, utilizing any of the 2 combinations of depth-damage curves. For a 10-year return period and 0.3m mean sea level rise scenario, more than 59 thousand euros of future damage costs could be saved by implementing renovation costs. However,

renovation works in the ordinary buildings in Obzidina ulica 2,4, and 8 would result in a negative financial balance when compared to the damage costs they are subjected to. It should be highlighted that despite the financial benefits not living up to the necessary to be considered feasible, these should not be the only benefits considered when deciding whether renovation interventions should be implemented in cultural heritage buildings. The irreplaceability and invaluable historic and social importance of cultural heritage buildings should be taken into account.

As previously mentioned in other sections, one of the biggest limitations of the present work is the lack of consideration of the contribution and potential alterations in the dynamics of storm surge action and wave heights to cultural heritage flood damage. The coastal dynamic processes are not considered for the estimation of the return periods of extreme events or the determination of flood depths, since a bathtub model is used. Nevertheless, it should be highlighted that Piran's city center is only a few hundred meters from the sea, and, according to Breilh et al. (2013), the bathtub model delivers reasonable results when predicting inundation for areas located less than 3 km away from the coast. However, the bathtub model results accuracy strongly depends on the local coastal area topography. Considering the uncertainty in sea level projections, the wide range of sea level rise and flood event scenarios created by Alivio (2020) would allow the consideration of several outcomes and, thus, account for the uncertainty of the projections. Analyzing the uncertainty bands considering the 42 flood scenarios with different return periods and sea level rise projections, for milder flood scenarios the difference in total damage cost to cultural heritage in the studied area is not very large (reaching a maximum of a million euros for T100). However, as the mean SLR scenarios get more severe and the return periods larger, the damage costs estimated by the curve gradually diverge more. This span of the simulated scenarios would account for the uncertainty associated with the damage estimations as it accounts for multiple different future outcomes. The lack of data limits the scope of the cost-benefit analysis since renovation costs of only 2 buildings are available. The small number of condition reports also hinders the creation of depth-damage curves tailored to the 51 buildings analyzed. In terms of salt weathering, data (building characteristics and identification of salts in the sea surrounding the area and in building materials) and resources limitations (possibility of extracting samples and performing tests) prevent the present work from delivering results on the impact of salt intrusion in cultural heritage buildings due to floods.

Despite the mentioned limitations, the present work delivers a more precise estimation of flood damage costs of cultural heritage buildings in Piran than the one presented by Alivio (2020) since they account for the vulnerability and building typology, and construction materials of the assets. The results obtained point out that a large percentage of the cultural heritage sites considered currently have moderate or high flood vulnerability. In the future, the building deterioration due to time along with the impacts of climate change and sea level rise will considerably increase the flood risk these cultural heritage assets are exposed to. This situation reinforces the demand for effective flood reduction and mitigation strategies that would protect the whole city of Piran, such as the ones presented in POPKLIMAS, and specific measures tailored to cultural heritage needs, such as the renovation of damaged buildings and retrofitting of the assets, including the installation of flood-resistant components and impermeabilization. Qualitative flood risk maps allow the population to better visualize and understand the risk their cultural heritage is under now and will be in the future, and possibly increase their awareness and proactivity in protecting and interacting with such assets. On the other hand, depth damage curves, damage costs per flood scenario, EAD, and reports on renovation costs support the decision-making of cultural heritage managers and local governments on which buildings to prioritize

and which flood measures to implement in order to avoid the most damage to cultural heritage. In addition, those responsible for cultural heritage management should investigate and continuously monitor their assets to better direct protection interventions and flood strategies. Furthermore, the quantitative damage assessments considering the vulnerability and building characteristics of cultural heritage can assist in the protection of this type of asset in other coastal areas, especially in the Adriatic Sea and the Mediterranean area.

### **7.3 Recommendations**

Considering the presented results and conclusions, the following suggestions for further research are made:

1. Incorporation of storm surges and wave configuration in sea level extreme models on the Slovenian coast.
2. Study of the direct impact of waves on cultural heritage buildings in Slovenia (hydrodynamic forces).
3. Calculation of FVIs for all types of buildings for the entire country of Slovenia.
4. In-depth investigation of the building materials of cultural heritage in Slovenia.
5. Identification of flood damage in cultural heritage sites in Slovenia and estimation of renovation costs.
6. Creation of monitoring campaigns to assess cultural heritage conditions.
7. Second-tier flood risk assessment for the most endangered cultural heritage buildings identified in Piran, allowing the creation of depth-damage curves for critical assets.
8. Investigation of the quantitative impact of saltwater on cultural heritage in Slovenia (including the identification of seawater and building material salts and experiments in the laboratory).
9. Estimate indirect flood damage due to loss of revenues (e.g. tourism reduction).

## 8 REFERENCES

- Alivio, M.B. (2020). Evaluation of flood damage caused by rising sea levels, MSc thesis, University of Ljubljana, Ljubljana, Slovenia
- Archive.org. (2019). Portorož/Portorose. [online] Available at: <https://web.archive.org/web/20041103041500/http://www.portoroz.si/EN/default.asp?id=546> [Accessed 29 Jul. 2023].
- Anaf, W., Leyva Pernia, D., Schalm, O. (2018) Standardized Indoor Air Quality Assessments as a Tool to Prepare Heritage Guardians for Changing Preservation Conditions due to Climate Change. *Geosciences* 2018, 8, 276.
- Arrighi, C., Brugioni, M. & Castelli, F. & Franceschini, S. & Mazzanti, B. (2015). Flood risk assessment in art cities: The exemplary case of Florence (Italy). *Journal of Flood Risk Management*. 11. n/a-n/a. 10.1111/jfr3.12226.
- Arrighi C. (2021). A Global Scale Analysis of River Flood Risk of UNESCO World Heritage Sites. *Front. Water*, 23 December 2021. Sec. Water and Climate. Volume 3 - 2021 | <https://doi.org/10.3389/frwa.2021.764459>
- Arrighi, C., Carraresi, A. and Castelli, F. (2022). Resilience of art cities to flood risk: A quantitative model based on depth-idleness correlation. *Journal of Flood Risk Management* published by Chartered Institution of Water and Environmental Management and John Wiley & Sons Ltd.. doi:<https://doi.org/10.1111/jfr3.12794>.
- Auger F. (1987). Alteration des roches sous influence marine; degradation des pierres en oeuvre et simulation acceleree en laboratoire. These Doctorat d'Etat es Sciences. Universite de Poitiers, France
- Balica, S.F., Wright, N.G., van der Meulen, F. (2012). A flood vulnerability index for coastal cities and its use in assessing climate change impacts. *Nat Hazards* 64, 73–105. <https://doi.org/10.1007/s11069-012-0234-1>
- Benčič, N. (2012). Embrace Piran. Tourist Board Portorož. Piran, Slovenia (M. Perpar, Trans.). <http://www.portoroz.si/si/files/default/PDF/Tiskovine/objemi-piran-zgibanka-eng.pdf>
- Benčič, N. (2018). *Istria Slovenia: Koper, Izola, Piran, Portorož* (V. Radulovič, Trans). Spirit Slovenia. Ljubljana, Slovenia. <https://www.slovenia.info/uploads/publikacije/slovenska-istra/istria-slovenia-en.pdf>
- Bertolin, C. (2019). Preservation of Cultural Heritage and Resources Threatened by Climate Change. *Geosciences*, [online] 9(6), p.250. <https://doi.org/10.3390/geosciences9060250>.
- Bogaards, R. (n.d.). Cost Benefit Analysis and Historic Heritage Regulation. [online] Available at: [https://oia.pmc.gov.au/sites/default/files/2021-06/wp3\\_rbogaards\\_historic\\_heritage.pdf](https://oia.pmc.gov.au/sites/default/files/2021-06/wp3_rbogaards_historic_heritage.pdf).
- Bolčič, L., Kne Š., Požar A. K., Mešl M., Mlakar I., Breznik A., Breznik K., Knaus A.J. (2020). Povečanje poplavn varnosti obalnega območja Piran zaradi globalnih klimatskih sprememb – POPKLIMAS
- Breilh, J. F., Chaumillon, E., Bertin, X., and Gravelle, M. (2013). Assessment of static flood modeling techniques: application to contrasting marshes flooded during Xynthia (western France). *Natural Hazards and Earth System Sciences*, 13(6), 1595–1612. Doi:10.5194/nhess-13-1595-2013
- Bricelj M. (2002) See the Sea. (n.d.). Available at: [https://www.gov.si/assets/ministrstva/MOP/Publikacije/morje\\_en.pdf](https://www.gov.si/assets/ministrstva/MOP/Publikacije/morje_en.pdf) [Accessed 22 Feb. 2023].
- Burnham, M. W. and Davis, D. W. (1997). Risk-based analysis for flood damage reduction studies. *Proceedings on Hydrology and Hydraulics*. United States Army Corps of Engineers Hydrologic Engineering Center, California, USA. <https://www.hec.usace.army.mil/publications/SeminarProceedings/SP-28.pdf>
- Cardell C., Delalieux F., Roumpopoulos K., Moropoulou A., Auger F., Van Grieken R., (2003) Salt-induced decay in calcareous stone monuments and buildings in a marine environment in SW France. *Construction and Building Materials*, Volume 17, Issue 3, Pages 165-179, ISSN 0950-0618. [https://doi.org/10.1016/S0950-0618\(02\)00104-6](https://doi.org/10.1016/S0950-0618(02)00104-6).
- Carroll P. and Aarrevaara E. (2018). Review of Potential Risk Factors of Cultural Heritage Sites and Initial Modelling for Adaptation to Climate Change. *Geosciences* 2018, 8, 322, doi:10.3390/geosciences8090322
- Casas, A., Lane, S. N., Yu, D., and Benito, G. (2010). A method for parameterizing roughness and topographic sub-grid scale effects in hydraulic modeling from LiDAR data. *Hydrology and Earth System Sciences*, 14(8), 1567–1579. Doi:10.5194/hess-14-1567-2010
- Charola, A.E. (2000) Salts in the Deterioration of Porous Materials: An Overview, *Journal of the American Institute for Conservation*, 39:3, 327-343, DOI: 10.1179/019713600806113176

- Ciantelli C., Palazzi E., Hardenberg J., Vaccaro C., Tittarelli F. and Bonazza A. (2018). How Can Climate Change Affect the UNESCO Cultural Heritage Sites in Panama? *Geosciences* 2018, 8, 296, doi:10.3390/geosciences8080296
- Climateforculture.eu. (2014). Climate for Culture. [online] Available at: <https://www.climateforculture.eu/index.php?inhalt=project.overview> [Accessed 27 Jul. 2023].
- Council of the European Union (2022). Council resolution on the EU Work Plan for Culture 2023-2026. Official Journal of the European Union. Available at: <https://www.consilium.europa.eu/media/60399/st15381-en22.pdf>
- CNR-ISAC (2007). Noah's Ark - Global Climate Change Impact on Built Heritage and Cultural Landscapes. Publishable executive summary
- Davis, L., Larionova, T., Patel, D., Tse, D., Juliá P.B., Santos P.P. and Ferreira T.M. (2023). Flood vulnerability and risk assessment of historic urban areas: Vulnerability evaluation, derivation of depth-damage curves and cost-benefit analysis of flood adaptation measures applied to the historic city center of Tomar, Portugal. [online] doi: <https://doi.org/10.1111/jfr3.12908>.
- Dassanayake D., Burzel A., Oumeraci H. (2012). Evaluation of Cultural Losses. [https://www.researchgate.net/publication/266458949\\_Evaluation\\_of\\_Cultural\\_Losses](https://www.researchgate.net/publication/266458949_Evaluation_of_Cultural_Losses)
- Deu, Ž. (2016). Dragocenosti starih mestnih jeder: monografija zgodovinskih mest Slovenije (J. Jarc, Trans.). Združenje zgodovinskih mest Slovenije. <https://issuu.com/simonpavlic/docs/dragocenosti-mestnih-jeder-issuu>
- Diaconu M.(2015). REPORT towards an integrated approach to cultural heritage for Europe | A8-0207/2015 | European Parliament. [online] Europa.eu. Available at: [https://www.europarl.europa.eu/doceo/document/A-8-2015-0207\\_EN.html#\\_part2\\_def1](https://www.europarl.europa.eu/doceo/document/A-8-2015-0207_EN.html#_part2_def1) [Accessed 29 Jul. 2023].
- Dutta, D., Herath, S., and Musiaka, K. (2003). A mathematical model for flood loss estimation. *Journal of Hydrology*, 277(1-2), 24–49. Doi:10.1016/s0022-1694(03)00084-2
- EEC (2005) Commission Recommendation of 20 December 1974 to Member States concerning the protection of the architectural and natural heritage. Official Journal L 021 , 28/01/1975 P. 0022 - 0023
- Englhardt, J., Hans de Moel, Huyck, C.K., de Ruiter M., Aerts, H. and Ward, P.B. (2019). Enhancement of large-scale flood risk assessments using building-material-based vulnerability curves for an object-based approach in urban and rural areas. [online] 19(8), pp.1703–1722. doi:<https://doi.org/10.5194/nhess-19-1703-2019>.
- Ernst, J., Dewals, B.J., Detrembleur, S., Archambeau, P., Erpicum, S., Piroton, M., (2010). Micro-scale flood risk analysis based on detailed 2D hydraulic modeling and high-resolution geographic data. *Natural Hazards*, 55(2), pp.181-209. Doi:10.1007/s11069-010-9520-y
- Erpicum, S., Dewals, B., Archambeau, P., Detrembleur, S., Piroton, M., (2010). Detailed inundation modeling using high-resolution DEMs. *Engineering Applications of Computational Fluid Mechanics*, 4(2), pp.196-208. Doi:10.1080/19942060.2010.11015310
- Eurocities (2022). Cultural Heritage in Cities and Regions - Challenges and trends throughout Europe. Cultural Heritage in Action. Available at: <https://www.heartsnminds.eu/culturalheritageinaction/#page=1> [Accessed 29 Jul. 2023].
- European Commission (2014). Towards an integrated approach to cultural heritage for Europe. Communication from the Commission to the European Parliament, the Council, the European Economic and Social Committee and the Committee of the Regions. Available at: <https://resources.riches-project.eu/wp-content/uploads/2015/10/CELEX-52014DC0477-EN-TXT.pdf>.
- European Commission (201). A New European Agenda for Culture. Communication From Commission to the European Parliament, the European Council, the Council, the European Economic and Social Committee and The Committee of the Regions. Available at: <https://eur-lex.europa.eu/legal-content/EN/TXT/?uri=COM:2018:267:FIN>
- European Commission, Directorate-General for Education, Youth, Sport and Culture, (2019) European framework for action on cultural heritage. Publications Office. <https://data.europa.eu/doi/10.2766/949707>
- Expoaus.org. (2015). Piran. [online] Available at: <https://www.expoaus.org/piran-uso9> [Accessed 1 Mar. 2023].
- FEMA, (2014): Flood Model Technical Manual, HAZUS-MH. [http://www.fema.gov/media-library-data/20130726-1820-25045-8292/hzmmh2\\_1\\_fl\\_tm.pdf](http://www.fema.gov/media-library-data/20130726-1820-25045-8292/hzmmh2_1_fl_tm.pdf) (accessed 7 March 2014)
- Fereshtehpour, M., & Karamouz, M. (2018). DEM Resolution Effects on Coastal Flood Vulnerability Assessment: Deterministic and Probabilistic Approach. *Water Resources Research*, 54(7), 4965–4982. Doi:10.1029/2017wr022318

- Fermo P., Goidanich S., Comite V., Toniolo L. and Gulotta D. (2018). Study and Characterization of Environmental Deposition on Marble and Surrogate Substrates at a Monumental Heritage Site. *Geosciences* 2018, 8, 349, doi:10.3390/geosciences8090349
- Figueiredo, R., Romão, X. and Paupério, E. (2021). Component-based flood vulnerability modeling for cultural heritage buildings. [online] 61, pp.102323–102323. doi: <https://doi.org/10.1016/j.ijdr.2021.102323>.
- Financial Administration of the Republic of Slovenia (2014). Legislation | Cultural heritage | Financial Administration of The Republic of Slovenia. [online] Available at: [https://www.fu.gov.si/en/customs/prohibitions\\_and\\_restrictions/cultural\\_heritage/#c1685](https://www.fu.gov.si/en/customs/prohibitions_and_restrictions/cultural_heritage/#c1685) [Accessed 27 Jul. 2023].
- Foudi, S. & Osés-Eraso, N. (2014). Flood risk management: Assessment for prevention with hydro-economic approaches. *Routledge Handbook of the Economics of Climate Change Adaptation* Chapter: 16
- Foudi, S., Osés-Eraso, N., & Tamayo, I. (2015). Integrated spatial flood risk assessment: The case of Zaragoza. *Land Use Policy*, 42, 278–292. Doi:10.1016/j.landusepol.2014.08.002
- Franke, L., and E Pinsler. 1998. Untersuchungen von Salztransportprozessen und deren Visualisierung mit Hilfe der Röntgen-analytik. *International Journal for Restoration of Buildings and Monuments* 4(3):187-207.
- Gerl, T., Kreibich, H., Franco, G., Marechal, D., and Schröter, K. (2016). A Review of Flood Loss Models as Basis for Harmonization and Benchmarking. *PLOS ONE*, 11(7), e0159791. Doi:10.1371/journal.pone.0159791
- Gesch, D. B. (2018). Best Practices for Elevation-Based Assessments of Sea-Level Rise and Coastal Flooding Exposure. *Frontiers in Earth Science*, 6. Doi:10.3389/feart.2018.00230 <https://www.frontiersin.org/articles/10.3389/feart.2018.00230/full>
- Grossi C.M., Brimblecombe P., Menéndez B., Benavente D., Harris I., Déqué M. (2011). Climatology of salt transitions and implications for stone weathering. *Science of the Total Environment* 409 (2011) 2577–2585. doi:10.1016/j.scitotenv.2011.03.029
- Haugen A., Bertolin C., Leijonhufvud G., Olstad T. and Broström T. (2018). A Methodology for Long-Term Monitoring of Climate Change Impacts on Historic Buildings. *Geosciences* 2018, 8, 370, doi:10.3390/geosciences8100370
- Herath, S. (2003). Flood Damage Estimation of an Urban Catchment using Remote Sensing and GIS. *International Training Program on Total Disaster Risk Management*. United Nations University, Japan. <https://www.adrc.asia/publications/TDRM2003June/10.pdf>
- Herein System. (2014). Slovenia - Herein System - [www.coe.int](http://www.coe.int). [online] Available at: <https://www.coe.int/en/web/herein-system/slovenia> [Accessed 27 Jul. 2023].
- Holický M. and Sýkora M. (2009) Assessment of Flooding Risk to Cultural Heritage in Historic Sites. *Journal of Performance of Constructed Facilities* 24(5) DOI:10.1061/(ASCE)CF.1943-5509.0000053
- Honeycombe DB. Weathering and decay of Masonry. In: Ashurst J, Dimes FG, editors. *Conservation of building and decorative stones*. 1998 edition. Oxford: Butterworth/-Heinemann; 1990. p. 153–78. paperback, part 1.
- Interreg Central Europe (2014). ForHeritage. [online] Available at: <https://programme2014-20.interreg-central.eu/Content.Node/ForHeritage.html> [Accessed 27 Jul. 2023].
- Interreg Central Europe (2018a). Forget Heritage. [online] Available at: <https://programme2014-20.interreg-central.eu/Content.Node/Forget-heritage.html> [Accessed 27 Jul. 2023].
- Interreg Central Europe (2018b). Forget Heritage. Policy Handbook for the Revitalization of Ghost Buildings in Central Europe Cities. Deliverable T.1.4.1.
- Interreg Central Europe (2018c). Forget Heritage. Management Manual. D.T1.3.1
- Interreg Central Europe (2022a). ForHeritage. D.T3.3.4 – The Model for Financing of Cultural Heritage in Ljubljana Urban Region
- Interreg Central Europe (2022b). D.T2.3.3 – Feasibility Study For The Vodnik Homestead For The Future Use Of Private Funding Sources
- Institute for the Protection of the Cultural Heritage of Slovenia (2020). Monuments with rehabilitation assessment. OE Piran and Restoration Center.
- Kang, J.-L & Su, M.-D & Chang, L.-F. (2005). Loss functions and framework for regional flood damage estimation in residential area. *Journal of Marine Science and Technology*. 13. 193-199. <https://jmst.ntou.edu.tw/marine/13-3/193-199.pdf>
- Kne Š. (2020). Piran in njegovi problem. *Revija študentov Fakultete za gradbeništvo in geodezijo v Ljubljani* | oktober 2020 | brezplačen izvod

- Kolega, N. (2015). Coastline changes on the Slovenian coast between 1954 and 2010. *Acta Geographica Slovenica*, 55(2). Doi:10.3986/ags.1887
- Kopp, R. E., DeConto, R. M., Bader, D. A., Hay, C. C., Horton, R. M., Kulp, S., Strauss, B. H. (2017). Evolving Understanding of Antarctic Ice-Sheet Physics and Ambiguity in Probabilistic Sea-Level Projections. *Earth's Future*, 5(12), 1217–1233. Doi:10.1002/2017ef000663
- Kuza, I. and Merc, M. (2015). In STAGE every inhabitant of Slovenia play his or her part. Republic of Slovenia Statistical Office. <https://www.stat.si/StatWeb/en/News/Index/5238>
- Li, Xingong and Rowley, Rex and Kostelnick, John and Braaten, David and Meisel, Joshua and Hulbutta, Kalonie. (2009). GIS Analysis of Global Impacts from Sea Level Rise. *Photogrammetric Engineering and Remote Sensing*. 75. 807-818. 10.14358/PERS.75.7.807.
- Loli A. and Bertolin C. (2018). Indoor Multi-Risk Scenarios of Climate Change Effects on Building Materials in Scandinavian Countries. *Geosciences* 2018, 8, 347, doi:10.3390/geosciences8090347
- Ličer, M. (2019). Podnebne spremembe in naraščanje gladine morja v Severnem Jadranu (Climate change and sea level rise in the North Adriatic). National Institute of Biology – Marine Biological Station Piran. <https://www.nib.si/mbp/sl/home/news/902-podnebne-spremembe-in-narascanje-gladine-morja-v-severnem-jadranu>
- Martínez-Gomariz E., Forero-Ortiz E., Guerrero-Hidalga M., Castán S., Gómez M. (2020). Flood Depth–Damage Curves for Spanish Urban Areas. *Sustainability*; 12(7):2666. <https://doi.org/10.3390/su12072666>
- Melin C. B., Hagentoft C.E., Holl K., Nik V.M. and Kilian R. (2018). Simulations of Moisture Gradients in Wood Subjected to Changes in Relative Humidity and Temperature Due to Climate Change. *Geosciences* 2018, 8, 378, doi:10.3390/geosciences8100378
- Menéndez B. (2018). Estimators of the Impact of Climate Change in Salt Weathering of Cultural Heritage. *Geosciences* 2018, 8, 401, doi:10.3390/geosciences8110401
- Merz, B., Kreibich, H., Thielen, A., and Schmidtke, R. (2004). Estimation uncertainty of direct monetary flood damage to buildings. *Natural Hazards and Earth System Sciences*, 4(1), 153–163. Doi:10.5194/nhess-4-153-2004
- Merz, B., Kreibich, H., Schwarze, R., and Thielen, A. (2010). Review article "Assessment of economic flood damage". *Nat. Hazards Earth Syst. Sci.* 10, 1697–1724. <https://doi.org/10.5194/nhess-10-1697-2010>
- Messner, F., Penning-Rowsell, E., Green, C., Meyer, V., Tunstall, S. and Veen, A. (2007). Evaluating flood damage: guidance and recommendations on principles and methods. FLOOD Site Project Report. [http://www.floodsite.net/html/partner\\_area/project\\_docs/T09\\_06\\_01\\_Flood\\_damage\\_guidelines\\_d9\\_1\\_v2\\_2\\_p44.pdf](http://www.floodsite.net/html/partner_area/project_docs/T09_06_01_Flood_damage_guidelines_d9_1_v2_2_p44.pdf)
- Massari, G., and Massari I. (1993). Damp buildings, old and new. Rome: ICCROM. 7-12.
- Mezek S., Bricelj M. (2002) A Review of Coastal Area Management in Slovenia. In: Sain B.C., Pavlin I., Belfiore S. (eds) Sustainable Coastal Management: A Transatlantic and Euro-Mediterranean Perspective. NATO Science Series (Series IV: Earth and Environmental Sciences), vol 12. Springer, Dordrecht. [https://doi.org/10.1007/978-94-010-0487-9\\_12](https://doi.org/10.1007/978-94-010-0487-9_12)
- Middelmann-Fernandes, M. H. (2010). Flood damage estimation beyond stage-damage functions: an Australian example. *Journal of Flood Risk Management*, 3(1), 88–96. Doi:10.1111/j.1753-318x.2009.01058.x
- Ministry of Culture of the Republic of Slovenia (2018). Selection from the register of immovable cultural heritage. OPSI - Odprti podatki Slovenije. <https://podatki.gov.si/dataset/izbor-iz-registra-nepremicne-kulturne-dediscine>
- Miranda F.N. and Ferreira T.M. (2019). A simplified approach for food vulnerability assessment of historic sites. *Natural Hazards* (2019) 96:713–730 <https://doi.org/10.1007/s11069-018-03565-1>
- Mlakar B and Zupančič T. (2022). Tourist arrivals and overnight stays, March 2022. [online] Available at: <https://www.stat.si/StatWeb/en/News/Index/10284> [Accessed 21 Feb. 2023].
- Mlasko, J. (2011). Lasersko Skeniranje in Aerofotografiranje 2011 Blok B21: Tehnično Poročilo Izdelave. Agencija Republike Slovenije za okolje (ARSO). Ljubljana, Slovenia. [http://gis.arso.gov.si/related/lidar\\_porocila/b\\_21\\_izdelava\\_izdelkov.pdf](http://gis.arso.gov.si/related/lidar_porocila/b_21_izdelava_izdelkov.pdf)
- Nicholls R. J., Hansoni S., Herweijerii C., Patmoreii N., Hallegatteiii S., Corfee-Morlotiv J., Châteauiiv J. and Muir-Woodii R. (2008). Ranking Port Cities with High Exposure and Vulnerability to Climate Extremes: Exposure Estimates. OECD Environment Working Papers, No. 1, OECD Publishing, Paris, <https://doi.org/10.1787/011766488208>
- Nicholls, Robert and Cazenave, Anny. (2010). Sea-Level Rise and Its Impact on Coastal Zones. *Science* (New York, N.Y.). 328. 1517-20. Doi: 10.1126/science.1185782.

[https://www.researchgate.net/publication/44683423\\_SeaLevel\\_Rise\\_and\\_Its\\_Impact\\_on\\_Coastal\\_Zones](https://www.researchgate.net/publication/44683423_SeaLevel_Rise_and_Its_Impact_on_Coastal_Zones)

- NOAA National Centers for Environmental Information. (2018). State of the Climate: National Climate Report for May 2018, published online June 2018, retrieved on March 3, 2021 from <https://www.ncdc.noaa.gov/sotc/national/2018/05/supplemental/page-1>
- Ntself.org. (2019). About tides – Tides: questions and answers | National Tidal and Sea Level Facility. [online] Available at: <https://ntself.org/about-tides/tides-faq#:~:text=Tides%20can%20be%20predicted%20far,very%20accurately%20into%20the%20future.> [Accessed 29 Jul. 2023].
- Olesen, L., Löwe, R., and Arnbjerg-Nielsen, K. (2017). Flood damage assessment – Literature review and recommended procedure. Cooperative Research Centre for Water Sensitive Cities. <https://watersensitivecities.org.au/content/flood-damage-assessment-literature-review-recommended-procedure/>
- Oppenheimer, M., B.C. Glavovic, J. Hinkel, R. van de Wal, A.K. Magnan, A. Abd-Elgawad, R. Cai, M. Cifuentes-Jara, R.M. DeConto, T. Ghosh, J. Hay, F. Isla, B. Marzeion, B. Meysignac, and Z. Sebesvari, 2019: Sea Level Rise and Implications for Low-Lying Islands, Coasts and Communities. In: IPCC Special Report on the Ocean and Cryosphere in a Changing Climate [H.-O. Pörtner, D.C. Roberts, V. Masson-Delmotte, P. Zhai, M. Tignor, E. Poloczanska, K. Mintenbeck, A. Alegría, M. Nicolai, A. Okem, J. Petzold, B. Rama, N.M. Weyer (eds.)]. Cambridge University Press, Cambridge, UK and New York.
- Pistrika, A., Tsakiris, G., and Nalbantis, I. (2014). Flood Depth-Damage Functions for Built Environment. *Environmental Processes*, 1(4), 553–572. Doi:10.1007/s40710-014-0038-2
- Poulter, B. and Halpin, P. N. (2008). Raster modelling of coastal flooding from sea-level rise. *International Journal of Geographical Information Science*, 22(2), 167–182. Doi:10.1080/13658810701371858
- Price, C. A., and :P.Brimblecombe. 1994. Preventing salt damage in porous materials. In *Preventive conservation, practice, theory and research*, ed. A. Roy and :P. Smith. London: International Institute for Conservation of Historic and Artistic Works. 90-93.
- Reimann L., Vafeidis A. T., Brown S., Hinkel J. & Tol R. S.J. (2018). Mediterranean UNESCO World Heritage at risk from coastal flooding and erosion due to sea-level rise. *Nature Communications* | (2018) 9:4161 | DOI: 10.1038/s41467-018-06645-9 | [www.nature.com/naturecommunications](http://www.nature.com/naturecommunications)
- Schröter, K., Kreibich, H., Vogel, K., Riggelsen, C., Scherbaum, F., & Merz, B. (2014). How useful are complex flood damage models? *Water Resources Research*, 50(4), 3378–3395. Doi:10.1002/2013wr014396
- Sesana E., Gagnon A. S., Bertolin C. and Hughes J. (2018). Adapting Cultural Heritage to Climate Change Risks: Perspectives of Cultural Heritage Experts in Europe. *Geosciences* 2018, 8, 305, doi:10.3390/geosciences8080305
- Sesana E., Gagnon A.S., Bonazzac A., Hughes J.J. (2019). An integrated approach for assessing the vulnerability of World Heritage Sites to climate change impacts. *Journal of Cultural Heritage* 41 (2020) 211–224
- Sesana E., Gagnon A. S., Ciantelli C., Cassar, J. Hughes (2021). Climate change impacts on cultural heritage: A literature review. *WIREs Climate Change*, Volume 12, Issue 4 e710 <https://doi.org/10.1002/wcc.710>
- Smith, D. (1994). Flood damage estimation - A review of urban stage-damage curves and loss functions. *Water SA*, 20, 231-238. [https://journals.co.za/Doi/10.10520/AJA03784738\\_1124](https://journals.co.za/Doi/10.10520/AJA03784738_1124)
- Snethlage, R., and E. Wendler. 1997. Moisture cycles and sandstone degradation. In *Saving our architectural heritage: The conservation of historic stone structures*, ed. N. S. Baer and R. Snethlage. Chichester: Elsevier. 7-24.
- STA (2019). Piran, Izola & Koper Flooded Due to Rain, Full Moon (Videos). [online] Total-slovenia-news.com. Available at: <https://www.total-slovenia-news.com/lifestyle/4964-piran-izola-koper-flooded-due-to-rain-full-moon-video> [Accessed 1 Mar. 2023].
- Statistical Office of the Republic of Slovenia (SURS). (2022). Settlement of Piran. <https://www.stat.si/KrajevnaImena/en/Settlements/Details/3227>
- Steiger, M., and W Dannecker. 1995. Hygroskopische Eigenschaften und Kristallisationsverhalten von Salzmischungen. In *Jahresberichte Steinzeitalter: Steinkonservierung 1993*, ed. R. Snethlage. Berlin: Ernst & Sohn. 115-28.
- Stephenson, V. and D'Ayala, D. (2013). A new approach to flood loss estimation and vulnerability assessment for historic buildings in England, *Nat. Hazards Earth Syst. Sci. Discuss.*, 1, 6025–6060, 201, doi:10.5194/nhessd-1-6025-2013

- Stieglitz, M., Shaman, J., McNamara, J., Engel, V., Shanley, J. and Kling, G.W. (2003). An approach to understanding hydrologic connectivity on the hillslope and the implications for nutrient transport. *Global Biogeochemical Cycles*, [online] 17(4), p.n/a-n/a. doi:<https://doi.org/10.1029/2003gb002041>.
- Strojan, I. and Robič, M. (2016). Sea level. Slovenian Environment Agency. <http://kazalci.arso.gov.si/en/content/sea-level-4>
- UCL (2017). NOAH's ARK Project. [online] UCL Institute for Sustainable Heritage. Available at: <https://www.ucl.ac.uk/bartlett/heritage/research/projects/project-archive/noahs-ark-project> [Accessed 22 Jul. 2023].
- UNESCO (2018). The Criteria for Selection. [online] Unesco.org. Available at: <https://whc.unesco.org/en/criteria/> [Accessed 29 Jul. 2023].
- UNEP/MAP-PAP/RAC. (2018). MAP Coastal Area Management Programme (CAMP) Slovenia: Final Integrated Report. MAP Technical Series No. 171. UNEP/MAP: Athens. <https://digitallibrary.un.org/record/648053?ln=en>
- Vahtar M. (2006). Institute for Integral Development and Environment. EuroSION case study on the Slovenian coast, EuroSION project. [http://copranet.projects.eucc-d.de/files/000152\\_EUROSION\\_Slovenian\\_coast.pdf](http://copranet.projects.eucc-d.de/files/000152_EUROSION_Slovenian_coast.pdf)
- Vidmar, A., Zabret, K., Lebar, K., Pergar, P., and Kryžanowski, A. (2019). Development of an application for estimating the benefits of constructional and non-constructional measures for flood risk reduction. Conference: 7. Hrvatska konferencija o vodama - Hrvatske vode u zaštiti okoliša i prirode, Opatija, Croatia. [https://www.researchgate.net/publication/333631413\\_Development\\_of\\_an\\_application\\_for\\_estimating\\_the\\_benefits\\_of\\_constructional\\_and\\_non-constructional\\_measures\\_for\\_flood\\_risk\\_reduction](https://www.researchgate.net/publication/333631413_Development_of_an_application_for_estimating_the_benefits_of_constructional_and_non-constructional_measures_for_flood_risk_reduction)
- Wang J. (2015). Flood risk maps to cultural heritage: Measures and process. *Journal of Cultural Heritage* 16 (2015) 210–220. <http://dx.doi.org/10.1016/j.culher.2014.03.002>
- Weatherspark.com. (2023). Piran Climate, Weather By Month, Average Temperature (Slovenia) - Weather Spark. [online] Available at: <https://weatherspark.com/y/75151/Average-Weather-in-Piran-Slovenia-Year-Round> [Accessed 22 Feb. 2023].
- Weber, H. 1984. Mauerfeuchtigkeit. Sindelfingen, Germany: ExpertVerlag. 15-37.
- Webster, T., Forbes, D., MacKinnon, E. and Roberts, D. (2006). Flood-risk mapping for storm-surge events and sea-level rise using lidar for southeast New Brunswick. *Canadian Journal of Remote Sensing*. 32. 194-211. 10.5589/m06-016.
- World Bank Blogs. (2022). Flood risk already affects 1.81 billion people. Climate change and unplanned urbanization could worsen exposure. [online] Available at: <https://blogs.worldbank.org/climatechange/flood-risk-already-affects-181-billion-people-climate-change-and-unplanned> [Accessed 1 Mar. 2023].
- World Weather & Climate Information. (2023). Average monthly rainfall and snow in Piran, Slovenia (millimeter). [online] Available at: <https://weather-and-climate.com/average-monthly-precipitation-rainfall.piran,Slovenia> [Accessed 22 Feb. 2023].
- Yunus, A. P., Avtar, R., Kraines, S., Yamamuro, M., Lindberg, F. and Grimmond, C. (2016). Uncertainties in Tidally Adjusted Estimates of Sea Level Rise Flooding (Bathtub Model) for the Greater London. *Remote Sensing*. 8. 366. 10.3390/rs8050366.ç'x